

**Geochemical processes associated with 'marine band'
formation in the Lower Carboniferous Bowland Shale
Formation, Northern England.**

Jack Walker

Doctor of Philosophy

Newcastle University, School of Natural and Environmental Sciences

Submitted: December 2019

Acknowledgements

I thank the collaborative efforts of Newcastle University (Dr. Sanem Acikalin, Dr. Shannon Flynn, Dr. Martin Jones, Dr. Cees Van der Land and Sam Graham), the British Geological Survey (Dr. Chris Vane, Dr. Ed Hough and Dr. Jan Hennissen), the Lyell Centre with Heriot-Watt University (Prof. Thomas Wagner) and Cuadrilla Resources (Lucy Craddock and Huw Clarke) for their input, feedback and contributions throughout.

I express a special thanks to Sanem and Shannon who, although they joined during a late and busy stage, proved savvy and exceptional assets to the project. For their help and hard work, I will always be thankful.

Thank you to the funders (NERC Centre for Doctoral Training Oil and Gas scheme), the British Geological Survey (British Geological Survey Funding Initiative) and Newcastle University. As an addition to the funding, the British Geological Survey with Chris Vane kindly provided important Rock-Eval(6) pyrolysis analysis as well as expertise and advice. Without the untiring efforts of Newcastle University technicians (David Earley, Paul Donohoe and Bernard Bowler), this project could not have achieved its goals.

Thank you in advance to the internal and external examiners for giving up their time to read this thesis.

Thank you to the past and current employees of Cuadrilla Resources and the NERC CDT Oil and Gas, who broadened my knowledge base and put this project into perspective. They, each of them, made the whole experience a lot of fun.

On a more personal note, I would like to thank Tom Fender, Claire McGhee, Sam Graham and Tom Charlton for making me laugh.

And thank you to my family and to Vicky, for everything.

Contents

Abstract-----	1
Chapter 1. Introduction -----	3
Chapter 2. Geological History -----	12
Chapter 3. Methodology -----	20
Chapter 4. The applicability of outcrop organic geochemistry. -----	29
Chapter 5. Geochemical well correlation of the Bowland Shale. -----	44
Chapter 6. Palaeoceanography of the Bowland Shale. -----	74
Chapter 7. Selecting an analogue for the Bowland Shale. -----	98
Chapter 8. Discussion -----	132
Chapter 9. Conclusions -----	144
References -----	150

Abstract

Natural gas is needed and used by the global population to minimise our reliance on coal powered electricity generation. Gas is also used to manufacture hydrocarbon-based products such as fertilizers, fabrics and pharmaceuticals. Gas can be extracted from low permeability “unconventional” systems, where laterally extensive beds enriched in hydrocarbons (“sweet spots”) are targeted for hydraulic fracturing. Mudstone dominated formations require complex techniques such as geochemistry to identify sweet spots. This study investigates the recent unconventional target, the Bowland Shale Formation in the Bowland Basin, Lancashire (UK), as a case study and as a promising target for gas production. As a case study, we use the Bowland Shale Formation to investigate the applicability of outcrop organic geochemistry to exploration (Chapter 4). The Bowland Shale Formation is also used as a case study to investigate key stratigraphic boundaries (e.g. highstands) that are globally recognised hydrocarbon targets and are used for targeting directional drilling (Chapter 5). As a target for natural gas, the palaeoceanography of the Bowland Shale Formation in the Bowland Basin is investigated to interpret organic matter burial, spatially across the basin (Chapter 6), and to select a suitable analogue (Chapter 7). This requires a multi-disciplinary approach using geochemistry (X-ray diffraction, X-ray fluorescence, Rock-Eval pyrolysis, molecular analysis and organic carbon isotopic analysis); sedimentology (logging and scanning electron microscopy); biostratigraphy and computational statistical modelling. We find that outcrop-derived total organic carbon and extractable organic matter contents are not representative of subsurface exploration cores from the same formation; X-ray fluorescence (redox sensitive Mo and U) and Rock-Eval pyrolysis (oil saturation index) can be used to identify highstands; the Upper Mississippian Bowland Basin was anoxic in the centre as well as at the basin margin and that the Barnett Shale is a suitable palaeoceanographic analogue to the Upper Mississippian Bowland Shale Formation.

Chapter 1. Introduction

Worldwide energy demand is growing (EU 2011; Salameh 2003).

However, in recent years, so too is the scientific understanding and public awareness of risks and repercussions associated with energy supply. This consequently influences politics. For example, the “NERC Centre for Doctoral Training Oil and Gas” funding for this project was a consequence of a heightened UK blackout risk in March 2013 (e.g. Huppert 2013). In 2011, the European Union recognised that a transition from coal powered electricity generation was desirable, but also achievable using natural gas (EU 2011). This EU report highlighted the need for “unconventional” sources of natural gas (EU 2011). This refers to the process of extracting hydrocarbons, typically gas, directly from a mudstone/shale source rock, requiring the use of an engineering technique called hydraulic fracturing, fracking or fracing. In the same year, the first UK onshore unconventional production well was hydraulically fractured by Cuadrilla Resources (De Pater 2011) and in 2014, the UK Government planned to go “all out for shale” (Withnall 2014). However, also in 2014, the UK Government acknowledged that people had “uncertainties and worries and concerns” about the ever-growing UK shale gas industry (Press Association 2014).

In 2015, this Newcastle University project began with the aim of better understanding UK shale gas exploration targets, such as the Bowland Shale Formation (as well as upper and lower informal subdivisions), from a geological and geochemical perspective. The aim was to integrate large scale (geology) and small scale (geochemistry) systems in this relatively unexplored target with direct implications for industry and academia. Public opinion is mixed with regards to the development of a UK shale gas industry (Murray 2015). However, opponents suggest that environmental risks associated with shale gas production are too high (Vickerstaff 2019). Some academic critics express concerns over resource size estimates (Whitelaw et al. 2019). However, the geological uncertainty related to any

previously unexplored petroleum target is high and therefore the true extractable gas volumes cannot be known until post-production.

Resource estimation of an unexplored basin is a global fundamental uncertainty associated with petroleum exploration (McGlade et al. 2013), therefore the outputs of this project are not confined to the UK. Minimising risk can be achieved by developing the geological, geochemical and geophysical knowledge of an area. For example, the best geological models manage uncertainty, but aim to synthesise the large and small scale (geophysical, geological and geochemical) using the available data (Craigie 2018). For the relatively unexplored Bowland Shale Formation target, this project uses production and exploration drillcores from Preese Hall-1 and Beconsall-1Z, spudded on 16th August 2010 and 23rd August 2011, respectively. This permitted a real-world opportunity to actively minimise geological uncertainty and subsurface risk during exploration. Limited available cores from this formation promotes the use of a myriad complex techniques for elemental (X-ray fluorescence), mineralogical (X-ray diffraction), textural (scanning electron microscopy), isotopic ($\delta^{13}\text{C}_{\text{org}}$) and molecular (Rock-Eval pyrolysis, gas chromatography / mass spectrometry and gas chromatography / flame ionised detection) analyses that are integrated with sedimentology, computational models and previous petrophysical / geophysical data.

These analyses are used to investigate the applicability of outcrop organic geochemistry (Chapter 4); correlate wells for improved play fairway analysis and directional drilling (Chapter 5); analyse the processes related to organic matter (OM) burial / preservation in the Bowland Shale Formation (Chapter 6) and identify a suitable palaeoceanographic analogue to this UK shale gas target (Chapter 7). Figure 1 illustrates the structure of this thesis and the rationale for each major chapter is listed below:

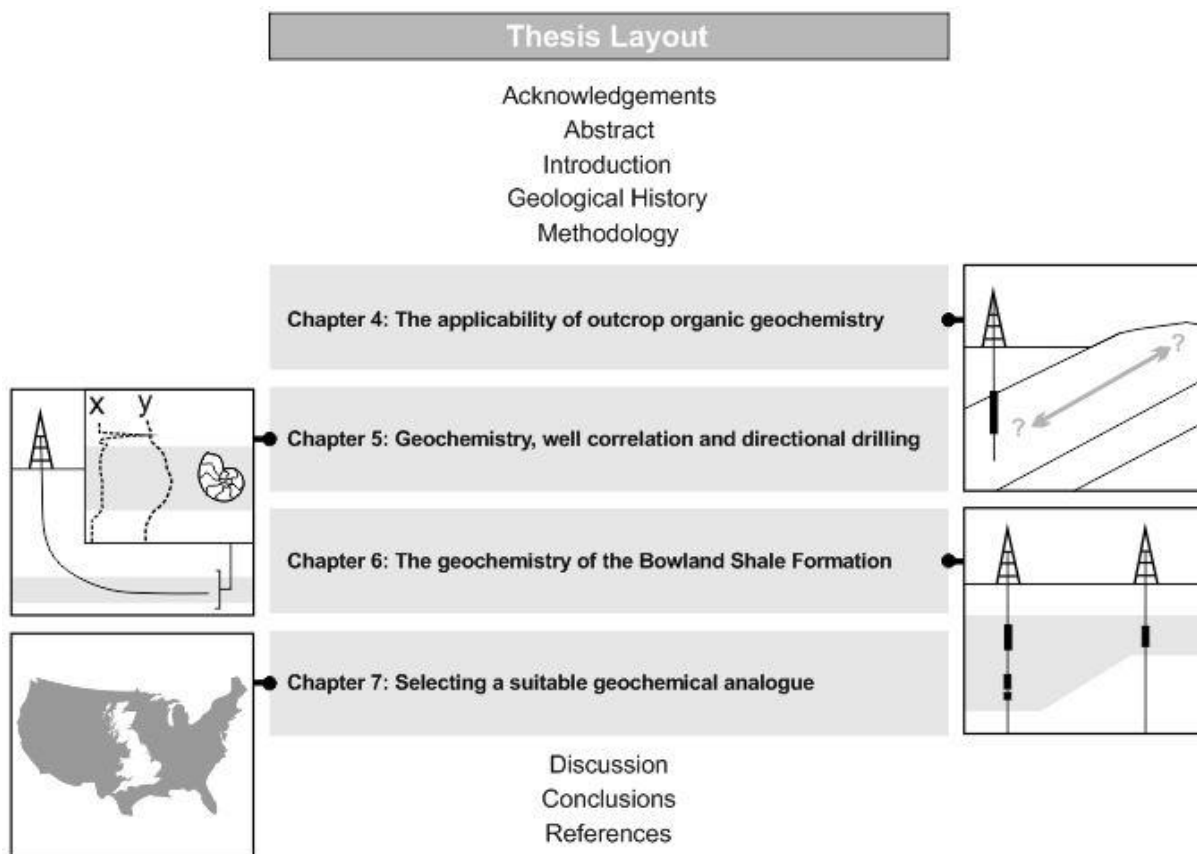


Figure 1: Outline and structure of thesis.

Chapter 4: The applicability of outcrop geochemistry in the Bowland Shale Formation.

In an unexplored basin, limited subsurface core material increases reliance on surface outcrop data, despite differences in thermal maturation history and weathering. For example, weathering is known to obscure pyrolysis-derived organic geochemical proxies (e.g. elevated oxygen index) needed for palaeoenvironmental reconstructions and

resource estimates (Emmings et al. 2017). Therefore, pyrolysis data of outcrop OM should be treated with caution in the Bowland Shale Formation. However, the effectiveness of more complex molecular analyses has not been previously investigated.

Chapter 4 uses molecular analysis to investigate the potential of using outcrop OM to supplement subsurface exploration core-derived organic geochemistry in unexplored formations, such as the Bowland Shale Formation. A secondary aim of this chapter highlights the challenges of investigating mature OM. Chapter 4 underscores the importance of the multi-disciplinary approach used in Chapters 5, 6 and 7.

Chapter 5: Geochemical well correlation in the upper Bowland Shale Formation

In mudstone dominated formations, stratigraphic intervals that are enriched in hydrocarbons (“sweet spots”) are typically good targets for hydraulic fracturing (Hashmy et al. 2012; Strickland et al. 2011). Therefore, it is important to identify laterally extensive target beds using core material. Subsurface stratigraphic navigation in mudstone successions is important for directional drilling as well as sweet spot discrimination. However, in mudstone successions, such as the Bowland Shale Formation, the identification of key stratigraphic layers is reliant upon petrophysics (gamma ray well ‘spikes’) and fossil abundance (Clarke et al. 2018; Riley 1993).

Therefore, this chapter introduces new proxies for improved well correlation in relatively unexplored shale gas targets, using organic and trace metal geochemistry. The upper Bowland Shale is used as a case study.

Chapter 6: Palaeoceanography of the Bowland Shale Formation (Mississippian, Carboniferous): a shale gas target.

Palaeoceanographic interpretations of source rocks are important because depositional environments and bottom water processes are linked to OM burial and preservation, which is essential for an economic source rock.

Therefore, it is crucial that the provenance, deposition and eogenesis of mudstone dominated target formations, such as the upper Bowland Shale, are understood.

Chapter 6 investigates the geology and geochemistry of the upper Bowland Shale and interprets Upper Mississippian Bowland Basin palaeoceanography. This chapter is crucial to the future of UK shale gas exploration and appraisal.

Chapter 7: Selecting an analogue for the Bowland Shale Formation using geochemistry.

Analogue studies are important to supplement well and core data in relatively unexplored basins and formations. For example, the well-explored Barnett Shale Formation is typically compared to the relatively unexplored upper Bowland Shale Formation because they were both deposited during the Mississippian (Andrews 2013b). However, the applicability of this analogue comparison is not extensively discussed in the literature.

An identical analogue is unattainable because no two formations/basins are indistinguishable. Formations that were deposited during different times and in different global positions (Blakey 2008) are typically expected to have different geochemical properties, particularly in organic matter (Craigie 2018; Peters et al. 2005). Therefore, geochemical analogue comparisons should be used with caution. However, attempts should still be made to minimise the subsurface risk of unexplored targets.

Therefore, Chapter 7 compares the elemental geochemistry of three Carboniferous formations (the upper Bowland, Barnett and Bakken shales) to select a suitable palaeoceanographic analogue for the upper Bowland Shale. One older formation (Mid-Devonian Marcellus Shale) is also compared to investigate the relative importance of basin morphology and a secondary aim of this chapter investigates the relative importance of time series and basin morphology in analogue selection.

Chemostratigraphy and sequence stratigraphy approaches are used extensively in this project. Therefore, it is important to provide a general introduction to chemostratigraphy and sequence stratigraphy in a mudstone context.

Chemostratigraphy and Sequence Stratigraphy in Mudstones

The geological uncertainty of an area or play can be minimised using a multi-proxy, multi-scale analysis that integrates large scale geological processes with geochemistry. Geochemistry is important because the constituents (elements and minerals) of any bed, member, formation and succession etc. can provide key insights into local and/or regional geological processes. As geochemical techniques become increasingly more precise and commonplace, the elemental and mineralogical make-up of a rock can be used to develop large scale interpretations and resource estimates (Craigie 2018). This approach leads to challenges linked to accurately interpreting the geochemistry of a rock with respect to sediment provenance, deposition and post-deposition. Therefore, the integration of geochemical techniques (e.g. chemostratigraphy using XRF) and large scale geological observations (e.g. sequence stratigraphy) are dependent upon accurate up-scaling. These challenges can be minimised by simultaneously using geochemistry to interpret basin-wide and/or regional processes and by using the large scale to direct appropriate geochemical interpretations (Craigie 2018).

Basin-wide and regional scale sediment deposition with respect to time and space can be interpreted using sequence stratigraphy (e.g. Posamentier et al. 1988). Sequence stratigraphy is a method of interpreting successions using a geometric framework associated with relative changes in sea level (e.g. Martinsen et al. 1995). This is most attainable where the contrast between different, well preserved depositional environments and strata are distinct (Davies and Elliott 1996; Davies and McLean 1996). For example, conventional systems typically show a distinct sequence of rock types (interbedded mudstones and

sandstones) that represent different stages and rates of basin infill and/or sediment accumulation (for more detail, see Posamentier et al. 1988). However, in unconventional systems, changes in regional relative sea level through time are not always apparent in terms of observable sedimentology (Clarke et al. 2018; Craigie 2018). Therefore, geochemical techniques are used to minimise knowledge gaps. However, Craigie 2018 also suggests that in this scenario it can be challenging to decipher the exact relationship between a geochemical observation and a sequence stratigraphic interpretation. Therefore, it is important to understand mudstone sequence stratigraphy, mudstone chemostratigraphy and how the two relate.

For example, Posamentier and Vail (1988) illustrate how the geometries of different systems tracts (ST) represent the products of deposition at different relative sea levels. This includes the Falling Stage ST (relative fall in sea level), Transgressive ST (shoreline retreats landward) and Highstand ST (sediment accumulation exceeds the rate of relative sea level rise), the base of the latter is formed by the maximum flooding surface (for more detail, see Posamentier and Allen 1999). However, in a prodeltaic depositional setting (a typical unconventional target) these changes in relative sea level with respect to sediment deposition are less distinct than in a typical conventional system (Clarke et al. 2018; Reading 2009).

Relative sequence stratigraphic interpretations and systems tracts can be used to predict lateral geometries. However, in mudstones, some authors (Emery and Myers 2009) suggest that the relativity, innate to the sequence stratigraphic method, may limit the applicability of sequence stratigraphy in source rock prediction or geochemistry. For example, sequence stratigraphy alone cannot be used to predict source rock hydrocarbon yield potential, especially in unconventional plays and general sequence stratigraphy rules-of-thumb can mislead interpretations in mudstone dominated formations (Emery and Myers 2009). Is it possible that the quantitative and the qualitative nature of geochemistry and

sequence stratigraphy, respectively, introduces challenges during integration? A fully synthesised sequence stratigraphic and geochemical model that accounts for regional scale as well as local changes in mudstone depositional processes is desirable, but this is currently a fundamental uncertainty.

Therefore, other techniques such as chemostratigraphy, biostratigraphy and petrophysics (e.g. gamma ray well logs), are typically used to identify key stratigraphic boundaries in mudstones (e.g. Clarke et al. 2018; Craigie 2018). The method broadly called chemostratigraphy identifies differences between rock types and stratigraphic boundaries using chemistry (Craigie 2018). This can involve a suite of techniques, but typically includes elemental analyses (Craigie 2018). Other techniques include isotopic analyses, but chemostratigraphic correlation crucially relies upon the contextualisation of geochemistry with respect to rock type, therefore chemostratigraphy is not limited to inorganic geochemistry (Craigie 2018). Some unconventional petroleum plays may be more dependent upon chemostratigraphic correlation than others. For example, biostratigraphic correlation is limited in the Bowland Shale Formation (Clarke et al. 2018) and therefore other techniques (e.g. sedimentology and biostratigraphy) must supplement these data to minimise subsurface uncertainty and improve the levels of confidence associated with one technique used in isolation.

Chemostratigraphy is a powerful method and it can be used to understand differences up succession in a mudstone dominated formation (Craigie 2018). For example, provenance determination cross-plots (e.g. Roser and Korsch 1988) can use relative abundances of Al, K, Mg, Zr and Ti to investigate the provenance of a rock. However, it is important not to over-interpret provenance plots that incorporate numerous elements because sorting, transportation, reworking and diagenesis can also influence the observed geochemistry (e.g. Craigie 2018). For example, Ti-bearing heavy minerals are relatively more resistant to physical and/or chemical weathering than most Na, Mg or K-bearing minerals (Craigie 2018).

Therefore, other elemental proxies must also be used alongside provenance plots.

Elemental abundances of U, Mo, Zn, Ni, Cu, Co and Zn (for example) can be used to identify zones with high TOC and elemental abundances of Mo, Zn, Ni, Cu, Co and V are proven to have links to palaeoenvironmental anoxia (e.g. Craigie 2018; Jones and Manning 1994). However, these are examples and may not always hold true in every scenario (Craigie 2015) and the driving factors that control these elemental abundances, related to anoxia, differ. For example, the water-sediment transportation of Mo relies upon the presence of thiomolybdate shuttles whereas the same process for U can be aided by the presence of organo-metallic compounds (Calvert and Pedersen 1993; Tribovillard et al. 2006) and is not reliant upon thiomolybdate shuttles. Furthermore, changes in sedimentary provenance and/or detrital input can control the changes in geochemistry and it is important not to confuse changes in provenance with changes in palaeoceanography (e.g. anoxia). For these reasons, this thesis explores basin-scale geometries and sedimentology prior to palaeoceanographic analyses.

Chapter 2. Geological History

Stratigraphy

Before 2009, the Bowland Shale Formation had group status (e.g. Aitkenhead 1992), however, it is currently situated within the Craven Group (Waters et al. 2009). The Bowland Shale Formation was deposited within the Bowland Basin (Figure 2) during the Mississippian (Waters et al. 2009). It is difficult to interpret Bowland Shale Formation stratigraphy in terms of members because the succession is mudstone dominated (Waters et al. 2011; Waters et al. 2009). However, some authors informally subdivide the succession into the lower (Middle Mississippian) and upper (Upper Mississippian) Bowland Shale Formation (Aitkenhead 1992; Clarke et al. 2018; Hennissen and Gent 2019) based on increased carbonate content in the lower Bowland Shale and biostratigraphy. For example, the base of highstand E_1A_1 , identified by goniatite fossil *Emstites leion*, marks the base of the upper Bowland Shale Formation (Andrews 2013b; Clarke et al. 2018; Riley 1993).

In Clitheroe, the Lancaster Fells and the Beconsall-1Z well (Figure 2), the base of the Bowland Shale Formation is marked by the top of the Pendleside Limestone (Clarke et al. 2018). However, the base of the lower Bowland Shale Formation was not cored in the Bowland Basin Preese Hall-1 well (Figure 2), therefore the stratigraphy below the Bowland Shale Formation here is uncertain (Clarke et al. 2018). The top of the Bowland Shale Formation is marked by the base of members of other formations, such as the Mam Tor Sandstone Member and Pendle Grit Member in Yorkshire and Lancashire or the Cren-y-Feow Formation in Merseyside (Earp et al. 1961; Fewtrell et al. 1981a).

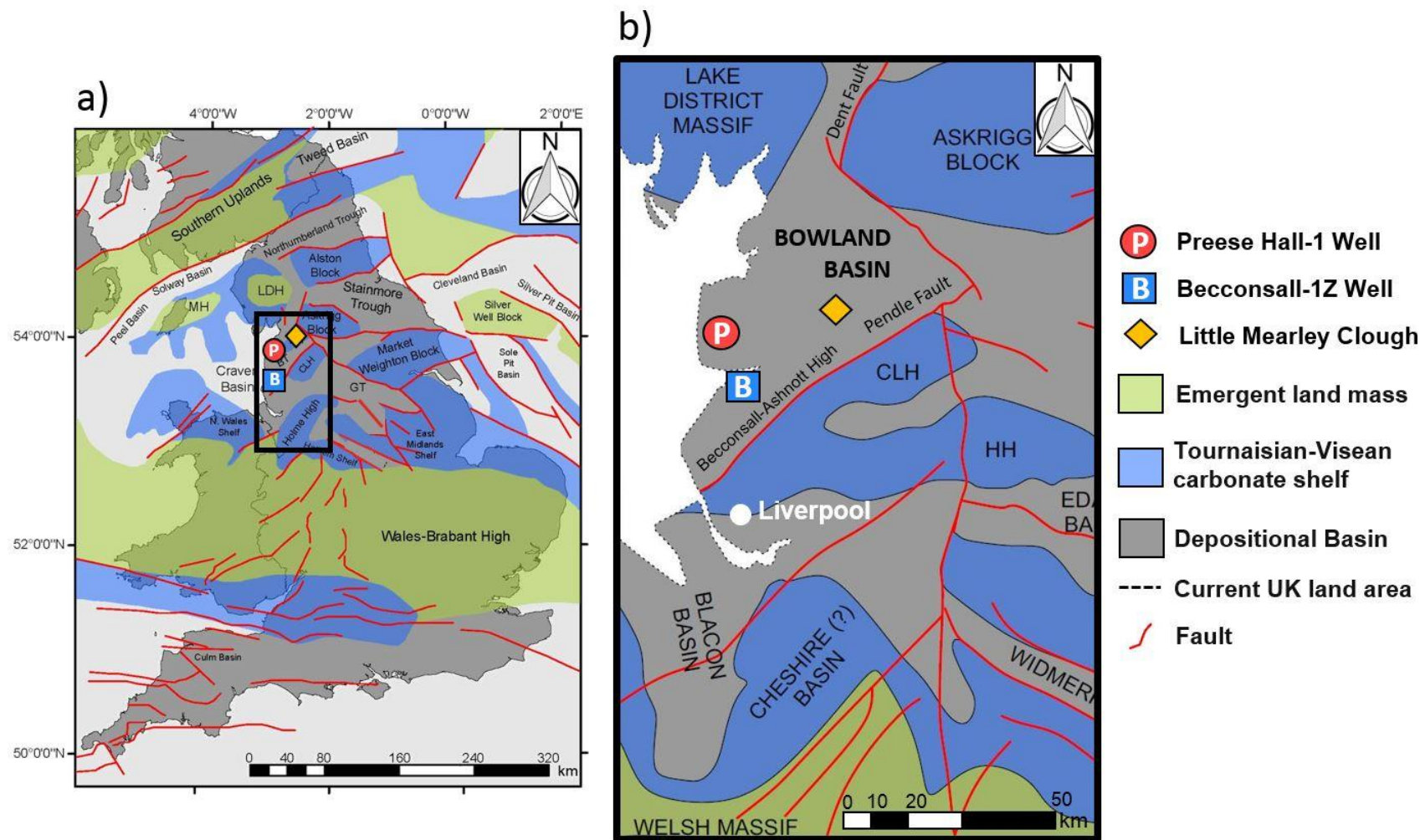


Figure 2: a) The palaeogeography of England and Wales. Major faults separate extensional basins and platforms (adapted from Waters et al. 2009). BH = Bowland High; BT = Bowland Trough; CLH = Central Lancashire High; DH = Derbyshire High; EG = Edale Gulf; GT = Gainsborough Trough; LDH = Lake District High; Manx High; WG = Widmerpool Gulf. b) Early Carboniferous palaeogeography including basins and platforms (adapted from Fraser and Gawthorpe 2003) and Becconsall-Ashnott High (Clarke et al. 2018). Presence of the Permo-Triassic Cheshire Basin (Smith et al. 2005 cf.; Waters et al. 2009) and Humber Basin (Hodge 2003; Kent 1966) are controversial (Andrews et al. 2012).

In the Bowland Shale Formation, key stratigraphic boundaries are typically identified using biostratigraphy and changes in the gamma ray log signal (Andrews 2013b; Clarke et al. 2018; Davies and McLean 1996). These techniques are also used to recognise key stratigraphic surfaces within the upper and lower Bowland Shale Formation, such as glacio-eustatic highstands which are also identified using goniatite index fossils (Bhattacharya 1993; Church and Gawthorpe 1994; Davies and McLean 1996; Dunham and Wilson 1985; Hampson et al. 1997; Isbell et al. 2003; Martinsen et al. 1995; Read et al. 1991). Beds that are enriched with goniatite index fossils are sometimes called 'marine bands' because they are suggested to represent a period of deposition related to high relative sea level (Holdsworth and Collinson 1988; Martinsen 1990). Marine bands typically, but not always, contain increased total organic carbon (TOC) and can correlate to spectral gamma ray spikes (Clarke et al. 2018; Davies and Elliott 1996; Davies and McLean 1996) and this makes them useful during directional drilling and as hydrocarbon sweet spots (Clarke et al. 2018).

Therefore, marine band E₁B₂, identified using goniatite index fossil *Tumulites pseudobilingue*, is used to correlate Beconsall-1Z (53° 41' 58.6291" N, 2° 53' 57.3813"; BGS reference number SD42SW/11) and Preese Hall-1 (53° 49' 19.006" N; 2° 56' 56.576"; BGS reference number SD33NE/38) (Figure 2; Clarke et al. 2018). Additionally, marine band E₁A₁ and goniatite fossil *Emstites leion* is used in Preese Hall-1 to identify the base of the upper Bowland Shale, but this was not identified in Beconsall-1Z (Clarke et al. 2018). Marine bands should be distinguished from barren sediment (sediment without goniatite index fossils) which can overlie and underlie marine bands (Gross et al. 2015). Additionally, marine bands should not be confused with 'marine band cycles' which represent glacio-eustatic cycles (Gross et al. 2015; Martinsen 1990; Martinsen et al. 1995; Waters and Condon 2012).

Controls on Bowland Basin Stratigraphy

The Craven Group (within which the Bowland Shale Formation sits) overlies the Bowland High Group (Andrews et al. 2012). The Bowland High Group was deposited during the initial phase of basin rifting (Hudson 1944; Arthurton et al. 1988). These older 'limestones-with-mudstones' are deeply buried and relatively unexplored with limited surface exposure (Andrews et al. 2012), but geophysical models suggest that this unit could be more than 3000 m thick (Arthurton et al. 1988). The lower Craven Group is suggested to comprise of syn-rift sediments (Andrews et al. 2012).

The lower Bowland Shale Formation is a mudstone dominated carbonate-rich succession within the Craven Group which laterally passes into age-equivalent limestones (Andrews et al. 2012; Clarke et al. 2018). It is suggested that deposition of the lower Bowland Shale Formation occurred during regional syn-rift processes in the basin (Andrews et al. 2012). However, sedimentation is suggested to be controlled by numerous other factors such as fluctuating sea levels, climate change and carbonate ramp growth at the perimeter of the basin (Arthurton et al. 1988; Andrews et al. 2012; Clarke et al. 2018). The relative importance of each factor is not certain. However, tectonic subsidence is not the singular or overriding control on Bowland Basin sedimentation in the upper or lower Bowland Shale Formation (Arthurton et al. 1988; Andrews et al. 2012). Therefore, chemostratigraphy is an applicable method of analyses in these circumstances and can be interpreted with respect to sedimentation and sea level changes.

The upper Bowland Shale Formation differs from the lower unit with respect to sedimentology because the beds are more laterally continuous in the upper unit (Andrews et al. 2012; Clarke et al. 2018). During the Upper Mississippian, the carbonate highs surrounding the basin were drowned (Andrews et al. 2012) which suggests that the Bowland Basin was more connected to adjacent basins in the Upper Mississippian, relative to the Middle Mississippian. Gradational increases in grain size at

the top of the Bowland Shale Formation transitions into the overlying Millstone Grit Group, associated with increased sediment supply from the north (Andrews et al. 2012).

Bowland Basin Structure and Development

In terms of palaeogeographical location, Beconsall-1Z is located towards the southern margin of the Bowland Basin and Preese Hall-1 is in the centre (Figure 2). The upper Bowland Shale Formation is 84 m thick in Beconsall-1Z and 499 m thick in Preese Hall-1 (Clarke et al. 2018).

The Bowland Basin was formed by the reactivation of normal faults during the closure of the Rheic Ocean (Clarke et al. 2018; Fraser and Gawthorpe 2003; Guion et al. 2000; Timmerman et al. 2009) linked to Mississippian crustal extension (Corfield et al. 1995; Leeder 1988b). Faults bound the Bowland Basin with the Southern Lake District High and Askrigg-Bowland High to the north and Central Pennine High to the south east (Gawthorpe and Clemmy 1987; Hough et al. 2014b; Figure 2). The Craven Fault System and Pendle Lineament bound the basin in the north and south east, respectively (Fraser and Gawthorpe 1990; Leeder 1982, 1988b; Worthington and Walsh 2011). North east-south west trending folds are the products of Variscan orogenic compression (Arthurton 1983, 1984; Corfield et al. 1996). Authors disagree on the relationship between the Beconsall and Ashnott highs to the south which are suggested to be topographically separate by some (Emmings et al. 2019b) and linked by others (Clarke et al. 2018).

The upper Bowland Shale Formation was deposited in the Bowland Basin via turbidite and hemipelagic sedimentation (Aitkenhead 1992; Andrews 2013b; Bisat 1924; Clarke et al. 2018; Smith et al. 2005). Previous work has used sedimentology (e.g. flow direction indicators) to suggest that primary sedimentation is sourced from the north, associated with the prograding and overlying Pendleside Sandstone Member of the Millstone Grit Group (Bisat 1924; Collinson 1968, 1969; Collinson et al. 1988; Fraser and Gawthorpe 2003; Holdsworth and Collinson 1988; Ramsbottom et al. 1978; Walker 1966).

Bowland Shale Formation Sedimentation, Sequence Stratigraphy and Chemostratigraphy

The relationship between sedimentation, sequence stratigraphy and chemostratigraphy is complex, varied and interconnected. Therefore, interpreting the geochemistry of the Bowland Shale Formation relies on an understanding of how sediment deposition influences geochemistry and the importance of regional processes during sedimentation. In any geochemical study, this should be determined prior to further geochemical analyses to prevent misinterpretation (Craigie 2018). However, this cannot always be practicably achieved with full certainty, particularly with respect to the dynamic, ancient and unexplored system of the Bowland Basin.

For example, differences in ocean connectivity in the lower and upper Bowland Shale, evident from the sedimentology (Andrews et al. 2012; Clarke et al. 2018) change how the geochemistry of each unit should be interpreted. Tribovillard et al. (2012) shows how differences in Mo and U abundances are linked to increased and/or sustained water column stratification in an open or connected system. Therefore, to integrate geochemistry with Bowland Basin stratigraphy it is important to recognise that the Mo/U relationship is applicable to the upper Bowland Shale, but perhaps not to lower unit. Correctly employing the Mo/U relationship is important because OM preservation is dependent upon specific palaeoenvironmental parameters, such as low oxygen (e.g. Peters and Moldowan 2005; Killips and Killips 2013).

To ensure that observed abundances of redox sensitive elements such as Mo and U are accurately interpreted with respect to oceanic redox states through time, it is important to prove that sedimentary input is not the control on their abundance (Craigie 2018). Heavy metal input proxies such as Zr and Ti can, in part, guide interpretations of sediment input (e.g. Craigie 2018). If the abundance of Zr and Ti (and other detrital proxies) in a mudstone formation does not change up succession, then it can be typically assumed that heavy metal input (and possibly sedimentation)

was relatively constant. Aluminium is predominantly associated with clay minerals and therefore Al can be used as a comparison standard for clay mineral abundance (Craigie 2018). These are examples, and geochemical correlation is limited only by available elemental abundances and the applicability of elements or elemental ratios. However, the upper Bowland Shale Formation has not been studied in detail with respect to geochemistry.

Therefore, each chapter of this thesis investigates the large scale influences of sedimentary input and structures before focussing further on the geochemistry. The investigation of Bowland Shale Formation geochemistry is reliant upon an understanding of the controls on sequence stratigraphy. For example, previous studies (e.g. Gross et al. 2015) have aimed to investigate possible links between geochemistry and sea level changes throughout the Bowland Shale Formation. Gross et al. (2015) suggest that the geochemistry of marine band cycles can be related to changes in palaeobathymetry and chemocline, indicating that marine band beds are the products of an increased rate of sea level change and/or a highstand. Sea level changes are suggested to be a driving factor of sedimentation within the Bowland Shale Formation (Gross et al. 2015). However, previous studies do not investigate the Bowland Basin; they primarily focus on marine band cycles and have not focussed on specific marine band beds. Crucially, this thesis fills these knowledge gaps. We investigate the relevance, applicability and limitations of the sequence stratigraphic-geochemical relationship, when applied to thin beds studied in high resolution. We achieve this by studying both the marine band beds (Chapter 4 and Chapter 5) and the Bowland Shale Formation as a whole (Chapter 6 and Chapter 7).

Palaeoclimate

The current consensus suggest that Britain was south of the equator at $\sim 5 - 10^\circ$ S during the Mississippian (Aitkenhead 1992; Cocks and Torsvik 2006; Scotese and McKerrow 1990; Woodcock and Strachan 2012). At this time, glacial influenced cyclicity is considered by some authors to be a

major control on Bowland Basin sea level fluctuation and sedimentation (Andrews 2013a). However, the influence and extent of Carboniferous glaciation is controversial. For example, some authors suggest that sedimentation was not influenced by glacio-eustatic cyclicity during the Lower and Middle Mississippian (Ramsbottom 1979). Conflicting theories likely stem from the lack of exposed Carboniferous sediments and structures.

Burial History

The thermal maturity of the Bowland Shale Formation is related to burial depth, time and heat flow, however the complicated tectogenesis/ uplift increases the reliance upon computational models (Andrews 2013b). These thermal depositional models suggest that the upper Bowland Shale Formation in Beconsall-1Z and Preese Hall-1 were buried to c. 5000 m before the Variscan inversion with a maximum burial depth of 5700 m in the Late Cretaceous (Andrews 2013a). Thermal maturity varies spatially across the Bowland Basin (Clarke et al. 2018), however limited surface exposure obscures the relationship between outcrop and core burial history interpretations.

Chapter 3. Methodology

Beaconsall-1Z, Preese Hall-1 and Marine Band E₁B₂

Mississippian marine band E₁B₂ (e.g. Waters et al. 2009) was previously identified in Beaconsall-1Z and Preese Hall-1 using the crushed, thick-shelled goniatite index fossil *Tumulites pseudobilingue* within the upper Bowland Shale Formation (Bisat 1922; Clarke et al. 2018; Hird and Clarke 2012; Hird et al. 2012; Horn 1960). Marine bands such as E₁B₂ are typically also associated with enrichments in saline fauna (Holdsworth and Collinson 1988; Ramsbottom et al. 1962). The bases of marine bands are transitions from underlying barren sediment overlain by mudstones containing gradationally increasing saline fauna (Holdsworth and Collinson 1988; Ramsbottom et al. 1962). Their centres are enriched in thick-shelled goniatite index species (e.g. *Tumulites pseudobilingue*), this is sometimes called the 'goniatite phase' (Holdsworth and Collinson 1988; Martinsen 1993; Ramsbottom et al. 1962). However, this phase could also be described as the 'minimum observed goniatite phase thickness' to account for post-depositional erosion as well as sampling and/or preservation bias. This phase is typically overlain by progressively less saline fauna (Holdsworth and Collinson 1988; Martinsen 1993; Ramsbottom et al. 1962). The tops of marine bands are gradational transitions to overlying barren sediment (Holdsworth and Collinson 1988; Martinsen 1993; Ramsbottom et al. 1962). Therefore, in this current study: (i) Zone 1 represents sediment below the thick-shelled goniatite phase (ii) Zone 2 represents goniatite phase sediments (marine band), and (iii) Zone 3 represents sediments above the thick-shelled goniatite phase. In Chapter 5, results are given with reference to zones.

At Beaconsall-1Z, the upper Bowland Shale Formation is 84 m thick (Hird et al. 2012). Depth ranges for *Tumulites pseudobilingue* identification were 2140.91 m (top) and 2142.59 m (base) (Clarke et al. 2018; Hird et al. 2012). Therefore, the E₁B₂ goniatite phase at Beaconsall-1Z is 168 cm.

At Preese Hall-1, the upper Bowland Shale Formation is 499 m thick (Clarke et al. 2018; Hird and Clarke 2012). At Preese Hall-1, depth ranges for *Tumulites pseudobilingue* identification were 2081.75 m (top) and 2081.81 m (base) (Hird and Clarke 2012). Therefore, the minimum thickness of the E₁B₂ goniatite phase at Preese Hall-1 is 6 cm.

Both cores were logged and sampled at high resolution (~10 cm intervals avoiding fractures) up succession through cored Mississippian marine band E₁B₂. All 20 g samples were cleaned thoroughly with a wire brush, dichloromethane and methanol to remove natural and/or artificial contaminants. Samples were crushed to a powder, homogenised and sub-sampled for multi-proxy comparisons. Different techniques use the same samples, however limited sampling availability forced lower sampling resolutions for some techniques (e.g. stable isotope geochemistry). Significant differences between cores were determined using two-sample T-tests. For accuracy, ratio errors consider the magnitude of propagated error (Holmes and Buhr 2007).

A high resolution sampling approach was selected for this study to better identify compositional differences indicative of a marine band across thin beds and many stratigraphic boundaries within, typically found in mudstones (Craigie 2018). Biostratigraphic correlation was relatively limited in Bowland Shale Formation cores in comparison the goniatite fossil abundance in outcrops of County Clare Basin (Davies and Elliott 1996). However, a combination of different disciplines (e.g. biostratigraphy and geochemistry) at high resolution is the best approach, with adequate attention to the expression of uncertainty during interpretation. Additionally, this project treated geochemical interpretations with caution, using more than one proxy to support any interpretation.

X-ray Fluorescence

Collected, cleaned and crushed core samples were run using X-ray fluorescence (XRF) with a SPECTROSCOUT ED-XRF machine (Chemostrat, Welshpool Laboratory). Elements were analysed using XRF over

Inductively Couple Plasma Optical Emission Spectrometry (ICP-OES) or Inductively Coupled Plasma Mass Spectrometry (ICP-MS) due to cost and time efficiency. This current study did not aim to investigate the effectiveness of these different elemental analysers, but XRF was selected to produce less expensive results, more rapidly than ICP analyses based on previous studies (Craigie 2018). However, previous studies have proven that XRF is not accurately responsive to sodium (Na) (Kawai et al. 1998). Therefore, in this current study, Na analyses and interpretations are expressed with caution, if at all. Furthermore, using XRF, we recorded the oxides (Chemostrat, Welshpool) and did not record the “fundamental parameters” such as oxygen. Therefore, the sum of all elements for each sample was not 100%.

The elemental geochemistry of 86 sub-samples (43 from Beconsall-1Z and 43 from Preese Hall-1 with an interval frequency c. 10 cm) were run using XRF. Powdered and homogenised sub-samples (4 g) were mounted and packed down to the bottom of a sample cup (without a binder) to minimise void space (homogenous sample). Internal reference standards were analysed every 10 samples to correct for machine drift (Chemostrat, Welshpool). Elemental analyses closely mirrored steps outlined by Craigie (2018). 6 control samples were run alongside for error from one bulk core sample.

Rock-Eval Pyrolysis

Sub-samples used for pyrolysis totalled 44 from Preese Hall-1, 43 from Beconsall-1Z and 33 from outcrops (Little Mearley Clough) with an interval frequency of c. 10 cm. All sub-samples were crushed, homogenised and sieved (250 µm) and then analysed using a Rock-Eval(6) analyser (British Geological Survey) configured in standard mode (Behar et al. 2001; Newell et al. 2016; Slowakiewicz et al. 2015). Dry sub-samples (60 mg) were heated and held at 300 °C for 3 minutes and then heated from 300 to 650 °C. These were then held for 3 minutes at 25 °C/min. Hydrocarbons that were released during this two-stage pyrolysis were measured using a flame ionization detector (FID). The amount of

free hydrocarbons (S1) and the amount of hydrocarbons generated from thermal cracking (S2) contribute to other proxies such as oil saturation index and production index (e.g. Killops and Killops 2013). Low S1 and S2 values in some Bowland Shale studies (e.g. Clarke et al. 2018) can obscure these proxies and therefore this study uses S1 and S2 derived proxies with caution to avoid misinterpretation related to bimodal program peaks (Killops and Killops 2013). The T_{max} was calculated from the T_{peak} S2 - 37 °C (Behar et al. 2001). Instrument quality was checked every 10 samples against the accepted values of the Institut Français du Pétrole (IFP) standard. We recognised that the strength of the RockEval and XRF techniques used in this study relies upon an accurate expression of error. Therefore, the use of RockEval Pyrolysis data in this study utilised IFP analyses in the calculation of error (British Geological Survey Laboratory, Keyworth). 6 control sample errors and IFP data pertinent to run batches were used for error from one bulk core sample.

X-ray Diffraction

Twenty-four dry powdered sub-samples (8 from Preese Hall-1 and 16 from Beconsall-1Z), each 100 mg, were crushed and mounted onto an oblique cut and zero background silicon wafer which was levelled using a glass slide (Newcastle University). Sample frequency was c. 10 cm. Mounted samples were inserted into the diffractometer and data were collected over range 3-85° 2 θ with step size 0.0167° 2 θ .

Bulk fraction X-ray diffraction (XRD) analyses used a PANalytical X'Pert Pro MPD multi-purpose diffractometer (Newcastle University). This was powered by a Philips PW3040/60 X-ray generator that was fitted with an X'Celerator detector and copper anodes with 40 kV and 40 mA of current. The scanning X'Celerator detector (with a secondary graphite crystal monochromator in the diffracted beam path) used a nominal time step length of 500 seconds. Fixed divergence and anti-scatter slits (0.5° and 1°) were used together with a 10 mm beam mask. Soller slits were 0.04 radians. All diffractometer scans were run in continuous mode. All mineral phase identifications and interpretations used PANalytical High Score Plus[©]

with databases "ICDD Powder Diffraction File 2" (PANalytical 2004) and "ICDD Powder Diffraction File 4" (ICDD 2018) as well as open databases (Cambridge 2016). PANalytical High Score Plus[©] calculated a percentage abundance of relative mineralogical abundance and this can limit the accuracy when comparing between samples ("closed sum"). Therefore, this study uses caution in any interpretations of XRD and XRD is strictly used as a complimentary technique, therefore clay fraction processes were desirable, but not a necessity for this study. Limited core material and sample availability prevented triplicates of each sub-sample. Therefore, 4 control samples from one bulk core sample were run alongside for error.

Mineralogical data were processed using bulk fraction XRD in a Newcastle University laboratory by a technician primarily due to budget. This study used XRD to broadly understand the differences between core mineralogy up succession in a marine band to identify major differences. Clay fraction XRD may have shown more precise results, however we were limited by cost and instead used bulk fraction XRD as a broad indicator of mineralogy.

Organic Carbon Isotopic Analysis ($\delta^{13}\text{C}_{\text{org}}$)

Twenty-five 400 mg sub-samples (10 from Preese Hall-1 and 15 from Beconsall-1Z) were selected for organic carbon isotopic analyses ($\delta^{13}\text{C}_{\text{org}}$). This used Elemental Analyser Isotope Ratio Mass Spectrometry (EA-IRMS; Iso-Analytical Laboratory, Cheshire). Sub-samples were placed in 1 M of hydrochloric acid and left overnight to liberate inorganic carbon as CO_2 . Sub-samples were then neutralised using distilled water and dried ($60\text{ }^\circ\text{C}$). Sub-samples were heated using a furnace ($1000\text{ }^\circ\text{C}$) and combusted (c. $1700\text{ }^\circ\text{C}$) in an oxygen rich environment. Oxygen (O_2) was removed and NO_x was converted to N_2 by sweeping the gases through pure copper wires ($600\text{ }^\circ\text{C}$). A packed column gas chromatograph ($100\text{ }^\circ\text{C}$) separated CO_2 from N. A magnetic field separated different gas species of differing mass. Synchronous measurements were taken of CO_2 isotopomers at m/z 44, 45 and 46 using a collector array (Faraday cup).

Wheat flour ($\delta^{13}\text{C}_{\text{V-PDB}} = -26.43 \text{ ‰}$) was used as reference material (Iso-Analytical). Instrument quality control checks used beet sugar ($\delta^{13}\text{C}_{\text{V-PDB}} = -26.03 \text{ ‰}$), cane sugar ($\delta^{13}\text{C}_{\text{V-PDB}} = -11.64 \text{ ‰}$) and an International Atomic Energy Agency, Vienna, inter-laboratory comparison standard (IAEA-CH-6). Error was calculated using duplicates run every 5 samples and reference material.

Organic carbon isotopic analyses in this study are used with caution in relation to organic matter input and used alongside GC/MS analyses for improved confidence during interpretation. With regards isotopic processing, these analyses were outsourced to an external laboratory (Iso-Analytical Laboratory, Cheshire). These isotopic data and expressed errors are suitable for the purposes of this study. However, future isotopic analyses may choose to use compound-specific $\delta^{13}\text{C}$ analysis improved instrumental accuracy and reproducibility (for an extensive review, see Sherwood et al. 2007).

Gas Chromatography / Mass Spectrometry – Selective Ion Monitoring

Ninety-one sub-samples were analysed using gas chromatography / mass spectrometry (GC/MS). However, peak integration was attainable for just 42 sub-samples (15 in Preese Hall-1 and 27 in Becconsall-1Z).

Surface oxides and other contaminants were removed prior to analyses using dichloromethane and a wire brush before being powdered in a methanol-cleaned Team Mill. Samples passed through a 250 μm sieve, cleaned with dichloromethane and homogenised. The mill was cleaned thoroughly between each sample. Crushed powder (15 g) was placed into a pre-extracted, clean SoxtecTM (FOSS) based on TecatorTM Technology (SoxtecTM) thimble (33 x 80 mm) overlain with pre-extracted cotton wool. Thimbles were placed into a FOSS SoxtecTM 2050 with 130 ml of azeotrope of dichloromethane and methanol mix in each SoxtecTM glass jar (93 % dichloromethane and 7 % methanol) with activated copper and anti-bumping granules. SoxtecTM extraction ran for 4 hours and 20 minutes. Post-extraction, solvent was blown down (Rotovac Vario Power Unit) to 10

ml before 1 ml was removed and blown to dryness using nitrogen to weigh the extractable OM (EOM) on SALTER HA-180M scales. Thin layer chromatography (TLC), with filter paper cleaned with dichloromethane, for over 1 hr was used to separate aliphatic from aromatic fractions.

Petroleum ether was used as the solvent for thin layer chromatography. Aliphatic and aromatic fractions were scratched off and each eluted using 100 % petroleum ether and 50:50 petroleum ether: dichloromethane, respectively.

Internal standards included 5 μ l of p-Terphenyl and 20 μ l heptadecylcyclohexane for aromatics and aliphatic fractions respectively at concentrations 1 mg/ml. Samples were run using Agilent 7890 GC/MS with Mass Selective Detector (MSD). Integration software used Enhanced Data Analysis RTE integration parameters.

Triplicate and duplicates were for GC/MS unattainable due to (i) width of the core (ii) sample depth limitations associated with high resolution sampling (iii) Low EOM values. Therefore, 3 control sub-samples gave error estimates from one sample from Preese Hall-1.

Gas Chromatography / Flame Ionised Detection

The same solvent and OM mixtures that were run using GC/MS were analysed using Gas Chromatography/Flame Ionization Detector (GC/FID) HP5890 (Newcastle University). Additionally, 15 outcrop sub-samples from Little Mearley Clough (LMC) used GC/FID. Internal standards used 20 μ l heptadecylcyclohexane at concentrations 1 mg/ml. Additionally, 5 sub-samples (from one upper Bowland mudstone core sample) were used for error.

Similar to GC/MS analysis, low EOM and low abundances of pristane and phytane resulted in attainable peak integration for 40 of the 91 processed sub-samples: 10 from Preese Hall-1, 13 from Beconsall-1Z and all 17 outcrop sub-samples. These molecular (GC/MS and GC/FID) processing were limited by minimal peak integration, therefore the data used in this study are that of the successfully integrated peaks. This, along with low

EOM, demonstrates the limitations of molecular analyses in the Bowland Shale Formation. With regards data analyses, this may increase sampling-related bias. However, the high precision of the instrument and preliminary observations show low error and limited variability between samples. Therefore, the accuracy and precision of extracted organic compounds are suitable for this long-term study. For improved precision, samples would have preferably been run in triplicate, however, this could not be achieved in this study because of limited sample size relative to the required OM extracts.

The multi-disciplinary approach used in this study increases confidence levels through myriad techniques and avoids interpretations based on one technique in isolation.

Scanning Electron Microscopy

Six dry stubs in total (3 from each well) were mounted on an aluminium stub with Achesons Silver Dag, dried overnight and then gold coated (5-10 nm) using a Polaron Scanning Electron Microscope (SEM) Coating Unit (Newcastle University).

Sub-samples were mounted as stubs and imaged using a Tescan Vega LMU SEM and Tescan-supplied software respectively. Bruker Flash 6130 Energy-Dispersive X-ray spectroscopy (EDX) with Espirit software version 2.1 was used for reconnaissance.

Statistical Analyses

Using Minitab, two sample T-tests with 95 % confidence interval (CI) determined significant differences.

Modelling Geochemical Similarities and Differences

Chapter 6, for the first time, used computational statistical methods to investigate the geochemical similarities between multiple source rocks to select an analogue for the upper Bowland Shale Formation. To investigate data similarities, a Gaussian Mixture Model (GMM) was created to group pooled XRF data from all study source rocks into a manually and

computationally determined number of groupings based on their distribution (called "Shale Formation n ").

Using MATLAB, 2D normal distributions (multivariate normal distributions) were used to conceptualise variance and covariance between elements in two dimensions. For each grouping, a unique matrix was allowed. This model allowed a full covariance matrix for each phase and each phase had a distinct covariance matrix. This permitted simultaneous variation between variables, as well as within variables. MATLAB populates the covariance matrices for each component and assesses the tolerance (fit) of all data. After iteratively processing the suite of data, a model was selected that fits a pre-defined error function (i.e. computation stopped when the tolerance falls below a threshold value) and this model was called the optimum solution. The GMM grouped two variables into a number of phases (N). To account for local undulations in $5N$ (5 manually selected groups) or $6N$ (6 manually selected groups, dependent upon how many "Shale Formations" that are being compared) dimensional space, this model was re-run with different starting conditions with aims of investigating numerous local minima to find the true minimum error.

This model was run on non-optimised (manually selected number of groupings based on the number of formations studied) and optimised (computationally derived number of groupings) modes and these clustered plots of hypothetical "Shale Formations" were compared to the original cross plots. Optimised settings use Computational Bayesian Information Criterion (BIC) to measure and select groupings that most likely represent true geochemical differences. To model cross plots that typically use logarithmic axes (e.g. Mo and U EF), values were converted to "ln" because the GMM required a normal distribution.

For all geochemical data, see Digital Identifier (DOI)[10.25405/data.ncl.12102492](https://doi.org/10.25405/data.ncl.12102492) at Newcastle University.

Chapter 4. The Applicability of Outcrop Organic Geochemistry in the Bowland Shale Formation.

Abstract

In relatively unexplored shale gas targets, such as the upper Bowland Shale Formation (Bowland Basin), core material is limited and reliance on surface outcrop material is high. In these scenarios, information from outcrops (e.g. organic geochemistry) contributes towards resource estimation. However, organic compounds can be altered by thermal maturation, weathering and OM differently across a basin/ formation. Therefore, we investigate the challenges and applicability of outcrop organic geochemical proxies (Little Mearley Clough, Lancashire, UK) relative to that of subsurface cores (from wells Becconsall-1Z and Preese Hall-1, Lancashire, UK). This study uses sedimentology, pyrolysis, extractable OM and GC/FID to identify the challenges associated with using outcrop organic geochemistry to aid basin analysis. Although outcrop data is necessary and useful to basin analysis, we recommend that caution is taken when attributing previously recognised effects linked to weathering, such as elevated T_{max} and oxygen indices (e.g. Emmings et al. 2017). We suggest this is because it is difficult to distinguish the relative importance of weathering from thermal maturity and spatial differences in OM burial. We find that low extractable OM and limited peak integration for pristane and phytane restricts the use of molecular analyses in mature upper Bowland Shale source rocks.

Introduction

Unexplored targets for shale oil and gas production have minimal subsurface core data. This increases reliance on surface outcrop analyses. However, weathering effects and differences in thermal maturities can alter observed outcrop compositions and obscure resource estimates (Petsch et al. 2000). Furthermore, the differences between outcrop and core derived data can obscure palaeoceanographic interpretations which are crucial to understanding locations of hydrocarbon accumulation. For

example, the UK upper Bowland Shale Formation is a relatively unexplored target for UK shale gas (Clarke et al. 2018), promoting academic and industrial interest in resource estimation (Andrews 2013b; Clarke et al. 2014; Whitelaw et al. 2019). However, limited core material from Preese Hall-1 and Beconsall-1Z (Bowland Basin, Lancashire, UK; Figure 2) increases reliance upon outcrop studies (e.g. Wiseall et al. 2018). However, fundamental problems associated with differences in geographical location, thermal maturity and surface exposure (Emmings et al. 2017) can limit the applicability of organic geochemical proxies (e.g. TOC) and obscure resource estimates.

Emmings et al. (2017) investigated the effects of weathering on geochemistry using outcrop-derived samples. Emmings et al. (2017) concludes that stream sampling provides the most accurate geochemical data in the absence of unaltered core material. However, the upper Bowland Shale is relatively unexposed (Earp et al. 1961; Waters et al. 2009), even in small rivers, which typically forces the collection of slope samples. Emmings et al. (2017) also suggests that weathering significantly effects the trace metal geochemistry of surface samples from slope outcrops. This limits palaeoceanographic interpretations. Weathering also obscures organic geochemical proxies (e.g. elevated OI and T_{max} in weathered rocks) when analysed using pyrolysis (Emmings et al. 2017; Leythaeuser 1973). However, previous studies have not used molecular analyses to study the organic geochemistry of Bowland Basin upper Bowland Shale outcrops. Furthermore, the applicability and potential of using Bowland Basin outcrop organic geochemistry has, until now, been uncertain.

We compare molecular and pyrolysis data from the Bowland Basin (upper Bowland Shale) to that of two cores (Beconsall-1Z and Preese Hall-1; Figure 2). We investigate the applicability and potential of using outcrop OM for resource estimations of this subsurface source rock. Analyses such as GC/FID are used to calculate pristane/ n -C₁₇ and phytane/ n -C₁₈ (from Shanmugam 1985 and Hunt 1996) and compare core and outcrop

biodegradation / thermal maturation. Other proxies, such as extractable organic matter (EOM) have been previously used to calculate the total bitumen (Bagnoud-Velásquez et al. 2013). However, this proxy is a precursor to other geochemical analyses and not typically used in petroleum exploration (e.g. chemostratigraphic or palaeoenvironmental analysis). This current study uses EOM to highlight the challenges associated with molecular analyses in thermally mature and/or weathered source rocks.

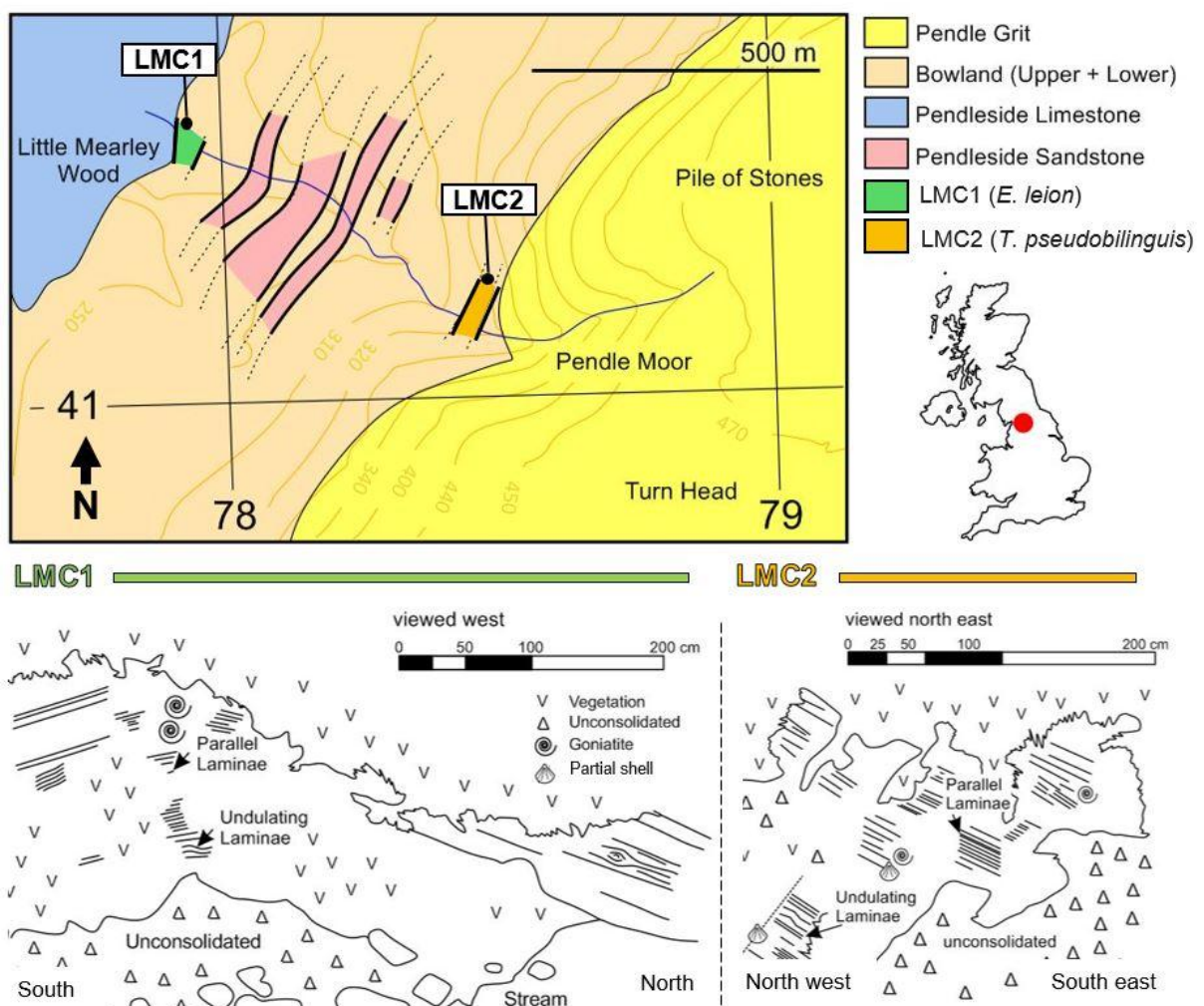


Figure 3: Little Mearley Clough outcrops (LMC1 and LMC2) at Pendle Hill, Lancashire, UK.

The type and abundance of OM can change up succession in a source rock (e.g. Clarke et al. 2018). This is controlled by processes that affect spatial and temporal differences in kerogen preservation and/or production (Katz

2005). For example, Carboniferous highstands and maximum flooding surfaces (sometimes called 'marine bands') are intervals that are typically enriched in TOC, goniatite index fossils and saline fauna (Bloxam and Thomas 1968; Davies and Elliott 1996; Riley 1993; Thomas and Bloxam 1969). These can act as sweet spots and targets for hydrocarbon production, but their fossil abundance and lateral extensiveness also makes them useful for well correlation (Bhattacharya 1993; Church and Gawthorpe 1994; Clarke et al. 2018; Davies and McLean 1996; Dunham and Wilson 1985; Hampson et al. 1997; Isbell et al. 2003; Martinsen et al. 1995; Read et al. 1991). For example, the Mississippian goniatite index fossil *Tumulites pseudobilingue* is used to stratigraphically correlate upper Bowland Shale marine band E₁B₂ in Preese Hall-1 and Beconsall-1Z (Clarke et al. 2018) as well as at outcrops such as LMC (Figure 2 and Figure 3; Waters et al. 2009). The upper Bowland Shale marine band E₁A₁, identified by goniatite *Emstites leion*, is found in Preese Hall-1 and at LMC, the type location for the upper Bowland Shale.

We compare the organic geochemical proxies of outcrop and subsurface core material using GC/FID, EOM and pyrolysis. We study the upper Bowland Shale to investigate the challenges associated with using time-equivalent rocks of different weathering grades, geographical locations and thermal maturities for resource estimation of an unexplored basin.

Methods

Outcrop Analysis

Marine band identification in core is difficult due to limited fossil availability, however it also difficult in outcrop due to weathering effects that make samples fissile and degraded. Therefore, this field study visited sites listed in previous studies (Waters et al. 2011; Waters et al. 2009) that identify the locations of Carboniferous highstands E₁A₁ and E₁B₂ in the upper Bowland Shale Formation. The outcrop location of LMC was selected for outcrop comparison of exposed E₁A₁ (-2° 20' 15.15", 53° 51' 56.30") and E₁B₂ (-2° 19' 42.31", 53° 51' 56.39") marine band successions, referred to in this chapter as locations LMC1 and LMC2

respectively and both were 160 cm successions from base to top (Figure 3). Marine bands were identified using fossil interpretations in the literature (Clarke et al. 2018; Horn 1960; Riley 1993) as well as archived biostratigraphic maps and grid references (Aitkenhead 1992; Waters et al. 2011; Waters et al. 2009).

Sampling

For this study, marine bands E_1A_1 and E_1B_2 were used for outcrop and core correlation. Thin marine band beds prevented extensive sample collection throughout the upper Bowland Shale. Therefore, a nested sampling approach was used that sampled all available material within and above/below the marine bands.

For marine band E_1B_2 , the goniatite phase ranges from burial depths 2081.75 – 2081.81 m (6 cm thick) in Preese Hall-1 (Hird and Clarke 2012) and from 2140.90 – 2142.52 m (162 cm thick) in Beconsall-1Z (Hird et al. 2012). For marine band E_1B_2 , sampling intervals in Preese Hall-1 ranges from 2072.64 - 2097 m depth (28 sub-samples at ~10 cm interval spacing) and in Beconsall-1Z from 2137.34 – 2146.04 m (43 sub-samples at ~10 cm intervals). At the exposed E_1B_2 outcrop succession LMC2 (Figure 3), 17 surface samples were taken, totalling 160 cm from base to top.

For marine band E_1A_1 , the goniatite phase ranges from burial depths 2501.40 – 2501.50 m (10 cm thick) in Preese Hall-1. To investigate the thermal maturity of rocks near to the base of the upper Bowland Shale (including marine band E_1A_1), Preese Hall-1 burial depths 2342.08 – 2501.60 m (16 samples) were analysed.

This chapter used outcrop and core sedimentological analyses, Rock-Eval pyrolysis, EOM and molecular analysis (GC/FID). See Methodology.

Results

Lithology

The marine band E_1A_1 at LMC1 (Waters et al. 2009; Figure 3), is c. 20 cm from base (marking the base of the upper Bowland Shale) to top where

vegetation and weathering obscures features. Two partially preserved and weathered goniatite fossils identified as *Emstites leion* are between c. 100 and 120 cm height from the base of the outcrop (Figure 3). The succession is brown-black and mudstone dominated. Strata range from thin bedded (8 cm thick) to thin laminae (0.4 cm thick). Most sedimentary structures are obscured by weathering effects. However, they are typically parallel laminated with some undulating laminae near the base of the outcrop.

The goniatite-enriched zone at LMC2 is c. 80 cm thick (Figure 3). This study succession is less weathered than at LMC1, however physical (fissile mudstone) and biological weathering (grass and roots) effects are still visually apparent at LMC2. The outcrop at LMC2 is mudstone dominated, grey-black and predominantly parallel laminated. Similar to LMC1, strata range from thin beds (9 cm thick) to thin laminae (0.3 cm thick).

Undulating laminae are apparent towards the base of this outcrop (c. 50 cm above the base). Partial fossils of goniatites, identified as *Tumulites pseudobilingue*, are poorly preserved, sparse and confined to the thin, parallel laminated strata. Partial-fossils of shell fragments are possible brachiopods.

Organic Geochemistry

Rock-Eval pyrolysis is used to compare outcrop and core material OM thermal maturity and type (Table 1). Figure 4 shows that cross plots of T_{max} (temperature that coincided with the maximum release of hydrocarbons during thermal cracking) and Hydrogen Index ($[100 \times S_2]/TOC$) show that Becconsall-1Z plots exclusively within the oil window (between T_{max} 435 and 470 °C) and ranges from 451.0 – 469.0 °C (Figure 4). T_{max} values in Preese Hall-1 plot within the oil (mature) and gas (post-mature) zones and range from 448.0 – 564.0 °C. Similarly, OM from the LMC1 outcrop-derived succession plots predominately within both the oil window and post-mature zones and ranges from 308.0 – 516 °C. This differs from the T_{max} of LMC2 OM that ranges from 434.0 – 444.0 °C. The OM from LMC2 predominantly falls within the oil window.

	Tmax (°C)	S1 (mg/g)	S2 (mg/g)	HI (mg/g)	OI (mg/g)	TOC (%)	EOM (g)	Pristane/n-C17	Phytane/n-C18
Outcrop (LMC1)									
Min	308.00	0.00	0.00	0.00	61.00	0.10	-	-	-
Max	516.00	0.10	0.89	64.00	2740.00	2.75	-	-	-
Average	474.75	0.01	0.18	17.00	541.38	0.91	-	-	-
StDev	50.69	0.03	0.26	16.47	788.36	0.82	-	-	-
Outcrop (LMC2)									
Min	434.00	0.64	3.25	98.00	1.00	2.92	0.0024	1.118	0.788
Max	444.00	1.64	9.35	231.00	16.00	4.39	0.0034	1.395	0.998
Average	441.06	1.19	6.45	183.41	5.59	3.49	0.0028	1.250	0.899
StDev	2.30	0.24	1.68	36.48	3.47	3.47	0.0003	0.071	0.065
Core (Preese Hall-1)									
Min	448.00	0.03	0.08	15.00	1.00	0.36	0.0001	0.117	0.000
Max	564.00	0.94	4.15	78.00	29.00	5.75	0.0011	1.962	0.016
Average	469.98	0.32	1.05	41.84	8.52	2.51	0.0004	0.463	0.003
StDev	19.58	0.25	0.82	18.10	7.60	1.40	0.0003	0.570	0.005
Core (Beaconsall-1Z)									
Min	451.00	0.36	1.15	41.00	1.00	2.14	0.0001	0.080	0.080
Max	469.00	1.00	3.02	93.00	16.00	4.52	0.0009	0.337	1.000
Average	458.60	0.64	1.77	55.03	4.15	3.20	0.0003	0.222	0.295
StDev	4.63	0.17	0.46	9.94	3.14	0.53	0.0002	0.072	0.225

Table 1: Organic geochemical results from outcrop and core data. (StDev = Standard Deviation).

The hydrogen index (HI) and oxygen index (OI) of OM are also used to investigate kerogen type and/or thermal maturity (Espitalie et al. 1977). In all successions, HI is low (<300 mg/g) and is close to the origin on a pseudo-van Krevelen diagram (Figure 4). Preese Hall-1 has an average HI of 41.8 ± 18.1 mg/g (values that follow \pm represent standard deviation) which is similar to Beconsall-1Z which has an average HI of 55.03 ± 9.94 mg/g. However, the HI of LMC2 and LMC1 differs from the cores and each other with averages of 183.4 ± 36.5 mg/g and 17.0 ± 16.5 mg/g, respectively.

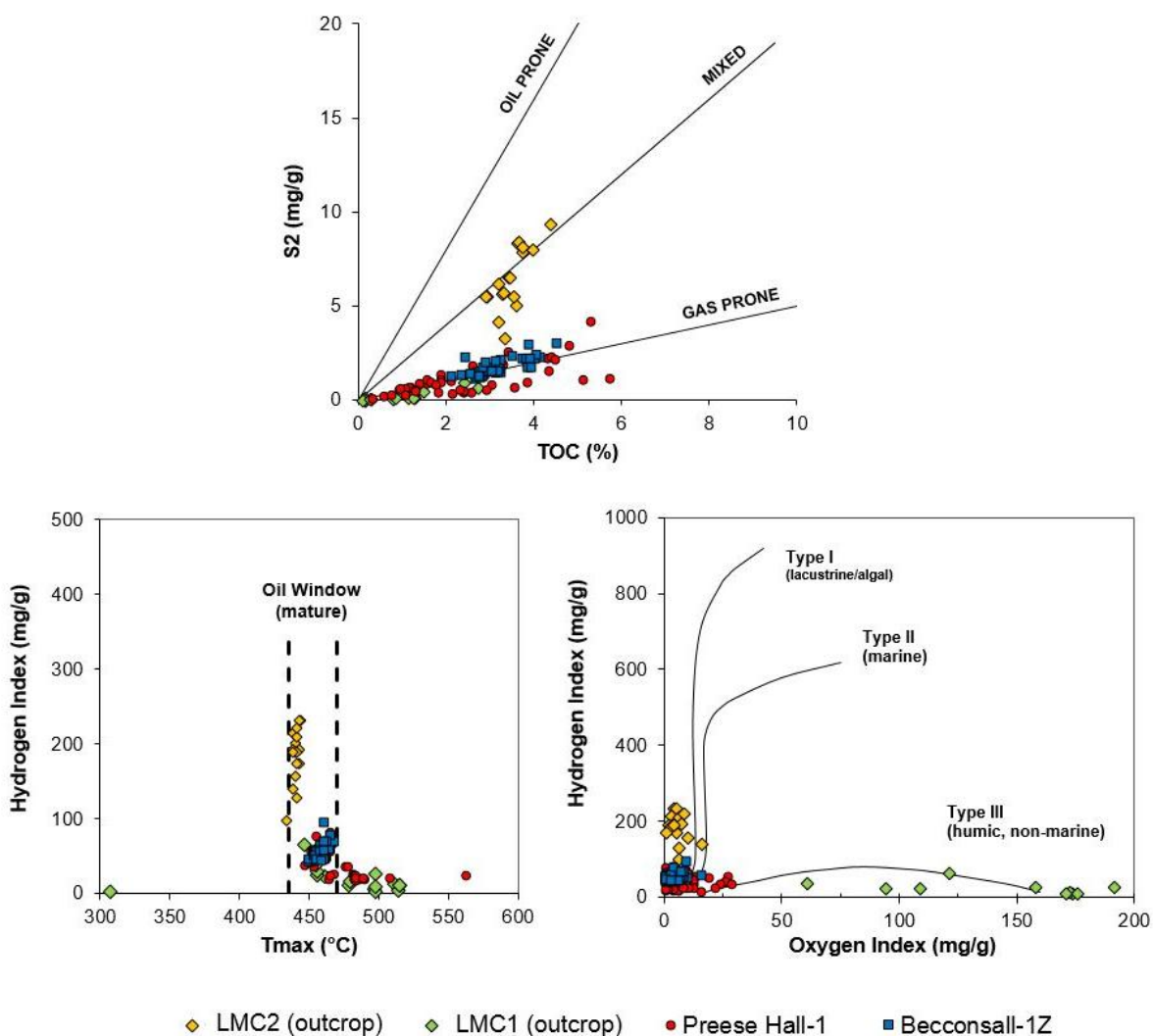


Figure 4: Rock-Eval pyrolysis of upper Bowland Shale Formation core and outcrop material using TOC versus S₂ (top, after Espitalié and Bordenave 1993 and Peters 1986), T_{max} versus HI and OI versus HI (after Espitalié et al. 1977).

The pseudo-van Krevelen diagram also shows a similarity in OI between Preese Hall-1 (average of 8.5 ± 7.6 mg/g), Beconsall-1Z (average of 4.2 ± 3.1 mg/g) and LMC2 (average of 5.6 ± 3.5 mg/g) (Figure 4). These values differ from that of LMC1 and has an elevated average OI of 541.3 ± 788.4 mg/g, relative to the other outcrop and core OM.

Cross plots of TOC and S₂ (hydrocarbons generated from thermal cracking) are used to compare the petroleum type (Figure 4). Therefore, Preese Hall-1, Beconsall-1Z and LMC1 OM are "gas prone". The OM of LMC2 is predominantly "mixed", although more gas prone than "oil prone". The average TOC was higher in Beconsall-1Z (3.2 ± 0.5 %) than in Preese Hall-1 (2.5 ± 1.4 %). Regarding the outcrops at LMC, the average TOC was higher at LMC2 (3.5 ± 3.5 %) than at LMC1 (0.9 ± 0.8 %). Using both cores and outcrop locations, the average TOC is 22 % lower in outcrop than in subsurface cores.

The quantified weight of bitumen extracted from the crushed mudstone is sometimes called EOM. LMC1 has negligible EOM using Soxtec™ extraction and therefore GC/FID was unattainable for this outcrop location. The average EOM (Table 1) was highest in LMC2 (28 ± 3 mg). The EOM in Preese Hall-1 has an average of 4 ± 3 mg, which is similar to Beconsall-1Z (average of 3 ± 2 mg). Figure 5 shows EOM versus depth. In Preese Hall-1 and LMC2, there is no clear increase in either EOM (g) or relative EOM (normalised to the rest of the succession) within the E₁B₂ marine band goniatite phase. In Beconsall-1Z, there is a clear increase in EOM and relative EOM within the E₁B₂ goniatite phase of LMC2. In Beconsall-1Z, EOM gradationally increases from 2145.64 m (1 mg) to 2143.30 (3 mg) (Figure 5). Bulk EOM gradationally decreases from 2140.80 (6 mg) to 2138.32 (3 mg) in Beconsall-1Z. Maximum EOM values in Beconsall-1Z (9 mg) and LMC2 (3 mg) are within the E₁B₂ goniatite phase. This is true for values of relative/normalised EOM (1 at 2141.00 m).

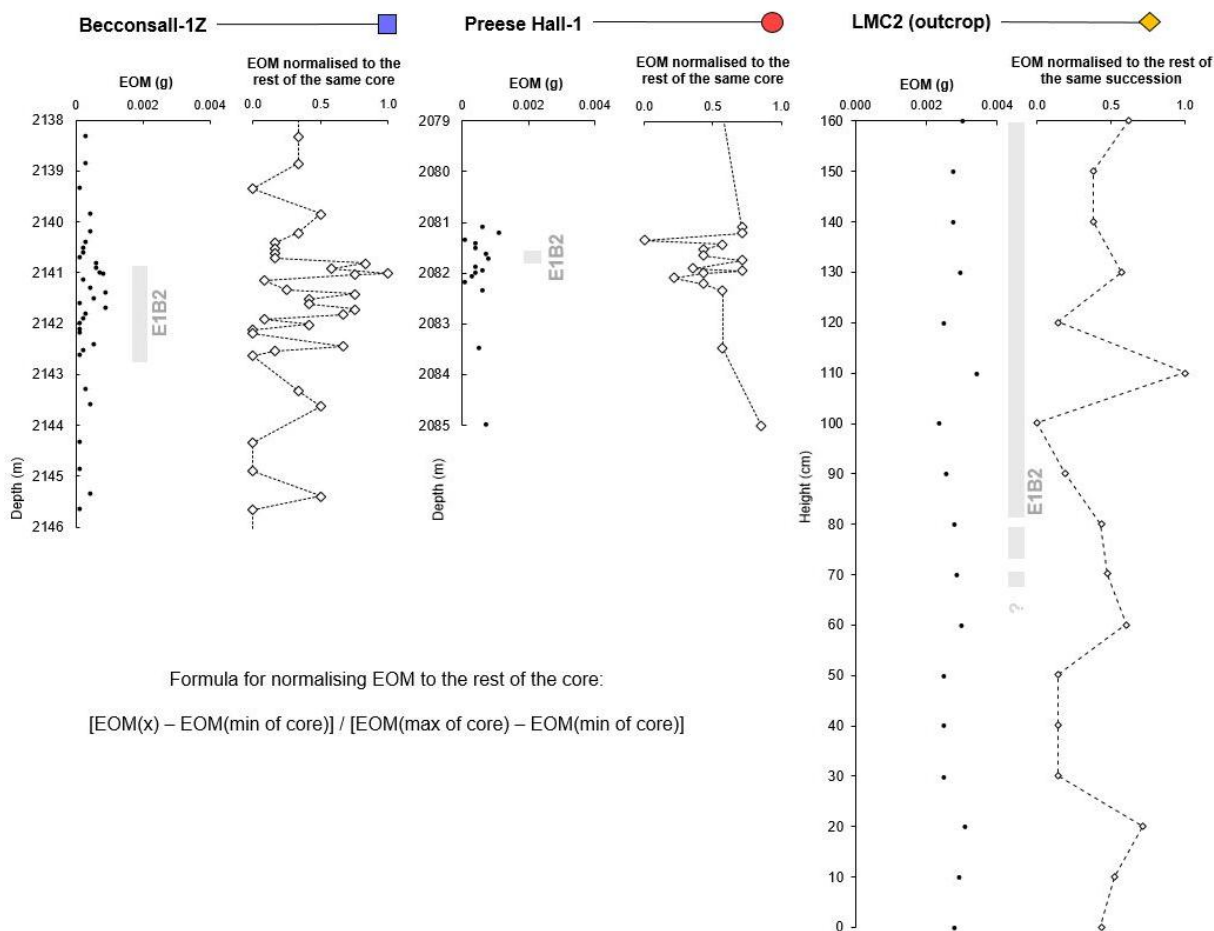


Figure 5: Extractable organic matter (EOM) in Beconsall-1Z, Preese Hall-1 and at LMC2.

Average pristane/ $n\text{-C}_{17}$ ratios are highest at LMC2 (1.250 ± 0.071) when compared with Beconsall-1Z and Preese Hall-1 core material (Table 1 and Figure 6). Pristane/ $n\text{-C}_{17}$ averages at Preese Hall-1 (0.463 ± 0.570) are higher than that at Beconsall-1Z (0.222 ± 0.072). Similarly, phytane/ $n\text{-C}_{18}$ averages are highest at surface outcrop LMC2 (0.899 ± 0.065) relative to Preese Hall-1 (0.003 ± 0.005) and Beconsall-1Z (0.295 ± 0.225). Cross plots of pristane/ $n\text{-C}_{17}$ and phytane/ $n\text{-C}_{18}$ from Preese Hall-1, Beconsall-1Z and LMC2 show that all OM is thermally mature. However, Preese Hall-1 is the most thermally mature and outcrop-derived OM are the least thermally mature (Figure 6).

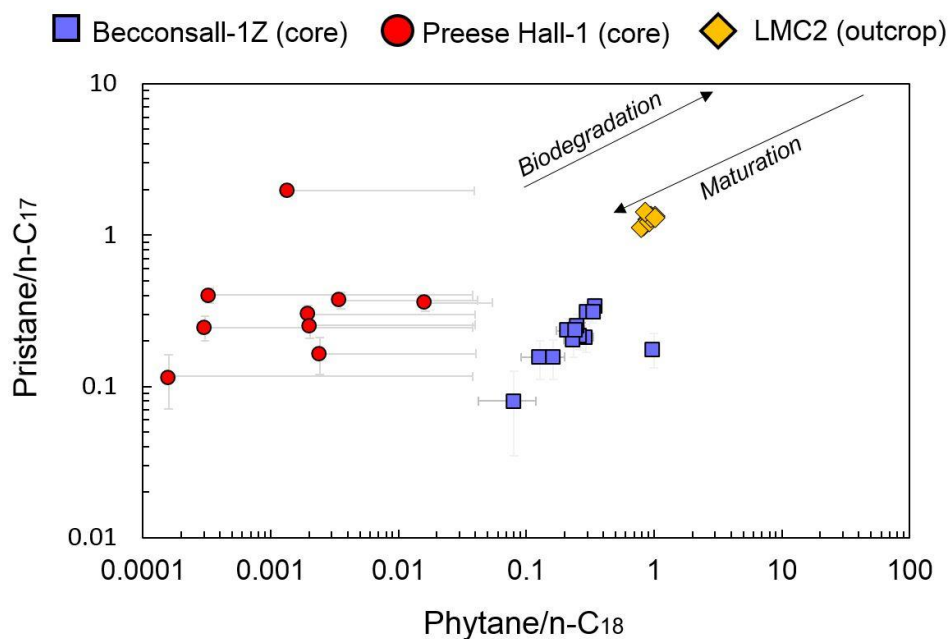


Figure 6: Binary plot of pristane/n-C₁₇ and phytane/n-C₁₈ from Preese Hall-1, Beconsall-1Z and LMC2.

Discussion

We investigate the applicability of molecular geochemistry to the Bowland Shale Formation (Bowland Basin) outcrops to subsurface data analyses. Rock-Eval pyrolysis is used in this study to compare the type and thermal maturity of Bowland Shale outcrop and core OM. A pseudo-van Krevelen is typically used for OM type identification (Espitalie et al. 1977). However, molecular analyses suggest that high thermal maturity in the upper Bowland Shale at outcrop and in core (Figure 6) obscures the type of OM that is typically determined from pyrolysis using cross plots of T_{max} and HI, OI and HI or TOC and S1. Binary plots of T_{max} and HI suggest that all upper Bowland Shale mudstones studied are mature and/or overmature (Figure 4). In previous studies, immature and early oil mature outcrops have been used to identify a mixture of type II, II-S, II/III and III (Emmings et al. 2019a; Emmings et al. 2019b). However, the maturity and/or over-maturity of the subsurface cores and outcrops, such as those used in this current study, prevents basin-wide interpretations using these Rock-Eval pyrolysis proxies. In this study, the near-origin clustering within the pseudo-van Krevelen (Figure 4) most likely represents hydrogen

expulsion due to thermal maturation (Killops and Killops 2013), rather than reflecting OM type. Therefore, Rock-Eval pyrolysis cannot be used to identify the OM type of these mature and/or over-mature upper Bowland Shale Formation source rocks.

Thermal maturity is crucial to the resource estimation of shale gas plays, such as the upper Bowland Shale (Espitalie et al. 1977; Soulsby and Kemal 1988; Whitelaw et al. 2019). However, at outcrop, weathering can elevate OI and T_{max} (Emmings et al. 2017), obscuring thermal maturity interpretations, leading to potentially inaccurate estimates. This study similarly observes high OI at LMC1 (61 – 2740 mg/g) relative to LMC2 (1 – 16 mg/g), Beconsall-1Z (1 – 16 mg/g) and Preese Hall-1 (1 – 29 mg/g). This is most likely linked to observed increases in apparent physical and biological weathering at LMC1. Therefore, visual observations of outcrop weathering grades are a good, qualitative indication of their organic geochemical applicability. This study also supports the use of weathering information in outcrop studies because without this the interpretations are obscured and/or limited.

Previous studies suggest that weathering can elevate T_{max} values, a proxy for thermal maturity (Emmings et al. 2017). However, in this current study, the similarities between T_{max} values of upper Bowland Shale cores and outcrops are more difficult to distinguish from “authentic” thermal maturation (Figure 4). Future outcrop studies should use T_{max} proxies alongside other thermal maturity indicators such as vitrinite reflectance. However, this is difficult in the upper Bowland Shale due to the abundance of indistinct amorphous OM (Emmings et al. 2019a). Therefore, visual observations of weathering grades at outcrop are useful as a rough guide. However, the complexity and variability of weathering makes geochemically altered signals difficult to distinguish from “authentic” maturation and OM type proxies.

Leythaeuser (1973) suggests that the TOC of OM rich mudstones can decrease to a maximum of 25 % under the influence of weathering, however Petsch et al. (2000) later recorded that weathering can decrease

TOC from 60 to approaching 100 %. This current study observes an average TOC decrease of 22 % in outcrop TOC relative to core, which is more similar to that of Leythaeuser (1973), based on both cores and outcrop locations. However, this difference in TOC is likely due to differences in geographical location and spatial differences in OM burial. Therefore, the organic geochemical study of outcrops must account for impacts of weathering, thermal maturation and differences in geographical location relative to the core.

The average EOM of upper Bowland Shale rocks were observed to be highest at LMC2 (28 mg) relative to Beconsall-1Z (3 mg) and Preese Hall-1 (4 mg). It is possible that increased EOM at LMC2, relative to both cores, is due to biological contamination of the OM extract (Peters et al. 2005). However, a more likely interpretation is that thermal maturation was greater in Preese Hall-1 and Beconsall-1Z. If true, OM destruction via the thermal maturation of subsurface upper Bowland Shale targets limits the potential for complex organic geochemical analyses from exploration cores. Cross plots of pristane/n-C₁₇ and phytane/n-C₁₈ support this interpretation (Figure 6) which infers increased thermal maturity in subsurface cores relative to outcrops. The geochemistry in this study supports previous thermal history burial models (Andrews 2013a) which suggest that the upper Bowland Shale Formation reached a maximum burial depth of c. 5700 m at the location of Beconsall-1Z and Preese Hall-1. However, previous thermal maturation models are based on core data. This further increases the uncertainty related to outcrop and core comparisons in the upper Bowland Shale Formation.

Additionally, it is possible that EOM is linked to goniatite abundance and marine band deposition (Figure 5), particularly with regards to the E₁B₂ marine band, because the maximum values of EOM in Beconsall-1Z (9 mg) and at LMC2 (34 mg) fall within the goniatite phase. However, this is not certain. One possible explanation for this may be that the processes (high salinity and low oxygen) that are related to enhanced goniatite preservation in the upper Bowland Shale (Bloxam and Thomas 1968;

Gross et al. 2015) may also result in differences in the abundance and/or type of OM. Future work should investigate the overriding controls on EOM abundance and the potential importance of EOM to marine band correlation.

In an unexplored basin with limited core material, options are limited for basin analysis and therefore reliance on outcrop-derived information is high. However, in these circumstances, we recommend that organic geochemistry be used with caution because the effects of thermal maturation, weathering and spatial differences in geochemical signals can be indistinguishable. Caution is also advised when interpreting the organic geochemistry of mature and/or post-mature upper Bowland Shale exploration cores and outcrops. This is because low EOM (<11 mg) in mature and/or over-mature cores limit the effectiveness of molecular analyses.

Conclusions

- The organic geochemistry of surface outcrops in the upper Bowland Shale is difficult to interpret because the chemical weathering and thermal maturity alterations are complex and variable. This makes interpretations of the original palaeoceanography (e.g. OM type) difficult to distinguish from thermal maturation and weathering signals. In this scenario, where pyrolysis techniques are obscured, caution should be taken when using these data in resource estimates.
- Visual guides to weathering in outcrop serve as a rough guide to direct sampling strategies. This study supports previous suggestions used in trace metal geochemical studies (Emmings et al. 2017) where care is taken to prioritise black, fresh mudstone outcrops from streams. We recommend that all future outcrop studies record weathering information.
- The upper Bowland Shale in Preese Hall-1 and Beconsall-1Z are mature and/or over-mature (evident from GC/FID and Rock-Eval pyrolysis). This supports previous computational models which

suggest that the upper Bowland Shale has been buried to a maximum depth of c. 5700 m (Andrews 2013a).

- The thermal maturation of upper Bowland Shale in the Bowland Basin, in cores and at LMC, limits the effectiveness of molecular analyses. For example, EOM in this study does not exceed 11 mg and this is an important precursor to GC/FID and other molecular analyses (e.g. GC/MS). Unattainable GC/FID peak integration for pristane and phytane in 51 out of 91 samples demonstrates the limitations of molecular analyses in mature source rocks which are reliant upon OM extracts. Therefore, the organic geochemistry of mature and over-mature rocks in the upper Bowland Shale have limited use for palaeoceanographic interpretations.
- Differences between outcrop and core EOM are most likely linked to spatial differences in thermal history, OM burial as well as weathering. All of these factors contribute to the uncertainty related to outcrop and core relationships. Therefore, a multi-proxy approach is recommended for upper Bowland Shale Formation studies (e.g. trace metal and mineralogical analyses).

Chapter 5. Geochemical Well Correlation in the Upper Bowland Shale Formation.

Abstract

Directional drilling and petroleum play fairway analysis is reliant upon the correlation of stratigraphic intervals observed in previously drilled wells. Well correlation during shale gas exploration is crucial for basin modelling and to successfully identify target intervals. However, stratigraphic correlation is difficult in shale gas plays where lithological variation is limited, and traditional marker horizons are rare. Typically, source rocks are correlated using biostratigraphic marker beds, for example so-called 'marine bands' in Carboniferous plays that contain age-diagnostic ammonoid fauna. However, this approach is often problematic due to poor index fossil preservation and difficulties in the identification of biota.

Marine bands are zones of enhanced petroleum production and are therefore a typical unconventional exploration target. In the Bowland Basin, a frontier shale gas target in Lancashire, UK, marine bands are also used to correlate wells. In exploration wells Beconsall-1Z and Preese Hall-1, only one marine band (E_1B_2) can be used to correlate the upper Bowland Shale Formation and therefore the reliability of this correlation is crucial to understanding time-equivalent, basin-wide depositional and eogenetic processes. Therefore, this study uses geochemistry to correlate wells in the Bowland Basin and develop the reliability of marine band correlation. Geochemical-assisted well correlation of Carboniferous marine band E_1B_2 in the Bowland Basin has been investigated using X-ray fluorescence, Rock-EvalTM pyrolysis, X-ray diffraction, $\delta^{13}C_{org}$ isotopic analysis, gas chromatography/ mass spectrometry and scanning electron microscopy at high resolution (10 cm intervals). The goniatite-bearing phase of marine band E_1B_2 in cores Beconsall-1Z and Preese Hall-1 show increases in oil saturation indices and stepped gradational increases in Mo/U up succession and thus are used as correlation proxies and as indicators of bottom water palaeoceanographic processes. Increases in the

Oil Saturation Index (OSI) within a marine band is proposed as an organic chemostratigraphic correlation proxy for the upper Bowland. Observed increases in OSI represent increased oil generation and/or retention within the E₁B₂ marine band. Trace metals are typically translated into the sediment less readily than OM. Therefore, sharp increases in Mo/U above the goniatite-bearing E₁B₂ interval are most likely linked to a period of increased and/or sustained water column stratification that promoted the preservation of goniatite fossils and OM.

Introduction

Economic unconventional petroleum production depends on reliable source rock characterisation, starting with a well-developed play framework. This framework typically relies on lithological, petrophysical and biostratigraphical correlation in order to identify zones of enhanced hydrocarbon potential. However, in most mudstone successions, key stratigraphic boundaries are difficult to identify due to textural and compositional homogeneity. Therefore, shale gas target formations are traditionally correlated by biostratigraphic marker beds, such as marine bands in Carboniferous plays (Clarke et al. 2018; Dusaar et al. 2000; Holdsworth and Collinson 1988; Leeder 1988b; Ramsbottom 1979; Ramsbottom et al. 1962; Waters et al. 2009).

Marine bands are mudstone intervals that are rich in saline fauna and goniatite index fossils, ranging in thickness from centimetres to a few metres (Holdsworth and Collinson 1988; Kombrink et al. 2008; Martinsen 1993; Ramsbottom et al. 1962; Waters et al. 2009). Marine bands accumulate during highstands and are consequently laterally extensive, making them useful for regional-scale correlation (Clarke et al. 2018; Waters and Condon 2012). Currently, reliable marine band identification and correlation relies on the presence of age-diagnostic ammonoid fossils, including goniatites, but the identification of goniatite fossils is challenging in scarcely populated and/or poorly preserved core samples. In recent years, new geochemical proxies, such as Th/K and Th/U, have been introduced to improve subsurface correlation accuracy in unconventional

plays (e.g. Davies and Elliott 1996; Hudson and Turner 1933). However, these studies have focussed on successions with distinct grain size variation (sandstone to mudstone) that directly impact geochemistry. This study therefore evaluates the geochemistry of a marine band with no distinct grain size variation (only composed of clay size fraction) with the aim to develop a geochemical tool for improved subsurface shale correlation. This study focuses on a palaeontological and sedimentological well-defined marine band in the Upper Mississippian upper Bowland Shale Formation, E₁B₂ in Preese Hall-1 and Beconsall-1Z wells, northwest England (Figure 2; Clarke et al. 2018).

Current Marine Band Identification

Many authors associate Mississippian marine bands with deposition during maximum flooding events (Bhattacharya 1993; Church and Gawthorpe 1994; Davies and McLean 1996; Dunham and Wilson 1985; Hampson et al. 1997; Martinsen et al. 1995; Maynard 1992; Read et al. 1991). These occurred during glacio-eustatic high stands, with each marine band differing in magnitude and geographical extent (Isbell et al. 2003; Maynard 1992; Stephenson et al. 2008; Veevers and Powell 1987). Brandon et al. (1995) suggest that marine band sedimentation is slow and thus represents a “major” portion of time, however they constitute a small percentage of the overall succession. Previous studies investigate the range of marine band periodicities (Martinsen 1993; Riley et al. 1995; Waters and Condon 2012), but each study links highstand cyclicity to glacio-eustatic mechanisms (Brandon et al. 1995; Church and Gawthorpe 1994; Earp et al. 1961). More specifically, marine band formation is linked to either highstands or maximum flooding surfaces (Church and Gawthorpe 1994; Davies and Elliott 1996; Davies and McLean 1996; Gross et al. 2015; Hampson et al. 1997; Holdsworth and Collinson 1988; Martinsen et al. 1995; Maynard 1992; Posamentier et al. 1988; Read et al. 1991).

Marine bands typically correlate with elevated gamma ray signals on down-hole gamma ray logs of natural radiation, suggested to be linked

with uranium concentrated in the organic-rich sediment (Clarke et al. 2018; Davies and Elliott 1996; Myers and Wignall 1987; Thomas and Bloxam 1969). Additionally, localised elevated authigenic kaolinite abundance (Hawkins et al. 2013) and elevated TOC (Fisher and Wignall 2001; Kombrink et al. 2008; Spears and Sezgin 1985; Thomas and Bloxam 1969) are linked to high gamma signals. Although marine bands have known links to high TOC, the amount and type of OM differs between intervals (Clarke et al. 2018; Gross et al. 2015; Hennissen et al. 2017). In some successions, marine band OM is typically dominated by aquatic organisms, mainly algae, whereas others contain increased contribution from land plant material (Gross et al. 2015; Hennissen et al. 2017; Könitzer et al. 2016). It is also suggested that some marine bands have been deposited in prodeltaic environments with photic zone anoxia (Gross et al. 2015), associated with periods of enhanced palaeosalinity (e.g. Holdsworth and Collinson 1988).

The aim of this study is to use geochemistry to develop the reliability of marine band E₁B₂ biostratigraphic correlation in the upper Bowland Shale Formation, UK, a target for frontier petroleum exploration.

Methods

This chapter used sedimentological observations, XRF, XRD, isotopic analysis of OM, molecular analyses (GC/MS), Rock-Eval pyrolysis and two sample T-test statistical analyses. See Methodology.

Sampling

Beaconsall-1Z and Preese Hall-1 were logged and sampled between 2138 – 2146 m and 2079 – 2085 respectively at high resolution (sampling at ~10 cm intervals avoiding fractures; 59 samples in total; Figure 2) up succession across marine band E₁B₂, identified using open access well reports (Hird and Clarke 2012; Hird et al. 2012) as the only marine band used to correlate the upper Bowland in these wells.

Results

Lithology and Mineralogy

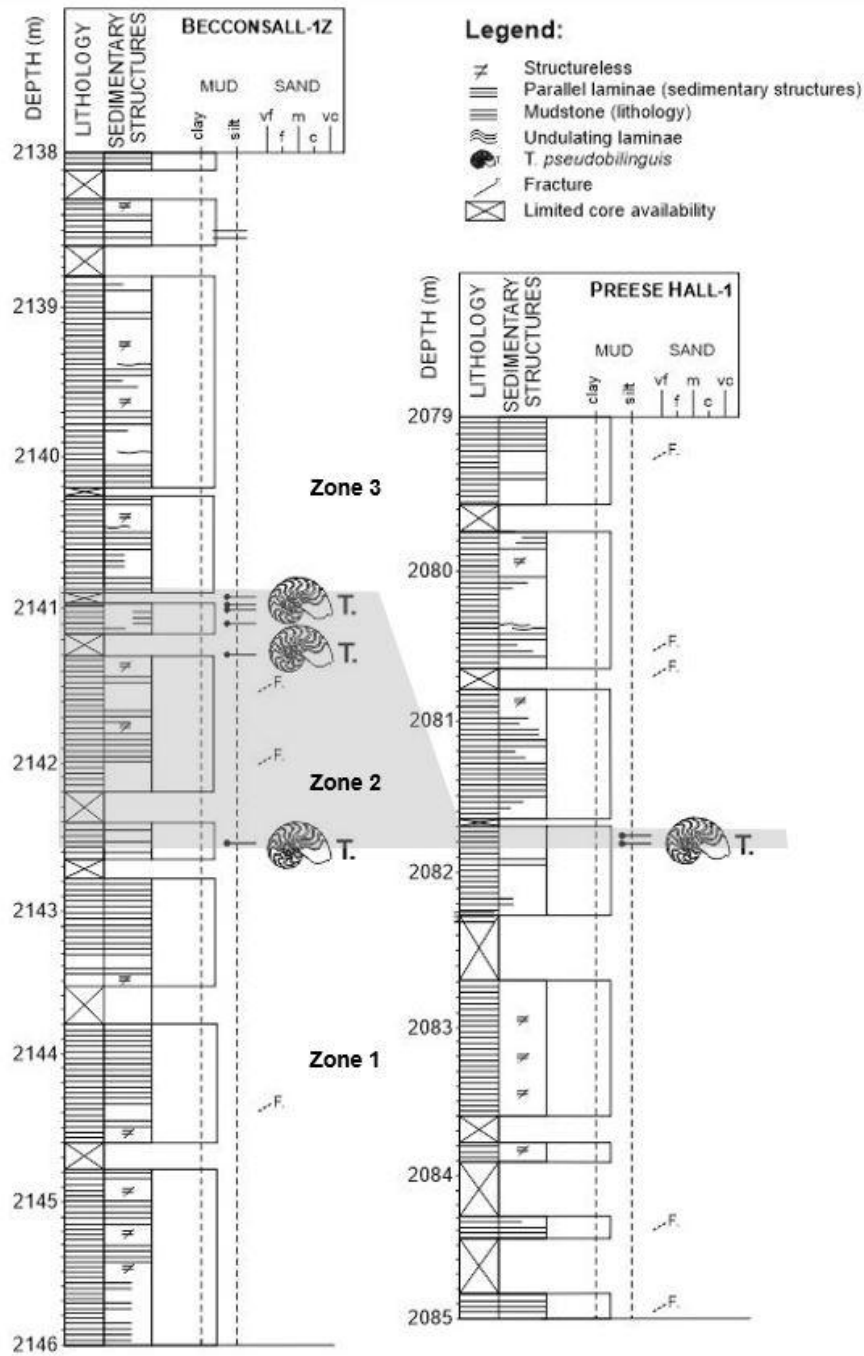


Figure 7: Becconsall-1Z and Preese Hall-1 lithology and biostratigraphic (*Tumulites pseudobilingue*- Zone 2) correlation.

In Preese Hall-1, the marine band E₁B₂ is 6 cm thick, located between 2081.75 m (top) and 2081.81 m (base) burial depth (adapted from Hird and Clarke 2012). In Beconsall-1Z, E₁B₂ is 168 cm thick and located between 2140.91 m and 2142.59 m (adapted from Hird et al. 2012). Approximately 3 m of sediment, above and below the marine band, were also selected for focussed geochemical analyses to compare goniatile enriched sediment (marine bands) to mudstone that was absent of goniatile fossils (barren sediment). Therefore the "study successions" range from 2138 m (top) – 2146 m (base) in Beconsall-1Z and 2079 m (top) – 2085 m in Preese Hall-1 (Figure 7).

Using lithofacies codes from Gross et al. (2015), barren sediments in this study correspond to lithofacies "m" and marine band sediments correspond to lithofacies "mb". Both cores (in marine band and barren sediment) is dominated by parallel laminated mudstone with minor cross lamination and brown-orange mudclasts. Undulating laminae is rare, but when present is typically within Preese Hall-1 barren sediment. Organic matter is typically amorphous forming OM rich laminae (lamalganite) in both cores and in lithofacies m and mb. For this study, the succession is subdivided into three sections called zones 1, 2 and 3, based on stratigraphic location and goniatile presence. Zone 1 is defined as sediment below the thick-shelled goniatile-bearing phase (lithofacies m), Zone 2 represents the goniatile-bearing sediments of marine band E₁B₂ (lithofacies mb) and Zone 3 represents sediments above the thick shelled goniatile-bearing phase (lithofacies m) (Figure 7).

		Percentage Mineral Abundance (%)						
		Quartz	Mg-Calcite	Muscovite/Illite	Pyrite	Dolomite	Chlorite	
Beaconsall-1Z	Zone 3	Min	46.4	2.4	31.0	0.6	2.4	0.5
		Max	55.9	5.3	44.3	6.3	2.4	4.7
		Average	51.5	4.0	38.0	4.1	2.4	2.6
		StDev	4.0	1.1	4.8	2.1	0.0	3.0
	Zone 2	Min	48.4	3.1	6.9	4.3	1.6	-
		Max	83.5	16.5	44.0	32.4	5.2	-
		Average	58.0	7.5	31.0	10.7	3.2	-
		StDev	13.1	5.0	13.9	12.2	1.8	-
	Zone 1	Min	36.2	5.7	17.5	2.3	-	-
		Max	63.3	16.9	41.0	7.3	-	-
		Average	52.5	10.0	30.1	5.5	8.1	-
		StDev	13.1	4.9	12.2	2.2	-	-
Preese Hall-1	Zone 3	Min	51.4	17.4	21.8	5.9	-	-
		Max	54.8	19.5	22.1	6.9	-	-
		Average	53.1	18.5	22.0	6.4	0.1	-
		StDev	2.4	1.5	0.2	0.7	-	-
	Zone 2	Min	38.6	16.2	6.3	0.2	-	-
		Max	56.8	54.9	24.2	2.8	-	-
		Average	47.7	35.6	15.3	1.5	-	-
		StDev	12.9	27.4	12.7	1.8	-	-
	Zone 1	Min	46.4	4.2	9.1	0.1	-	-
		Max	59.5	44.4	23.9	3.3	-	-
		Average	56.0	22.1	15.9	1.2	20.8	-
		StDev	6.4	16.7	6.1	1.8	-	-

Table 2: Mineralogical relative abundances of Zone 1, 2 and 3. (StDev = Standard Deviation).

In Beconsall-1Z and Preese Hall-1, both cores are dominated by quartz, Mg-calcite and muscovite/illite (Table 2). The mineralogy of both cores are relatively homogenous up succession (**Error! Reference source not found.** and Figure 8). In Beconsall-1Z, relative average quartz abundances are similar in Beconsall-1Z (52.5, 58.0 and 51.5 % in zones 1, 2 and 3, respectively) and Preese Hall-1 (56.0, 47.7 and 53.1 % in zones 1, 2 and 3, respectively). This mineralogical homogeneity up succession is also true for illite/muscovite, which is the dominant clay mineral, with relative average abundances of 30.1, 31.0 and 38 % in zones 1, 2 and 3, respectively, for Beconsall-1Z as well as 15.9, 15.3 and 22 % in zones 1, 2 and 3, respectively, for Preese Hall-1. Additionally, the relative Mg-calcite abundance is similar between all zones in both cores. For example, Beconsall-1Z contains relative abundances of 10.0 % in

Zone 1, 7.5 % in Zone 2 and 4.0 % in Zone 3. Preese Hall-1 contains more Mg-calcite (approximately double) than Becconsall-1Z with 22.1 % in Zone 1, 35.6 % in Zone 2 and 18.5 % in Zone 3. Average pyrite abundances are low in Preese Hall-1 with 1.2, 1.5 and 6.4 % in zones 1, 2 and 3, respectively. Pyrite relative abundances are higher in Becconsall-1Z than Preese Hall-1 with average relative abundances of 5.5 % in Zone 1, 10.7 % in Zone 2 and 4.1 % in Zone 3. Textural observations indicate that, in Preese Hall-1 and Becconsall-1Z, there is little difference in texture between the cores and zones (Figure 9).

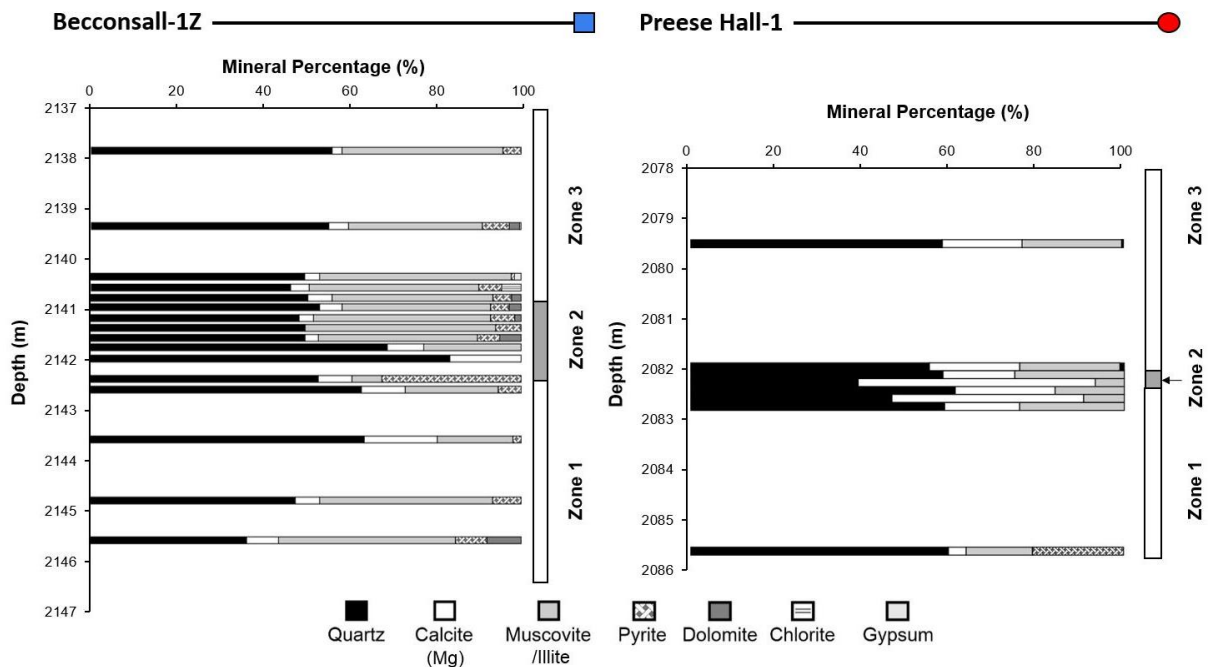


Figure 8: Relative mineralogy across Zone 1, 2 and 3 in Becconsall-1Z and Preese Hall-1.

Beaconsall-1Z

Preese Hall-1

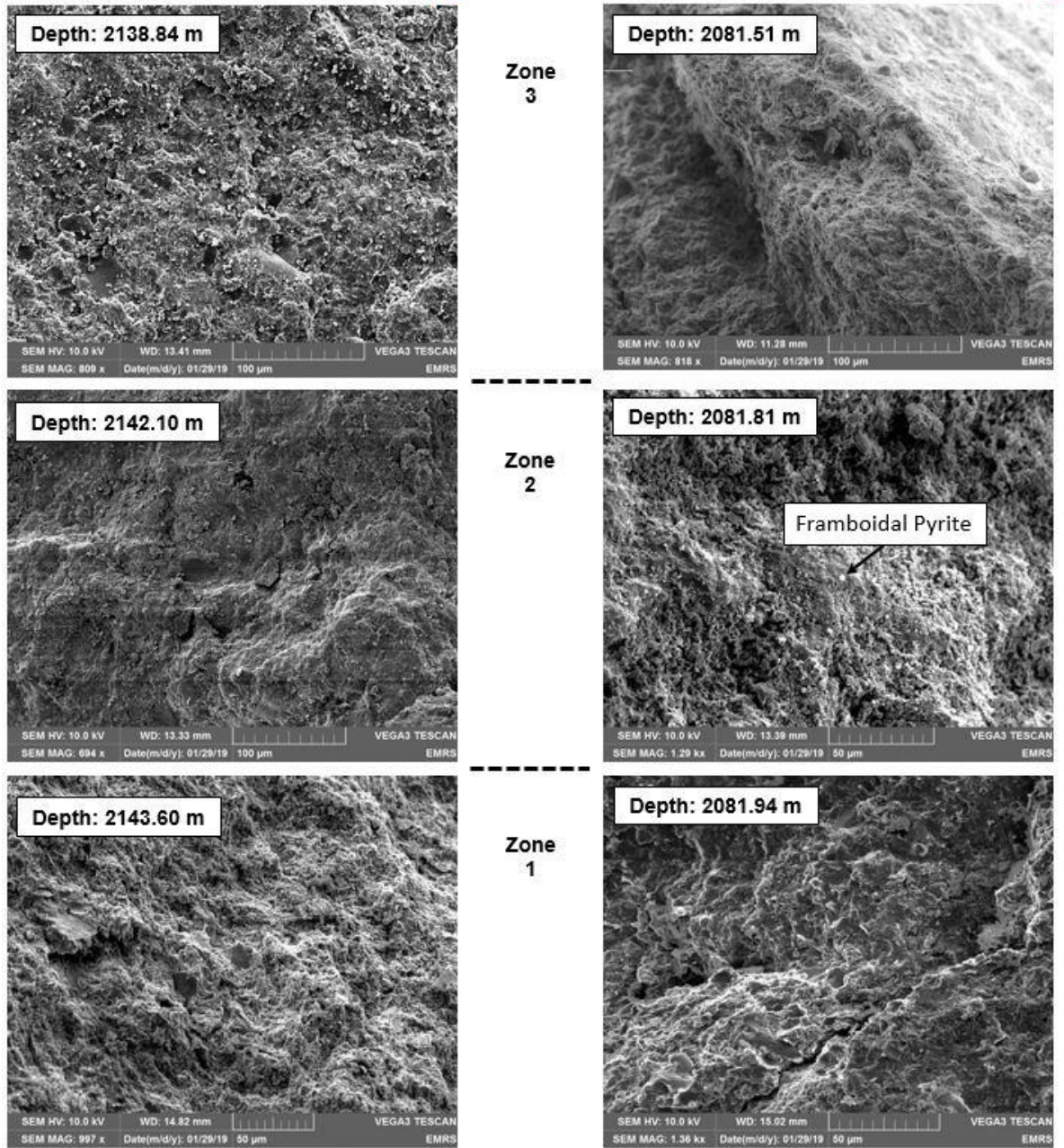


Figure 9: Scanning electron microscopy (secondary electron) data showing the topographic information and textures of Zone 1, 2 and 3 in Beaconsall-1Z and Preese Hall-1.

Provenance

Table 3 and Figure 10 record and illustrate the values of detrital proxies Ti/Al, Zr/Al and Th/K between zones in Beconsall-1Z and Preese Hall-1.

Both Ti/Al and Zr/Al show relatively constant distributions up succession in both wells. For example, average Ti/Al values in Beconsall-1Z are 0.049 ± 0.002 in Zone 1 (values that follow \pm represent the standard deviation of each zone), 0.051 ± 0.002 in Zone 2 and 0.053 ± 0.002 in Zone 3. This is similar in Preese Hall-1 where Ti/Al values are 0.056 ± 0.007 (Zone 1), 0.060 ± 0.002 (Zone 2) and 0.062 ± 0.018 (Zone 3). Preese Hall-1 similarly shows relatively unchanging average values in Zr/Al between zones 1, 2 and 3 of 0.0014 ± 0.0002 , 0.0016 ± 0.0001 and 0.0019 ± 0.0013 , respectively. The same is true for Beconsall-1Z with average Zr/Al of 0.0013 ± 0.0001 (Zone 1), 0.0015 ± 0.0001 (Zone 2) and 0.0015 ± 0.0001 (Zone 3). Similar to Ti/Al and Zr/Al, detrital and grain size proxy Th/K is relatively unchanging up succession in Beconsall-1Z with averages of 2.66 ± 1.49 (Zone 1), 3.47 ± 0.76 (Zone 2) and 2.78 ± 1.14 . This is also similar to Preese Hall-1 which has averages of 5.32 ± 1.50 (Zone 1), 4.29 ± 2.87 (Zone 2) and 4.24 ± 1.51 (Zone 3). In Beconsall-1Z, low Th/K standard deviations are clear within Zone 2 (Figure 10), however this differs from Preese Hall-1 where standard deviations are higher in Zone 2 relative to zones 1 and 3.

Ti/Al ranges from 0.038 - 0.058 in Beconsall-1Z and 0.047 - 0.105 in Preese Hall-1. Zr/Al ranges from 0.001 - 0.002 in Beconsall-1Z and 0.001 - 0.005 in Preese Hall-1. The Th/K ratios in Beconsall-1Z ranges from 0.42 - 6.01 ppm/%, whilst this ratio has a wider range in Preese Hall-1 (0.93 - 8.02 ppm/%). Two sample T-tests (Table 4) show differences in Ti/Al, Zr/Al and Th/K between zones 1 and 2 as well as 2 and 3, in both cores, are not significant (95 % CI).

		Ti/Al	Zr/Al	Th/K	U/Al	Mo/Al	V/Al	Mn/Al	S/Al	Fe/Al	Mo/U	TOC	PI	S1	S2	OSI	
		(ppm/%)					(ppm/%)					(%)	(mg/g)		(mg/g)		
Beaconsall-1Z	Zone 3	Min	0.049	0.0013	0.42	0.00010	0.0003	0.0003	34.8	0.41	0.61	1.07	2.1	0.23	0.36	0.00	12.9
		Max	0.057	0.0017	4.18	0.00035	0.0007	0.0022	88.3	0.61	0.87	5.26	3.3	0.34	0.84	1.78	27.3
		Average	0.053	0.0015	2.78	0.00022	0.0005	0.0018	55.8	0.52	0.72	2.70	2.9	0.27	0.53	1.43	18.0
		StDev	0.002	0.0001	1.14	0.00006	0.0001	0.0005	13.9	0.07	0.07	1.14	0.3	0.03	0.14	0.18	4.1
	Zone 2	Min	0.048	0.0013	2.73	0.00016	0.0003	0.0020	41.7	0.27	0.47	1.33	2.4	0.21	0.61	1.30	15.1
		Max	0.058	0.0017	6.01	0.00048	0.0008	0.0115	128.1	0.90	1.50	2.32	4.2	0.36	1.00	2.43	31.2
		Average	0.051	0.0015	3.47	0.00029	0.0006	0.0046	65.0	0.56	0.79	1.95	3.3	0.29	0.77	1.88	23.7
		StDev	0.002	0.0001	0.76	0.00008	0.0002	0.0032	22.2	0.15	0.23	0.29	0.5	0.05	0.14	0.35	4.9
	Zone 1	Min	0.038	0.0012	0.55	0.00014	0.0002	0.0016	28.0	0.34	0.59	0.29	2.4	0.17	0.44	1.23	11.1
		Max	0.054	0.0016	4.41	0.00053	0.0007	0.0685	211.8	0.70	1.17	3.48	4.5	0.32	0.86	3.02	25.5
		Average	0.049	0.0013	2.66	0.00029	0.0004	0.0162	104.4	0.49	0.77	1.66	3.3	0.23	0.59	2.06	18.3
		StDev	0.004	0.0001	1.49	0.00013	0.0002	0.0201	60.0	0.15	0.18	0.94	0.7	0.05	0.12	0.62	4.9
Preese Hall-1	Zone 3	Min	0.051	0.0012	0.93	0.00010	0.0003	0.0016	19.0	0.26	0.50	2.24	0.6	0.16	0.08	0.20	12.6
		Max	0.105	0.0051	5.79	0.00031	0.0019	0.0216	257.4	0.66	1.00	6.56	4.4	0.29	0.93	2.57	21.1
		Average	0.062	0.0019	4.24	0.00021	0.0011	0.0099	69.7	0.52	0.75	3.48	2.9	0.25	0.51	1.59	3.0
		StDev	0.018	0.0013	1.51	0.00006	0.0006	0.0057	82.7	0.14	0.16	1.33	1.5	0.05	0.31	0.83	3.0
	Zone 2	Min	0.059	0.0015	1.20	0.00018	0.0003	0.0057	25.3	0.26	0.41	2.27	1.1	0.25	0.25	0.58	18.8
		Max	0.062	0.0016	6.85	0.00035	0.0005	0.0194	120.0	0.30	0.58	2.71	1.9	0.30	0.36	1.04	23.1
		Average	0.060	0.0016	4.29	0.00026	0.0005	0.0108	65.5	0.28	0.48	2.46	1.5	0.27	0.30	0.83	20.8
		StDev	0.002	0.0001	2.87	0.00008	0.0001	0.0075	48.9	0.02	0.09	0.22	0.4	0.03	0.06	0.23	2.2
	Zone 1	Min	0.047	0.0010	2.80	0.00016	0.0000	0.0021	16.7	0.20	0.34	0.09	1.0	0.18	0.17	0.48	14.0
		Max	0.066	0.0016	8.02	0.00048	0.0006	0.0106	498.5	0.81	0.92	6.53	5.3	0.30	0.94	4.15	20.1
		Average	0.056	0.0014	5.32	0.00029	0.0004	0.0065	143.1	0.36	0.58	2.17	2.6	0.25	0.43	1.43	16.8
		StDev	0.007	0.0002	1.50	0.00010	0.0002	0.0036	175.7	0.19	0.21	1.93	1.6	0.03	0.26	1.11	1.8

		$\delta^{13}C_{V-PDB}$	Averages		
		(‰)	C27	C28	C29
Beaconsall-1Z	Barren Sediment (no goniatites – averaged zones 1 and 3)	-27.7	0.36	0.32	0.37
	Marine Band (Zone 2)	-28.2	0.37	0.28	0.36
Preese Hall-1	Barren Sediment (no goniatites: averaged zones 1 and 3)	-29.4	0.36	0.28	0.37
	Marine Band (Zone 2)	-29.5	0.34	0.28	0.38

Table 3: Elemental proxies and results from Beconsall-1 and Preese Hall-1 (Zone 1, 2 and 3). (StDev = Standard Deviation).

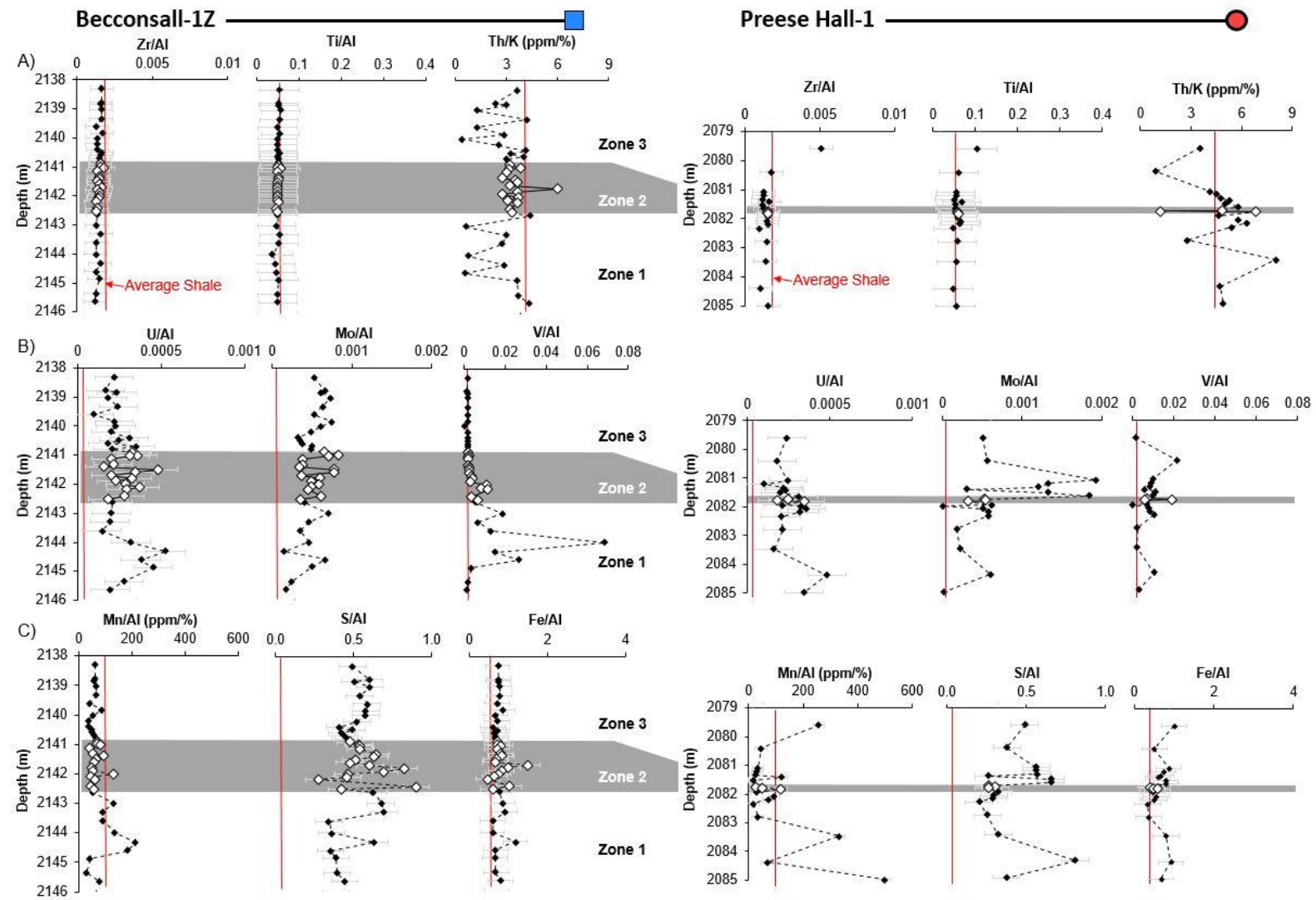


Figure 10: Elemental proxies up succession (Zone 1, 2 and 3) in Becconsall-1Z and Preese Hall-1.

	Proxy	Zone Comparison	Significance	Confidence Interval	P Value
Beaconsall-1Z	Ti/Al	2 & 3	Insignificant	95%	0.163
		1 & 2	Insignificant	95%	0.112
	Zr/Al	2 & 3	Insignificant	95%	0.112
		1 & 2	Insignificant	95%	0.077
	Th/K	2 & 3	Insignificant	95%	0.068
		1 & 2	Insignificant	95%	0.138
	V/Al	2 & 3	Significant	95%	0.004
		1 & 2	Insignificant	95%	0.102
	Mn/Al	2 & 3	Insignificant	95%	0.278
		1 & 2	Insignificant	95%	0.678
	Mo/U	2 & 3	Significant	95%	0.032
		1 & 2	Insignificant	95%	0.357
	TOC	2 & 3	Significant	95%	0.021
		1 & 2	Insignificant	95%	0.920
OSI	2 & 3	Significant	95%	0.002	
	1 & 2	Significant	95%	0.001	
Preese Hall-1	Ti/Al	2 & 3	Insignificant	95%	0.312
		1 & 2	Insignificant	95%	0.144
	Zr/Al	2 & 3	Insignificant	95%	0.559
		1 & 2	Insignificant	95%	0.069
	Th/K	2 & 3	Insignificant	95%	0.978
		1 & 2	Insignificant	95%	0.613
	V/Al	2 & 3	Insignificant	95%	0.867
		1 & 2	Insignificant	95%	0.446
	Mn/Al	2 & 3	Insignificant	95%	0.921
		1 & 2	Insignificant	95%	0.288
	Mo/U	2 & 3	Insignificant	95%	0.073
		1 & 2	Insignificant	95%	0.686
	TOC	2 & 3	Significant	95%	0.039
		1 & 2	Insignificant	95%	0.104
OSI	2 & 3	Insignificant	95%	0.079	
	1 & 2	Insignificant	95%	0.136	

Table 4: Two sample T-test results, showing insignificant or significant differences between elemental proxies of Beaconsall-1Z and Preese Hall-1 zones.

Redox Sensitive Elements

Bottom water redox conditions are typically studied using U/Al, Mo/Al, V/Al, Mn/Al, S/Al and Fe/Al ratios (e.g. Craigie 2018). This study focuses on U/Al, Mo/Al and V/Al due to their known reliability and conservative nature (Craigie 2018). Proxies of Mn/Al, S/Al and Fe/Al were also analysed for this study to aid understanding of bottom water redox conditions.

Figure 11 shows that in Beconsall-1Z, U/Al increases from 0.0001 to 0.0005 from the base of the core to the midpoint of Zone 1 (2145.64 m - 2144.32 m). This gradational increase is later followed by gradational decreases up to the base of Zone 2 (2144.32 m - 2142.52 m). Similar trends are present in Preese Hall-1, but with decreased confidence due to the reduced thickness of the marine band. Preese Hall-1 U/Al increases from 0.0003 - 0.0004 from 2084.98 - 2084.37 m, respectively, then drops to 0.0002 at 2083.46 m. Mo/Al gradationally increases from 0.00017 at the base of the Beconsall-1Z succession (2145.64) to 0.00053 at the top (2138.32 m) with the maximum value near the top of Zone 2 at 0.00083 (2141.00 m). In Preese Hall-1, Mo/Al gradationally increases up succession from 0.00002 at 2084.98 m to 0.0005 at 2079.60 m with sharp peaks of 0.00183 and 0.00192 at 2081.63 m and 2081.08 m, respectively, near the base of Zone 3. Figure 11 shows that, in Beconsall-1Z, V/Al gradationally increases from 0.002 at 2146.04 m at the base of Zone 1 to 0.069 at 2144.00 m near the midpoint of Zone 1. V/Al gradationally decreases from 2144.00 to 0.004 at 2141.80 m. Above 2141.80 m, the V/Al is relatively constant until 2138.32 m (0.002), the top of Zone 3. Preese Hall-1, V/Al averages range from 0.007 ± 0.004 (Zone 1) to 0.011 ± 0.008 (Zone 2) and 0.010 ± 0.006 (Zone 3). Two sample T-tests (Table 4) indicate that the differences in V/Al of zones 2 and 3 are significant in Beconsall-1Z, but not in Preese Hall-1 (95 % CI). Differences in V/Al between zones 1 and 2 are not significant in both cores (95 % CI).

Figure 11 shows that, in Beconsall-1Z, Mo/U values gradationally increase from 0.29 (2144.32 m) - 3.48 from (2143.00 m) in Zone 1 and

average at 1.66 ± 0.94 . Zone 2 Mo/U average values are relatively constant, averaging at 1.95 ± 0.29 . Maximum Beconsall-1Z Mo/U values are observed in Zone 3 at 2139.60 m marking a peak 1.3 m above the base of Zone 2. This trend is also present in Preese Hall-1, where the Mo/U signal is relatively constant in Zone 1 with an average of 2.17 ± 1.93 , but with a slight increase near the top of Zone 1 (2.32 at 2082.07 m). In Preese Hall-1, Zone 2 has an average Mo/U of 2.46 ± 0.22 . Similar to Beconsall-1Z, Zone 3 in Preese Hall-1 has a marked peak in Mo/U near the base of Zone 3 (5.26 at 2081.20 m). Two sample T-tests indicate that differences in the Mo/U of zones 1 and 2 are not significant (95 %) in both cores (Table 4). In Beconsall-1Z, differences between Mo/U in zones 2 and 3 are significant (95 %) but are not significant in Preese Hall-1 (95 %).

The Mn/Al values range from 28.0 - 211.8 ppm/% in Beconsall-1Z and 16.7 - 498.5 ppm/% in Preese Hall-1 (Table 3 and Figure 11). In Beconsall-1Z, average Mn/Al decreases from 104.4 ± 175.7 ppm/% (Zone 1) to 65.0 ± 22.2 ppm/% (Zone 2) to 55.8 ± 13.9 ppm/% (Zone 3). High Mn/Al averages in Zone 1 are also present in Preese Hall-1 (104.4 ± 60.0) relative to zones 2 (65.0 ± 22.2 ppm/%) and 3 (69.7 ± 82.7 ppm/%). In Preese Hall-1 and Beconsall-1Z, two sample T-tests indicate that the differences between Mn/Al in zones 1 and 2 as well as zones 2 and 3 are not significant (95 %). In Preese Hall-1, average S/Al values in zones 1, 2 and 3 are 0.36 ± 0.19 , 0.28 ± 0.02 and 0.52 ± 0.14 , respectively (Table 3 and Figure 10). S/Al for each zone are overall higher in Beconsall-1Z with averages of 0.49 ± 0.15 (Zone 1), 0.56 ± 0.15 (Zone 2) and 0.52 ± 0.07 (Zone 3). In Beconsall-1Z, average Fe/Al values are relatively unchanging between zones 1 (0.77 ± 0.18), 2 (0.79 ± 0.23) and 3 (0.72 ± 0.07). Preese Hall-1 has less similarity between the average Fe/Al of each zone including 0.58 ± 0.21 (Zone 1), 0.48 ± 0.09 (Zone 2) and 0.75 ± 0.16 (Zone3).

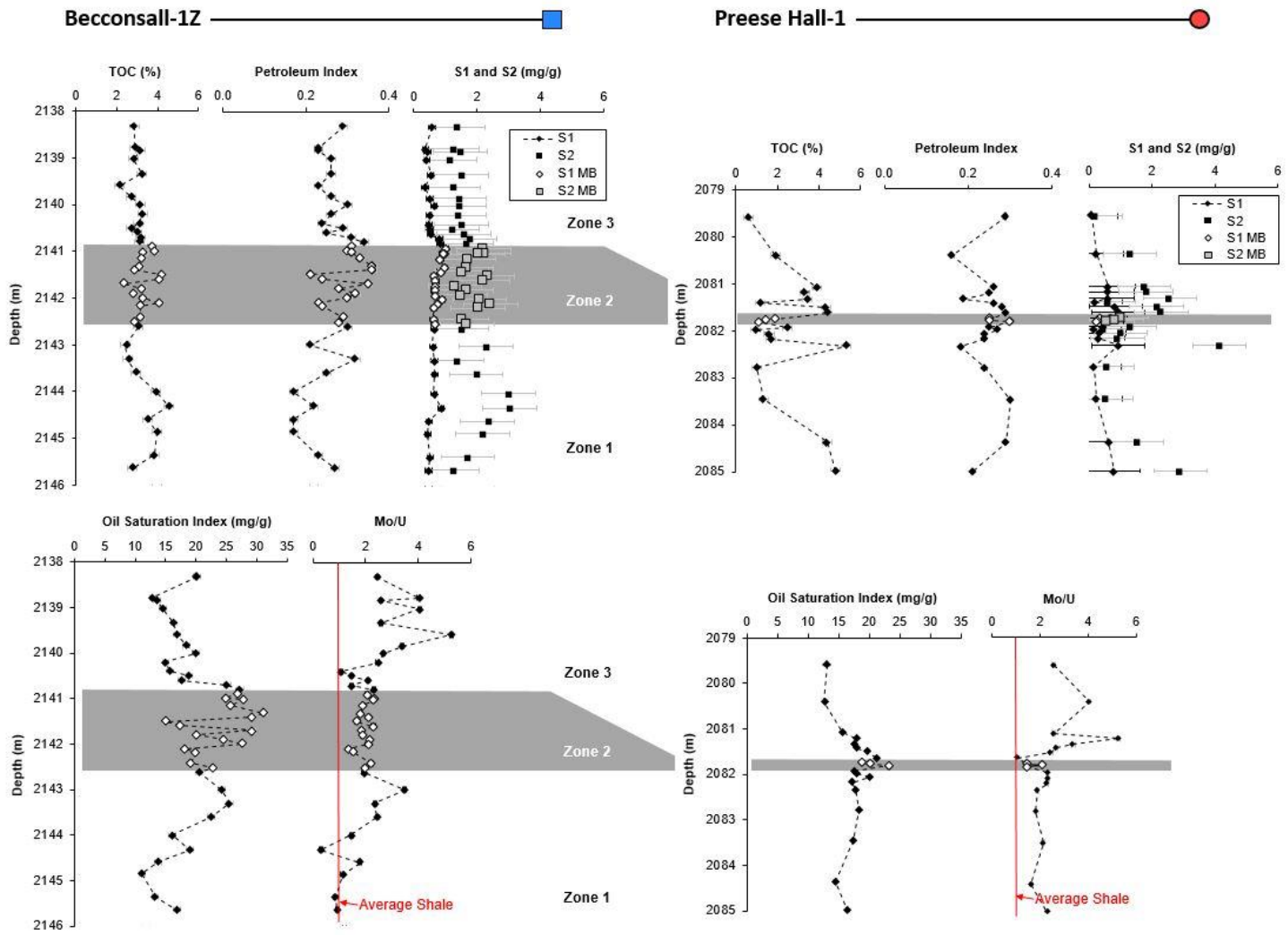


Figure 11: Organic and trace metal proxies up succession in Becconsall-1Z and Preese Hall-1 (Zones 1, 2 and 3).

Organic Geochemistry

The TOC ranges from 2.1 % to 4.5 % in Beconsall-1Z and 0.6 % to 5.3 % in Preese Hall-1 (Table 3 and Figure 10). Averages of TOC are higher in Beconsall-1Z (3.20 %) than Preese Hall-1 (2.43 %). In Beconsall-1Z, Zone 1 has an average TOC content of 3.3 ± 0.7 , Zone 2 the average TOC is 3.3 ± 0.5 and in Zone 3 the average TOC is 2.9 ± 0.3 (Table 3 and Figure 11). In Preese Hall-1, average TOC contents differ between 2.6 ± 1.6 (Zone 1), 1.5 ± 0.4 (Zone 2) and 2.9 ± 1.5 (Zone 3). In Beconsall-1Z and Preese Hall-1, two sample T-tests indicate that the differences in TOC signals between zones 2 and 3 are significant (95 %). In both cores, two sample T-tests (Table 4) indicate that the differences in TOC between zones 1 and 2 are not significant (95 %).

The pyrolysis-derived proxy S1 represents the amount of free hydrocarbons and S2 values represent the amount of hydrocarbons generated through thermal cracking of non-volatile OM (Peters et al. 1980). S1 ranges from 0.36 - 1.00 mg/g in Beconsall-1Z and 0.08 - 0.94 mg/g in Preese Hall-1. S2 ranges from 0.00 - 3.02 mg/g in Beconsall-1Z and 0.20 - 4.15 mg/g in Preese Hall-1. Increased error ranges in S2 decrease confidence in trends.

Petroleum Index (PI) values typically reflect thermal maturity, calculated as $PI = S1/[S1 + S2]$ (Farrimond et al. 1998). PI values range from 0.17 to 0.36 in Beconsall-1Z and 0.16 to 0.30 in Preese Hall-1. Both maximum values in both cores are recorded in Zone 2. All PI values are < 0.4 in both cores (Table 3 and Figure 12).

Figure 12 and Table 3 shows that OSI values range from 11.1 to 31.2 mg/g in Beconsall-1Z and 12.6 to 23.1 mg/g in Preese Hall-1. In Beconsall-1Z, OSI gradationally increases from 2145.64 m, the base of Zone 1 (16.91 mg/g) to 2142.62, the top of Zone 1 (20.59 mg/g). OSI values in Beconsall-1Z Zone 2 record an average of 23.7 ± 4.9 mg/g. Maximum OSI values in Beconsall-1Z (31.2 mg/g) are within Zone 2. OSI values gradationally decrease from 2140.90 m, the base of Zone 3 (26.7 mg/g) to 2138.78 m, near the top of Zone 3 (12.89 mg/g) (Table 3 and

Figure 11). Similar increases in OSI within Zone 2 (marine band) are present in both cores (maximum OSI in Zone 2 in both cores), although this characteristic is more pronounced in Becconsall-1Z than Preese Hall-1. Two sample T-tests indicate that differences in OSI between Becconsall-1Z zones 1 and 2, as well as 2 and 3, are significant (95 % CI).

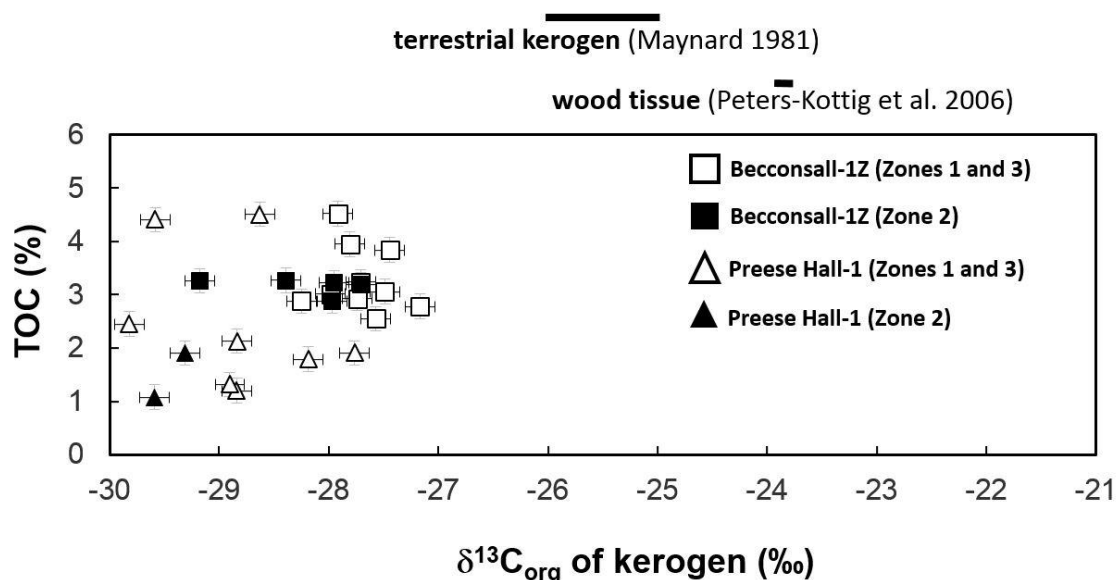


Figure 12: Organic carbon isotopes versus TOC (Preese Hall-1 and Becconsall-1Z). For reference, Carboniferous terrestrial material standards from Peters-Kottig et al. (2006) and Maynard (1981) are included above.

Average $\delta^{13}\text{C}_{\text{org}}$ (‰) values for barren sediment in Becconsall-1Z combines zones 1 and 3. Becconsall-1Z barren sediment, mudstones without goniatites, average at -27.7 ‰ (Table 3 and Figure 12) and Zone 2 in Becconsall-1Z has an average of -28.2 ‰. Becconsall-1Z OM is isotopically heavier than Preese Hall-1 in both barren sediment (-29.4 ‰) and Zone 2 (-29.5 ‰).

Steranes of C_{27} , C_{28} and C_{29} are investigated for OM provenance (Huang and Meinschein 1979; Shanmugam 1985). All values plot on or near to the transition between estuarine/ open marine and terrestrial zones in a sterane ternary plot (Figure 13). Steranes of C_{27} in barren sediment average at 0.36 in Becconsall-1Z and Preese Hall-1. Zone 2 has higher C_{27} sterane values in Becconsall-1Z (0.37) than in Preese Hall-1 (0.34). In Preese Hall-1, barren sediment and Zone 2 both have average C_{28} sterane

values of 0.28. Beconsall-1Z records C_{28} sterane values of 0.32 for barren sediment and 0.28 for Zone 2. C_{29} sterane values average at 0.37 for barren sediment and 0.36 for Zone 2 in Beconsall-1Z. Similarly, C_{29} sterane values average at 0.37 for barren sediment and 0.38 for Zone 2 in Preese Hall-1.

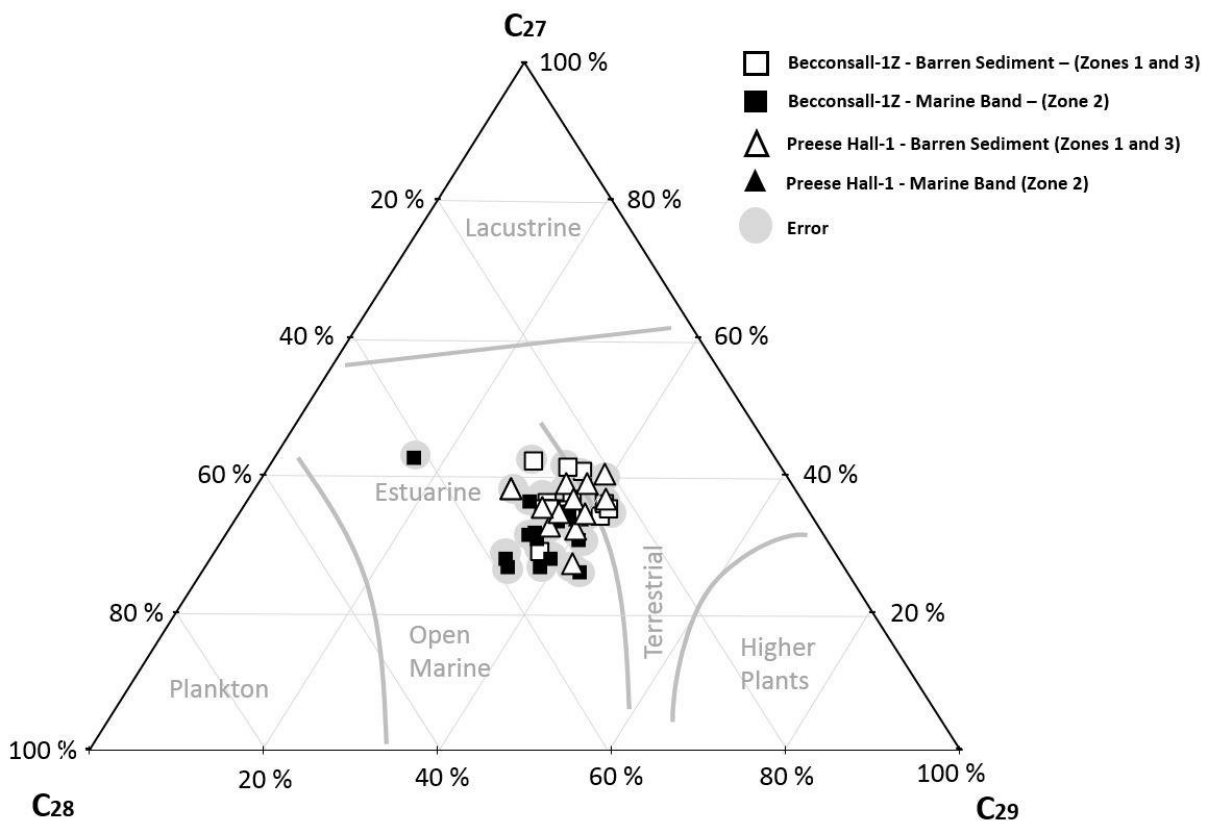


Figure 13: Ternary plot of C_{27} , C_{28} and C_{29} steranes from Beconsall-1Z and Preese Hall-1 barren (Zone 1 and 3) and marine band (Zone 2) sediment.

Discussion

Lithology and Mineralogy

The studied intervals in Beconsall-1Z and Preese Hall-1 are dominated by parallel laminated mudstone with localised cross and undulating laminations. Similarities in sedimentary texture and structure suggests a similar depositional environment for upper Bowland Shale Formation mudstones in this study interval. The unchanging distribution of provenance proxies (Ti/Al, Zr/Al and Th/K) throughout the cores, textural observations under SEM and clay mineralogy suggest that the provenance and the mode of deposition was constant throughout this succession. Therefore, changes in trace metal geochemistry are controlled by other palaeoceanographic conditions. For example, stratigraphic changes in redox sensitive element abundances (e.g. Mo and U) in this upper Bowland succession are predominantly controlled by bottom water redox conditions, such as anoxia (Calvert and Pederson 1993) and not by changes in heavy mineral and/or detrital influx.

Marine band E₁B₂ represents Zone 2 in this study. As this stratigraphic interval is defined by the first and last occurrence of goniatite fossil *Tumulites pseudobilingue*, marine band thickness refers to the “observed minimum goniatite phase thickness”. While using marine band as a correlation tool, care should be taken to account for marine band thickness uncertainties. For example, sampling bias, fossil preservation and goniatite fossil scarcity are likely to affect the reported thickness of the marine band (Zone 2). Although these factors can influence geochemical interpretations (Craigie 2018), biostratigraphy is highly reliant upon variables of which XRF is not, such as fossil occurrence.

Due to the above limitations of goniatite index fossil identification, previous studies aimed to use inorganic geochemistry for improved correlation (Davies and Elliott 1996; Hawkins et al. 2013). In the majority of previous case studies, provenance and heavy mineral input proxies (e.g. Th/K) were used for correlation. These proxies typically reflect grain size variation between the marine band and barren sediments above and

below. Analyses of detrital input to the basin (Figure 2) used Ti/Al, Zr/Al and Th/K ratios (Table 3 and Figure 10) as suggested by Kumpan et al. (2014). In Preese Hall-1 and Beconsall-1Z, these proxies do not differ significantly between zones (Table 3, Figure 10 and Table 4) which importantly suggests that changes in heavy mineral input and grain size do not obscure redox sensitive element abundances (e.g. Mo).

From proximal (Preese Hall-1) to distal (Beconsall-1Z), however, this succession differs in Th/K, Ti/Al and Zr/Al, reflecting subtle differences in cross-basinal heavy metal input and deposition. This does not affect correlation, however, because this study compares differences between zones. These cross-basin differences are subtle and likely do not represent a difference in provenance to each core location (Fraser and Gawthorpe 1990; Fraser and Gawthorpe 2003; Waters et al. 2009). Instead, the differences in heavy metal input/deposition may be linked to local sedimentation and/or differences in basinal subsea topography associated with local features such as the Beconsall-Ashnott High (Clarke et al 2018; Lawrence et al. 1987; Figure 2). In this scenario, seabed topography drives fluctuations in bottom water currents/energy, but the relative importance of these local factors to the primary sedimentary input is uncertain.

Other marine bands in the literature record increases in authigenic kaolinite which further supports bottom water anoxia during deposition and eogenesis (Hawkins et al. 2013). However, this is not observed in this current study (Table 2). The absence of observed authigenic kaolinite may be a result of burial depths that exceed c. 2500 m that led to high illite/muscovite abundances in place of typical authigenic kaolinite through illitization (Bjørlykke et al. 1995; De Pater 2011; Hawkins et al. 2013; Williams and Ferrell 1991). For example, thermal depositional models of the upper Bowland suggest that these successions have been buried >5000 m (Andrews 2013a). However, organic-illitization relationships are complex and varied with high uncertainty (Thomas 1986; Worden et al. 2003). Mineralogical abundances in this current study are consistent with

other upper Bowland Shale Formation studies (Fauchille et al. 2017; Gross et al. 2015) which show relatively unchanging mineral abundances throughout the formation. However, Table 2 and Figure 8 observe the upper Bowland to be quartz dominated whereas Gross et al. (2015) records it to be clay mineral dominated. This difference may be a factor of provenance proximity, for example the sample suite used in Gross et al. (2015) are further from the northern primary sedimentary provenance (Fraser and Gawthorpe 2003) than Beconsall-1Z and Preese Hall-1.

Redox Sensitive Elements

Differences between Mo, Mn, U and V signals are known to record differences in redox sensitivities and/or water to sediment transport mechanisms (Algeo and Tribovillard 2009; Beck et al. 2008; Tribovillard et al. 2012). Redox sensitive elements U and Mn share similar trends across all three zones in both cores and may therefore be reliable indicators of marine bands, at least in this study area. Differences between Mo and U trends may reflect relative changes in the chemocline above goniatite-bearing sediments (Curtis 1964; O'Mara and Turner 1997; Spears 1964b) and/or fluctuations in palaeosalinity known to be closely linked with Mo dissolution (Prange and Kremling 1985). For example, Mo uptake in sediments is typically reliant upon thiomolybdate whereas uptake of U is accelerated by the formation of organo-metallic ligands, however there are numerous variables (Algeo and Tribovillard 2009). For this study area, it is possible that the relative abundance of thiomolybdate shuttles, relative to organo-metallic ligands increased up succession. Furthermore, marine band U enrichment has been recognised elsewhere in Britain, such as the Mansfield Marine Band in the Yorkshire-Derbyshire Coalfield (Spears 1964a) and *Gastrioceras listeria* in Sheffield (Fisher and Wignall 2001) as well as *Gastrioceras subcrenatum* in South Wales (Bloxam and Thomas 1968).

Therefore, Mo and U relationships can be useful in establishing marine band correlation, and importantly can be characterised with non-destructive techniques. The Mo/U signals may suggest that the most

intense and/or sustained water column stratification occurred just above the goniatite-bearing zone during oceanic anoxia (Tribovillard et al. 2012). However, this current study illustrates the relevance of marine band associated Mo/U signals in relatively enclosed basins, such as the upper Bowland. Mo/U can document changes in intense and/or sustained water column stratification (Tribovillard et al. 2012). For example, high Mo/U at the base of Zone 3 may be linked to the preservation of goniatites in Zone 2. In this scenario, increases in Mo/U document increased and/or sustained water column stratification, resulting in low oxygen bottom waters, during and after goniatite fauna deposition, resulting in enhanced Mo relative to U. Alternatively, this trend may indicate Mo and U decoupling, perhaps related to enhanced palaeosalinity and high salinity water influx, previously recorded by the biomarker gammacerane in the Widmerpool Trough (Gross et al. 2015). Further evidence is necessary from basin-wide analyses to resolve whether Mo-U covariation and/or palaeosalinity can explain Mo/U correlation.

Limitations of trace metal geochemical marine band correlation include the reliance upon marine band thickness, which is also true for biostratigraphy. For example, geochemical interpretations are qualitatively more reliable in a thick marine band (168 cm Beconsall-1Z) than a thin one (6 cm in Preese Hall-1). However, this is most likely a universal challenge. Therefore, future geochemical marine band studies should aim to characterise marine bands with thicknesses greater than 6 cm.

Redox sensitive trace metal proxies of Mo/Al, U/Al, V/Al, Mn/Al and Mo/U (Figure 10 and Figure 11) show different stratigraphic increases to the relatively unchanging signals of Th/K, Ti/Al and Zr/Al. Therefore, redox sensitive element proxies most likely represent water column stratification with limited association to sedimentary input. Each of the U/Al, Mo/Al, V/Al and Mo/U typically indicate increased abundance of redox sensitive trace metals, relative to "average shale" (Wedepohl et al. 1991; Wedepohl 1969-1978) in both cores. This suggests that bottom water anoxia / water column stratification occurred in both the central and southern Bowland

Basin. Therefore, it is possible that anoxia was basin-wide and possibly beyond the basin margins because the E₁B₂ marine band extends beyond the Bowland Basin, into Germany (Horn 1960; Korn and Horn 1997) and North America (Nikolaeva 2013). However, future work should aim to test the limits of this hypothesis.

Organic Geochemistry

Organic geochemistry (e.g. $\delta^{13}\text{C}_{\text{org}}$ and C₂₇, C₂₈, C₂₉ steranes) is not a time efficient marine band correlation proxy, particularly in mature mudstones (Romero-Sarmiento et al. 2014; Smith et al. 2017).

Relative abundances and distributions of TOC, $\delta^{13}\text{C}_{\text{org}}$ and C₂₇, C₂₈, C₂₉ steranes across the zones suggest that OM provenances are constant between Beconsall-1Z and Preese Hall-1. However, significant differences in TOC between zones 2 and 3 (two sample T-test) as well as qualitative and interpreted increases in isotopically heavier $\delta^{13}\text{C}_{\text{org}}$ in Zone 2 may reflect relative increases in algal input/preservation in the central basin compared with the more distal south. Marine band E₁B₂ may be subtly more enriched in relative algal abundance than barren sediment. This is perhaps due to increased productivity and/or preservation of OM during a highstand (Canfield 1994; Hedges and Keil 1995).

This study shows that OSI is an unexpected proxy for the identification of marine bands because increases in OSI may reflect increased oil generation and/or retention (Lopatin et al. 2003). Therefore, it is possible that these OSI signals reflect a secondary response to increases in relative OM productivity/ preservation during marine band formation and/or increases in mudstone oil retention.

Relationships Between Geochemistry and Sequence Stratigraphy

Integrating sequence stratigraphy and geochemistry requires a synthesis of large and small scale schematics from previous studies which suggest that the levels of anoxia (Gross et al. 2015; Holdsworth and Collinson 1988) and/or sediment deposition (Martinsen et al. 1995; Maynard 1992) can be used to interpret key sequence stratigraphic boundaries. These key

boundaries include transgressive systems tract (TST), maximum flooding surfaces (MFS), highstand systems tract (HST) and falling stage systems tract (FSST).

In previous studies, TOC and gamma ray well logs are used to interpret sea level changes and sequence stratigraphic boundaries (Gross et al. 2015; Slatt and Rodriguez 2012). However, in this current study, TOC significantly differs between zones 2 and 3, but not between zones 1 and 2. Therefore, TOC is not always a useful proxy for all stratigraphic correlation and interpretation.

Zone 1 (below marine band) likely represents the transgressive systems tract (TST) because sediments are not fossiliferous and OSI values increase gradationally (most likely representing relative gradational increases in terrestrially sourced OM abundance). Therefore, sea levels of Zone 1 were not sufficiently high to preserve the thick-shelled goniatites of E₁B₂ (Figure 14). Furthermore, the fluctuating Th/K, Mn/Al, U/Al and V/Al signals in Zone 1, relative to Zone 2 (Figure 10), suggest that the boundary marked by the occurrence of *Tumulites pseudobilingue* is linked to a sea level and chemocline instability. Additionally, Mo/U signals gradationally increase up Zone 1 in both cores and the transition from Zone 1 to Zone 2 is marked by a decrease in Mo/U, further supporting a link between goniatite preservation and chemocline behaviour, related to increasing palaeobathymetry (transgression).

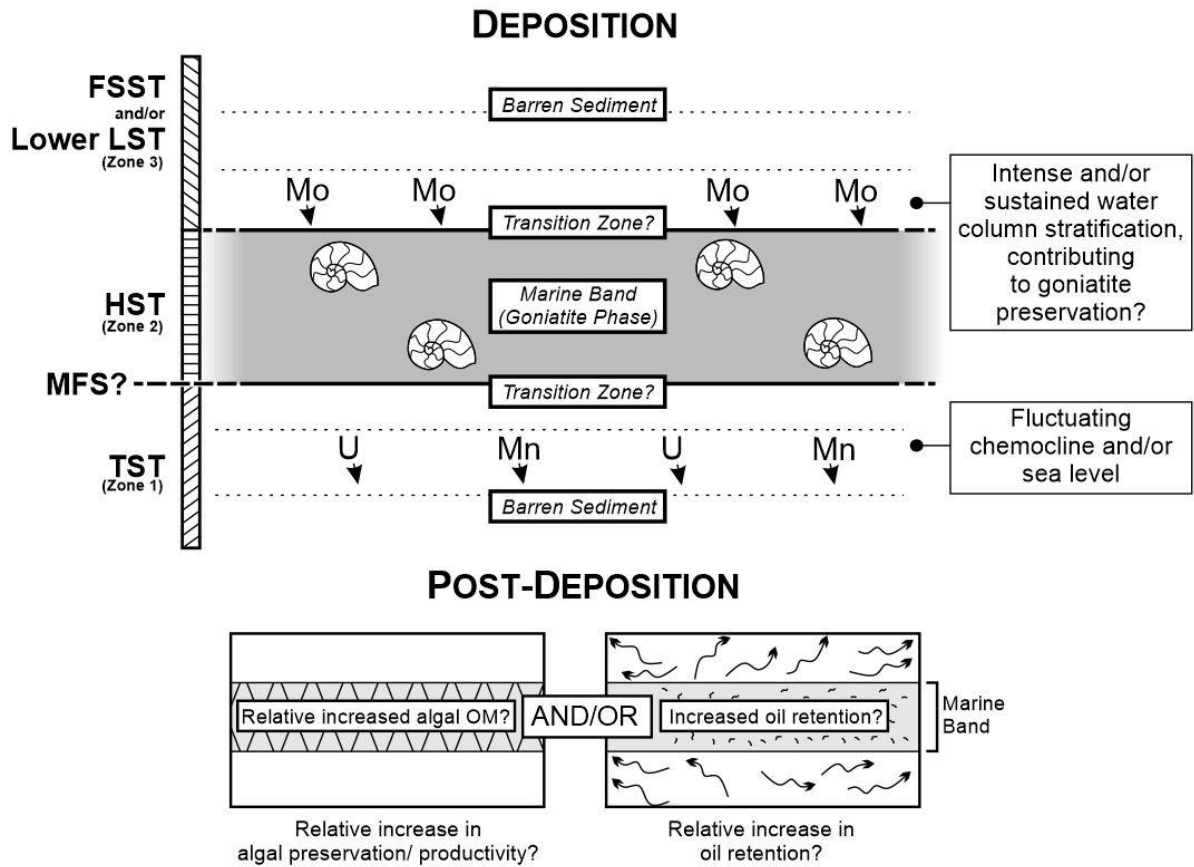


Figure 14: Summary diagram of marine band correlation using geochemistry.

Zone 2 (goniatite-bearing marine band) may broadly represent the highstand systems tract (HST) and/or the maximum rate of sea level rise (Figure 14). This is because goniatites are observed, OSI values are elevated (most likely representing relative increases in marine-derived OM abundance). Zone 2 was most likely deposited during a period of increased water column stratification (leading to goniatite preservation). The timing of this increased and/or sustained water column stratification is unclear, in part because differences between OSI (organic) which peaks within the marine band, and Mo/U (trace metal) which peaks above Zone 2 (marine band), may be representative of the characteristic difference between OM and trace metal abundances and how they are preserved in the rock record. For example, OM can be more readily translated into the sedimentary record and less susceptible to eogenetic processes and the link between TOC and redox sensitive elements is not always direct (Craigie 2018; Craigie 2015). However, the transition from goniatite-rich and high OSI (Zone 2) to barren and low OSI (Zone 3) sediment is linked to the Mo/U peak at the base of Zone 3. Therefore, alternatively, the relative increase in preserved marine OM (leading to elevated OSI) alongside goniatite fossils are the product of increased water column stratification represented by Zone 2 and sustained water column stratification during the stratigraphic transition from Zone 2 to Zone 3 (high Mo/U directly above Zone 2).

Zone 3 likely represents the falling stage systems tracts (FSST) or lower part lowstand systems tract (LST) (Figure 14). The stratigraphic boundary between Zone 2 and Zone 3 is marked by a significant difference (two sample T-test) in the TOC signal in both cores, supporting previous work that suggests TOC is a useful indicator of the HST to FSST transition (Slatt and Rodriguez 2012). The gradational decreases in OSI up Zone 3 may reflect a return back to the original palaeobathymetry. However, increased fluctuation of Mn/Al and U/Al, relative to the FSST suggest that the chemocline was more stable during the TST than the FSST.

Therefore, if these stratigraphic interpretations are accurate, the boundary between Zone 1 and Zone 2 likely represents the maximum flooding surface (MFS). This supports previous models (Martinsen et al. 1995) that suggest the MFS lies near the base of the marine band (Figure 14).

Barren sediments (zones 1 and 3) are separated by what may be interpreted as a marine band goniatite phase transition zone (Zone 2). For example, S/Al, U/Al, V/Al in Beconsall-1Z and Mn/Al typically show more heterogeneity below the marine band than above. This may suggest that the chemocline and the associated transgression (and/or rate of transgression) is less stable than regression. Suggestions of local and/or eustatic Mississippian sea level changes and/or rate of sea level change (Maynard and Leeder 1992; Maynard 1992) transgressed and regressed asymmetrically, perhaps fluctuating more during transgression than regression. This model does not complement previous, more symmetrical schematics (Gross et al. 2015; Holdsworth and Collinson 1988) that imply sea level changes transgress and regress similarly. Instead, the geochemistry of marine band E₁B₂ in Preese Hall-1 and Beconsall-1Z is similar to asymmetrical TST and FSST, which are typical of dynamic eustatic curve models (Algeo et al. 2004; Slatt and Rodriguez 2012).

Inconsistencies and uncertainties concerning high resolution stratigraphic models limit the development of sequence stratigraphic interpretations. Future work on marine bands should apply a similar methodology to the one presented in this study.

Conclusion

1. Pyrolysis-derived OSI is introduced as a proxy for marine band identification in mature, buried OM rich sediments, such as the upper Bowland Shale Formation. Increases in oil retention and/or generation are typically related to the thermal maturation of OM. However, in Beconsall-1Z and Preese Hall-1, OSI is proposed for identification of marine bands >6 cm thick. Future work on marine band identification should investigate (i) the relative importance of

- oil retention to oil generation within marine bands and (ii) elevated OSI in other marine bands.
2. Correlation of upper Bowland marine band E₁B₂ may be achievable using Mo/U, reflecting increased and/or sustained water column stratification or changes in chemocline stability in the transition from Zone 2 to Zone 3. Increases in Mo/U likely represent low oxygen bottom waters during and after goniatite fauna deposition, most likely reflecting preservation processes associated with goniatite preservation.
 3. The changes in redox sensitive trace metal abundances proxies (e.g. V/Al) up succession and between Beconsall-1Z and Preese Hall-1 indicate that the level of bottom water oxygen depletion in the Preese Hall-1 and Beconsall-1Z was spatially and temporally variable.
 4. Despite differences in the spatial and temporal abundances of redox sensitive elements, proxies such as Zr/Al, Ti/Al and Th/K are relatively constant in Preese Hall-1 and Beconsall-1Z, suggesting that the provenance was constant through time.
 5. This study does not observe elevated authigenic kaolinite abundances within marine band E₁B₂ that are previously recorded in other marine bands (Hawkins et al. 2013). However, the relative absence of kaolinite and presence of illite is most likely linked to diagenesis-induced illitization associated with high temperatures (Huyghe et al. 2011). Interpretations of high temperatures are supported by PI values, all >0.16 (mature oil window) and relatively low maximum S₂ values (4.15 mg/g in Preese Hall-1 or 3.02 mg/g in Beconsall-1Z) and this agrees with previous studies that model upper Bowland burial depth of > 5000 m (Andrews 2013c).
 6. Preserved organic $\delta^{13}\text{C}_{\text{org}}$ infers that upper Bowland OM is algal (autochthonous) dominated with some subordinate land-derived (terrestrial) contribution, recorded by sterane ternary diagrams that suggest upper Bowland OM could have had both an estuarine and terrestrial provenance.

7. Goniatite enrichment in upper Bowland marine band E₁B₂ is most likely the product of oxygen-poor bottom waters that promoted fossil preservation. A period of sustained water column stratification may have occurred during and/or immediately after goniatite deposition, causing relatively high Mo/U values (5.3 in both cores) immediately above the marine band. Values of OSI typically an indication of thermal maturity, may be elevated within the marine band as a result of minor differences in OM preservation during deposition and eogenesis, perhaps promoting small increases in the generation potential post-deposition. Alternatively, differences between organic and trace metal signals (e.g. maximum OSI within the marine band and maximum Mo/U above) may be because the mechanics that preserve OM and redox sensitive element abundances are different (Craigie 2018; Craigie 2015).
8. Future marine band correlation studies should aim to synthesise the large scale (sequence stratigraphy) and the small scale (geochemistry). A multi-disciplinary (biostratigraphical, sedimentological, geochemical and computer science) approach is recommended.

Chapter 6. Palaeoceanography of the Bowland Shale Formation (Mississippian, Carboniferous): a Shale Gas Target.

Abstract

Palaeoceanographic processes in geological basins directly translate into the geochemistry of petroleum source rocks and their hydrocarbon generation potential. Despite the benefits that geochemistry provides to petroleum systems interpretation, these analyses are complicated for thermally mature source rocks and therefore have not been fully utilised in the Bowland Shale Formation in the UK, a promising shale gas target. In this study, the palaeoceanography of the upper Bowland Shale Formation in the Bowland Basin, Lancashire, UK is reconstructed using X-ray fluorescence (XRF), Rock-Eval pyrolysis and molecular data from gas chromatography with flame ionisation detector (GC-FID) applied to two cores, Preese Hall-1 and Beconsall-1Z. The geochemistry of the upper Bowland Shale Formation in both cores reflects similarities in provenance, despite Preese Hall-1 being more proximal to the primary sedimentary source compared to Beconsall-1Z. Elemental abundances suggest that the mudstones were quartzo-feldspathic in origin, similar to the proximal Millstone Grit Group that overlies the Bowland Shale Formation. Redox sensitive trace metal abundances and enrichment factors (e.g. Mo and U) in combination with low pristane/phytane ratios suggest that bottom water redox conditions were low oxygen (dysoxic and/or anoxic) in both cores, supporting basin-wide enhanced organic carbon burial. Bottom waters in the centre of the Bowland Basin at Preese Hall-1 were possibly euxinic, as indicated by high molybdenum and uranium enrichment factors. These gradual changes in ocean redox were likely related to a topographic high (Beconsall-Ashnott High) that favoured differences in bathymetry and the depth of the chemocline. We compare the restriction of the Bowland Basin with the time-equivalent Fort Worth Basin (Barnett Shale) in the USA to conclude that the Barnett Shale was deposited under extreme basin restriction whereas comparatively low TOC and high Mo in

the Bowland indicates weak restriction during deposition, similar to the Gainsborough Trough.

Introduction

The Early Carboniferous (Mississippian) Bowland Basin (Figure 2) is currently being explored as the primary target for shale gas and onshore petroleum production (Clarke et al. 2018). Prior to any large-scale production of shale gas plays, onshore companies need to confidently identify subsurface target intervals rich in hydrocarbons ('sweet spots'). During this critical exploration phase, geochemistry plays a crucial role in developing detailed palaeoceanographic models of a basin and identifying and characterising intervals of high organic carbon richness (e.g. Craigie 2018). Palaeoceanographic and palaeogeographic conditions are important because zones with abundant organic carbon burial are associated with the centres of basins and ocean water anoxia, in combination favouring carbon burial (e.g. Schlanger and Jenkyns 1976). Sedimentology and X-ray diffraction (XRD) are important techniques typically used to identify stratigraphic intervals between exploration and production wells (e.g. Hancock and Taylor 1978). However, in mudstone dominated formations such as the Bowland Shale Formation, and informal subdivisions such as the upper and lower Bowland Shale Formation (Aitkenhead 1992; Hennissen and Gent 2019), sedimentology and XRD alone do not provide detailed of sufficiently specific information to interpret basin palaeoceanography.

It is important that the geochemistry of time equivalent beds and laminae are compared to best capture stratigraphically related depositional processes. However, this is difficult in the mudstone dominated Bowland Shale Formation (Clarke et al. 2018) where index fossils are typically confined to glacio-eustatic high stands (Bhattacharya 1993; Church and Gawthorpe 1994; Davies and McLean 1996; Dunham and Wilson 1985; Hampson et al. 1997; Isbell et al. 2003; Martinsen et al. 1995; Read et al. 1991) and core material is limited to cored intervals in two wells that have been successfully correlated, Beconsall-1Z and Preese Hall-1.

Well-correlation in the Bowland Basin is typically attained using beds enriched in saline fauna and goniatite index fossils, termed 'marine bands' (e.g. Bloxam and Thomas 1968; Brandon et al. 1995; Davies and McLean 1996). These marine bands are useful time-equivalent stratigraphic marker beds that stretch across large parts of the Bowland Basin (e.g. Gross et al. 2015), but also into Germany (e.g. Korn and Horn 1997) and North America (Nikolaeva 2013). Using biostratigraphy, marine band E₁B₂, identified by the goniatite *Tumulites pseudobilingue* (Hird and Clarke 2012; Hird et al. 2012; Riley 1993), has been used to correlate wells Becconsall-1Z and Preese Hall-1 in the Bowland Basin (Figure 2 and Figure 15). Additionally, marine band cycles in the Bowland Basin and worldwide have previously been linked to well log gamma 'spikes' (Clarke et al. 2018; Davies and McLean 1996; Myers and Wignall 1987; Thomas and Bloxam 1969), but this is not always the case in the Bowland Shale Formation (Clarke et al. 2018). Therefore, low stratigraphic abundances of index fossils (barren sediment) in the Bowland Shale Formation (Clarke et al. 2018) limits the application of time series plots.

However, the Bowland Shale Formation has previously been subdivided into informal lower and upper Bowland Shale Formation stratigraphic successions (Aitkenhead 1992; Hennissen and Gent 2019), suggested to represent the Middle and Upper Mississippian, respectively using gamma ray well logs (Clarke et al. 2018). The upper Bowland Shale Formation is selected for nested, high resolution analyses using available core material with previously collected (Clarke et al. 2018) gamma ray well log and mineralogical data. These data are placed in the context of large scale Upper Mississippian Bowland Basin processes.

Previous interpretations of the Bowland Basin have suggested that the primary sedimentary input to the Bowland Basin (Figure 2) are hemipelagic and turbidite sediments sourced from deltas located to the north (Clarke et al. 2018; Cliff et al. 1991; Collinson et al. 1988; Drewery et al. 1987; Gilligan 1920; Lawrence et al. 1987; Leeder 1988a; Reading 1964), towards the Southern Uplands (Figure 2). In time-equivalent UK

basins, such as the Gainsborough Trough located to the south east of the Bowland Basin (Figure 2), trace metal geochemistry has been used to investigate depositional and eogenetic (early diagenetic) processes (Hennissen et al. 2017; Riley et al. 2018). For example, in the Gainsborough Trough, the relative abundances of redox sensitive elements (i.e. Mo and U) helped identify ocean redox conditions as suboxic and/or anoxic (Riley et al. 2018). Aligned with this approach, this current study uses high resolution organic and inorganic geochemistry to reconstruct the palaeoceanographic and palaeoredox conditions to the Bowland Basin. Palaeomorphology and palaeobathymetry are not well constrained for this basin and have led to conflicting interpretations of topographic highs (e.g. Becconsall-Ashnott High, the Ashnott High, the Bowland High; Figure 15) and their interconnectivity (seismic and gravity maps in Clarke et al. 2018 and sedimentology in Emmings et al. 2019a). This aspect is of relevance for ocean redox development, carbon burial and the correlation of marker horizons (e.g. marine bands).

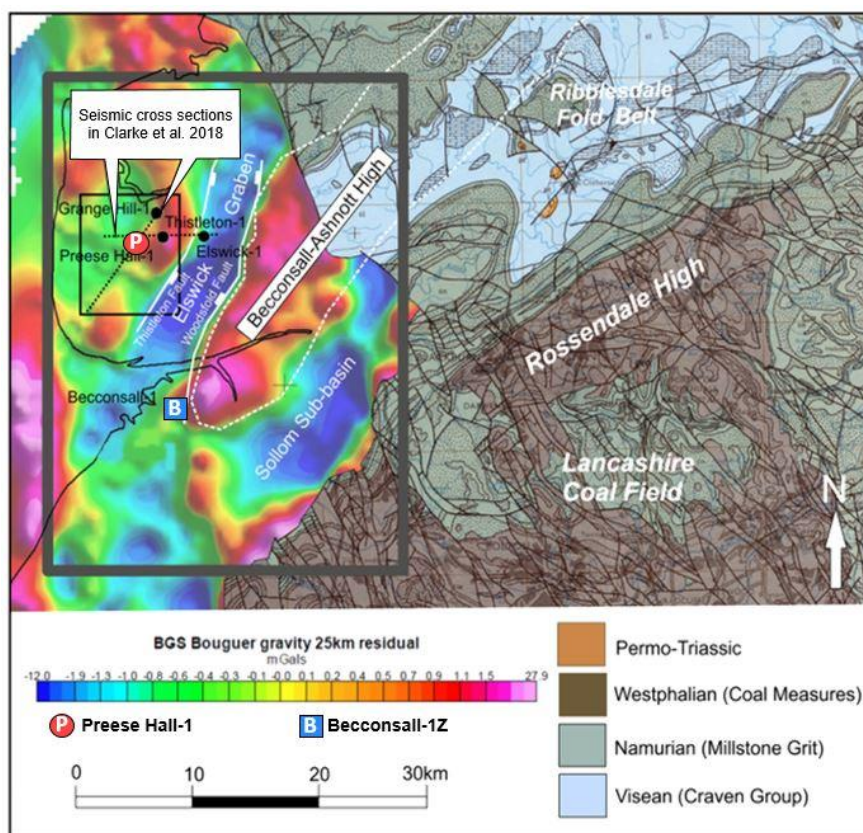


Figure 15: Gravity (Bouguer Anomaly) map of the Bowland Basin (adapted from Clarke et al. 2018).

Two wells proving the upper Bowland Shale Formation, Beconsall-1Z (53° 41' 58.6291" N, 2° 53' 57.3813; BGS reference number SD42SW/11) and Preese Hall-1 (53° 49' 19.006" N; 2° 56' 56.576"; BGS reference number SD33NE/38), were selected for this study. Both cores contain the time-equivalent *T. pseudobilingue* marine band (E₁B₂) defined by goniatite index fossils (Clarke et al. 2018).

The primary aim of this study is to utilise multi-proxy geochemical time series to reconstruct the palaeoceanography of the upper Bowland Shale Formation and prominent mechanisms favouring organic carbon burial. In a secondary step, we investigate similarities and differences of the Upper Mississippian Bowland Basin to other time-equivalent basins in the UK (Gainsborough Trough) and the USA (Fort Worth).

Methods

All upper Bowland Shale cores in Beconsall-1Z and Preese Hall-1 were utilised for geochemical analysis, but uncertainty related to limited core data prevents time series correlations beyond the reference to marine bands. Therefore, a nested sampling strategy was necessary.

This chapter integrated sedimentology (logged using engineering geological standard method BS 5930:1999 lithological determination), digitized gamma ray well data from well reports (Hird and Clarke 2012; Hird et al. 2012), XRD, XRF, Rock-Eval and molecular analyses (see Methodology).

Statistical analyses used two sample T-tests with 95 % CI, however the results must be taken with caution in this chapter because unavoidable core gaps forced unavoidable inconsistencies in sample spacing.

Results

Lithology and Mineralogy

The upper Bowland Shale Formation (Figure 16) comprises 499 m in Preese Hall-1 and 84 m in Beconsall-1Z based on the gamma ray well log and biostratigraphic boundaries (Hird and Clarke 2012; Hird et al. 2012). In both wells, the upper Bowland Shale Formation was mudstone

dominated with cyclical and argillaceous limestone beds. At Preese Hall-1, 334.98 m of upper Bowland Shale was cored with a core recovery of 89.0 % (calculated from Hird and Clarke 2012). At Beconsall-1Z, 9.14 m of the upper Bowland Shale was cored with a core recovery of 88.9 % (calculated from Hird et al. 2012).

Sedimentary logs of Preese Hall-1 indicate extensive interbedded parallel laminae with minor zones of cross-lamination (Figure 16). Beconsall-1Z is dominated by parallel lamination. Both cores contain small lenticular brown-orange clasts (possibly pyrite-rich mud clasts). Overall, logs indicate that Preese Hall-1 contains more undulating laminae and fluid escape structures than Beconsall-1Z.

Gamma values in Beconsall-1Z range from 26.79 - 238.69 with an average of 111.96 ± 45.79 (values that follow "±" represent standard deviation). In contrast, Preese Hall-1 GR values range from 25.33 - 178.66 with an average of 80.00 ± 25.04 . A two sample T-test indicates that there is a significant difference in GR between Beconsall-1Z and Preese Hall-1 (95 % CI).

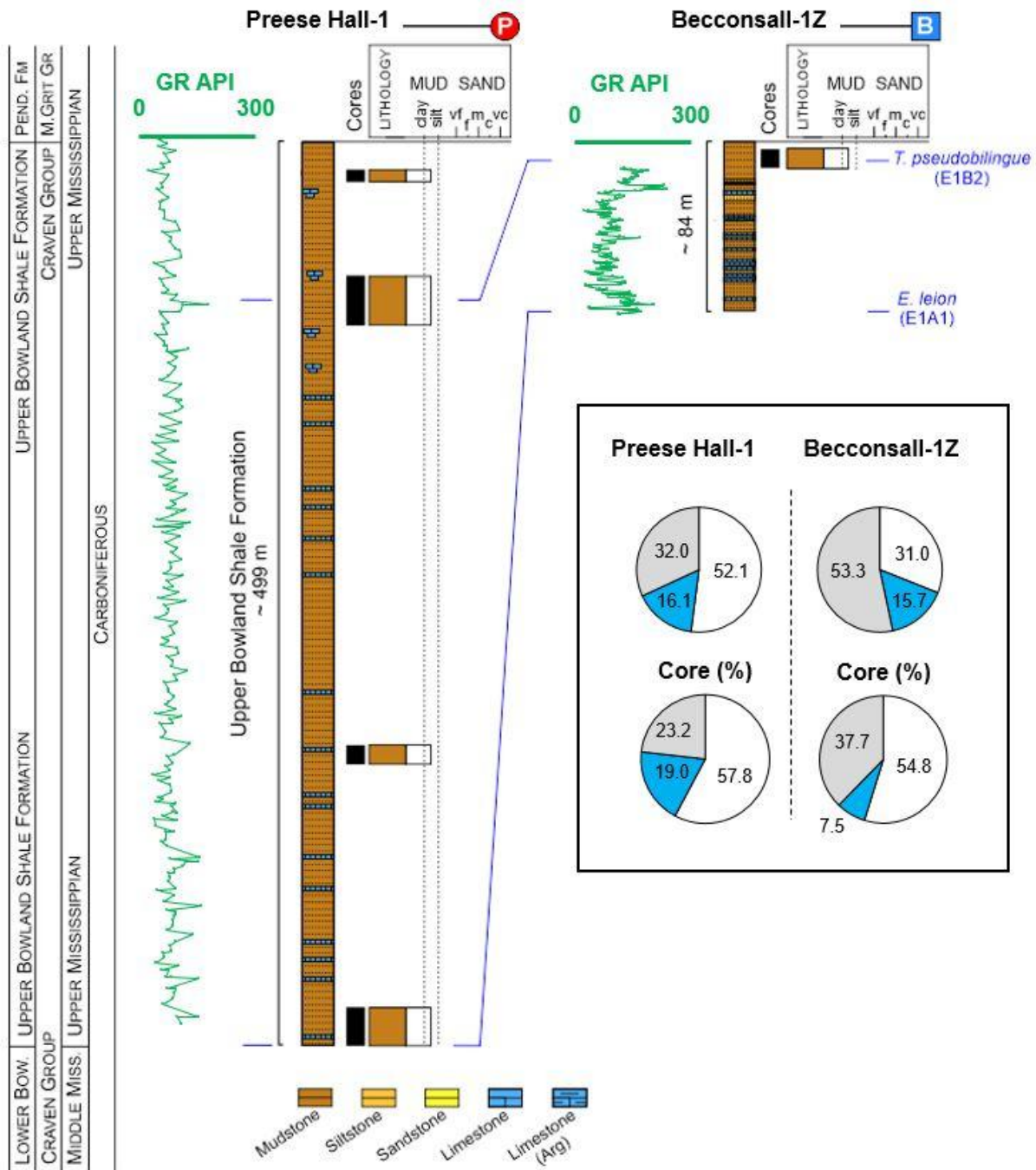


Figure 16: Lithology of the upper Bowland Shale Formation.

The mineralogy of Beconsall-1Z and Preese Hall-1 significantly differ using a two sample T-test. X-ray diffraction (XRD) analysis indicates that the quartz content in Beconsall-1Z ranges from 39.05 - 78.11 % with an average of 56.88 %, relative to total clay mineral and carbonate (Figure 17). Similarly, Preese Hall-1 ranges from 38.68 – 61.32 % with an average of 54.67 %, relative to total clay and carbonate. Additionally, the total clay mineral content for Beconsall-1Z ranges from 10.21 – 46.62 % with an average of 34.57 %, relative to total quartz and carbonate. Preese Hall-1 has significantly lower total clay mineral content (determined by a two sample T-test) and ranges from 6.31 – 24.90 % with an average of 17.53 %, relative to total quartz and carbonate. In contrast, Beconsall-1Z has significantly (determined by a two sample T-test) lower total carbonate content and ranges from 2.51 – 17.30 % in Beconsall-1Z with an average of 8.55 %, relative to total clay mineral and quartz. Preese Hall-1 has a larger range of total carbonate content 16.67 – 55.01 % with an average of 27.80 %, relative to total clay and quartz (Figure 17).

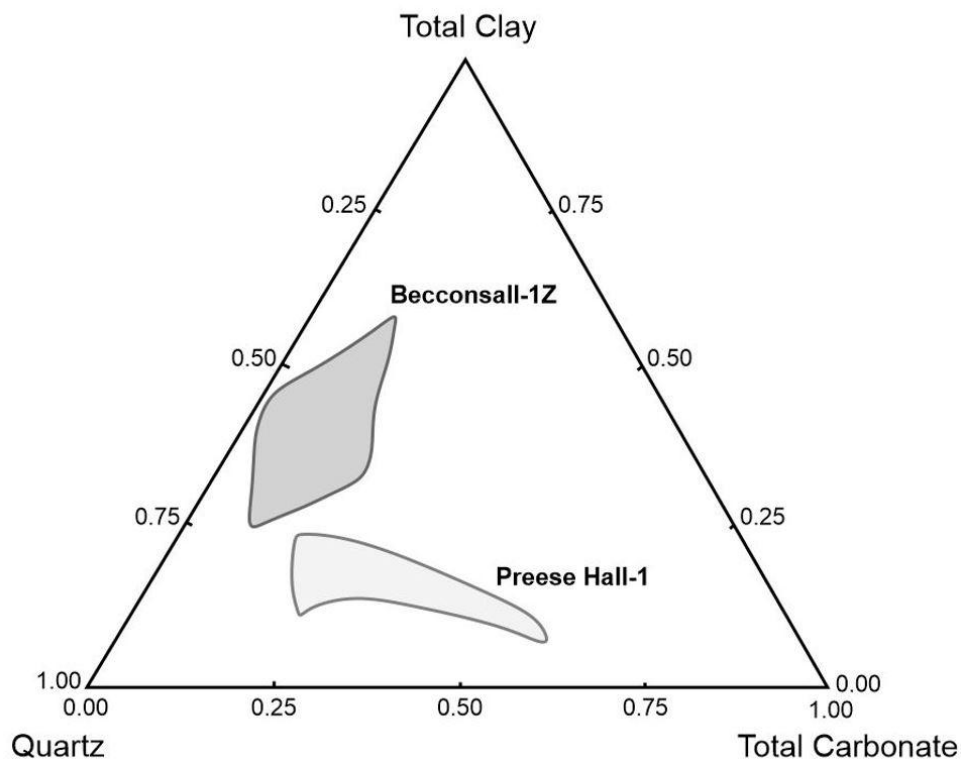


Figure 17: Mineralogy (XRD) in Beconsall-1Z and Preese Hall-1 upper Bowland Shale Formation.

Provenance

Roser and Korsch (1988) proposed using variations of Ti, Al, Fe, Ca, Na and K in a binary diagram, plotted as Discriminant Function (DF) 1 ($-1.773 \text{ Ti} + 0.607 \text{ Al} + 0.76 \text{ Fe} - 1.5 \text{ Mg} + 0.616 \text{ Ca} + 0.509 \text{ Na} - 1.224 \text{ K} - 9.09$) and DF2 ($0.445 \text{ Ti} + 0.007 \text{ Al} - 0.25 \text{ Fe} - 1.142 \text{ Mg} + 0.438 \text{ Ca} + 1.475 \text{ Na} + 1.426 \text{ K} - 6.861$) to interpret mudstone provenances. In Beconsall-1Z, DF1 ranges from 0.23 - 8.61 with an average of 2.72, whereas for Preese Hall-1 the average DF1 was 7.99 and therefore greater, ranging from 1.72 - 20.81. The average DF2 value differs between both wells, -2.43 and -2.51 for Beconsall-1Z and Preese Hall-1, respectively (Figure 18 and Table 5). Preese Hall-1 DF2 values have a larger range of -2.88 - 13.35 compared to Beconsall-1Z which ranges from -5.48 - 2.55. For both wells, DF values typically plot within the intermediate, felsic and quartzose sedimentary provenance zones. In contrast, Preese Hall-1 DF values plot almost entirely within the quartzose sedimentary provenance zone, with two values in the felsic igneous provenance zone. A two sample T-test indicates that there are significant differences in both DF1 and DF2 between the two cores.

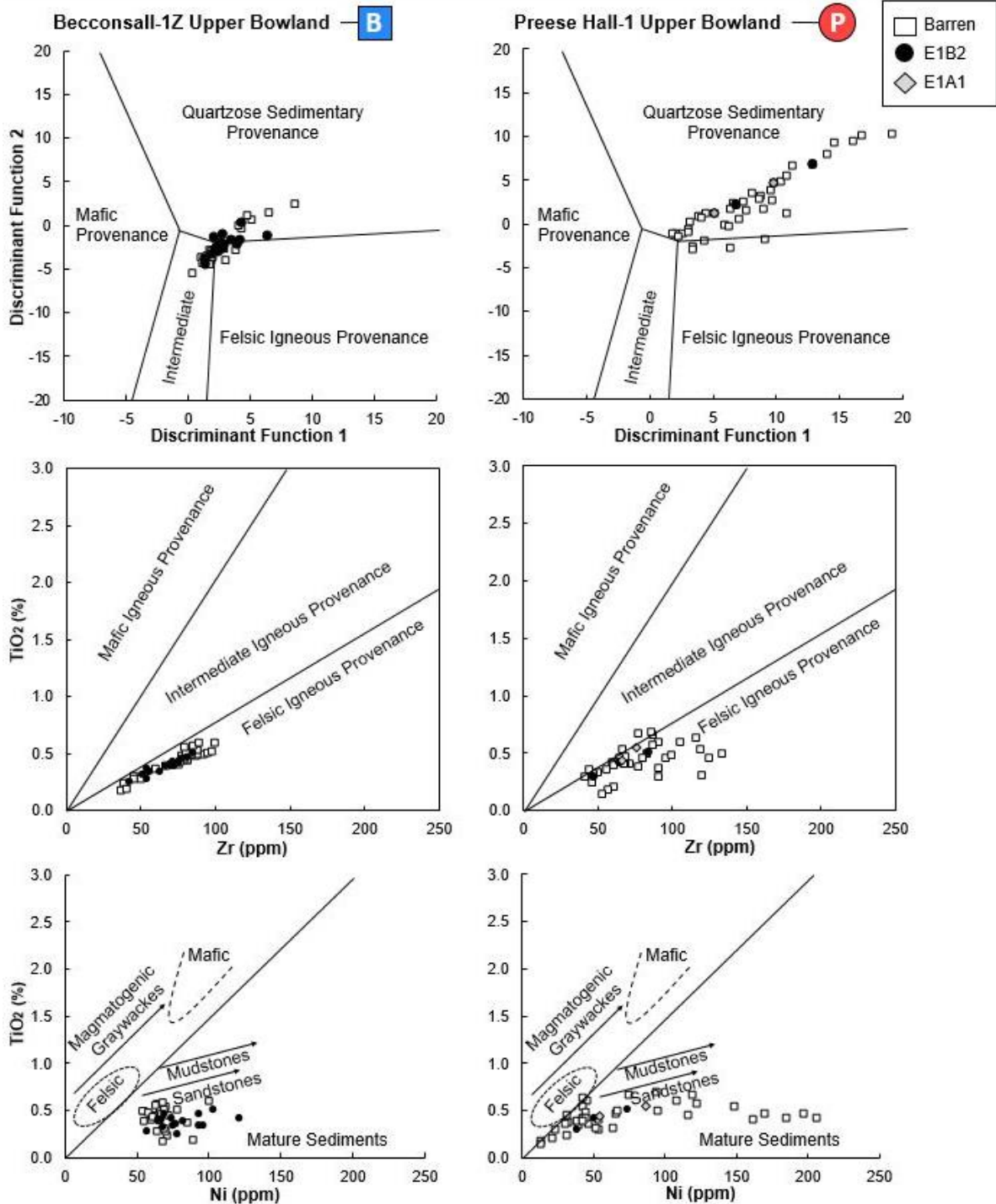


Figure 18: Trace metal provenance proxies for the upper Bowland Shale Formation using Discriminant Function 1 and 2 (after Roser and Korsch 1988), Zr versus TiO_2 (after Hayashi et al. 1997) and Ni versus TiO_2 (after Floyd et al. 1989).

Becconsall-1Z and Preese Hall-1 do not significantly differ (two sample T-test) in their TiO_2 values, 0.42 ± 0.10 % and 0.44 ± 0.13 %, respectively (Figure 18 and Table 5). Similarly, Zr values do not significantly differ (two sample T-test) between Becconsall-1Z and Preese Hall-1 $70.69 \pm$

17.17 ppm and 75.73 ± 23.21 ppm, respectively (Table 5 and Table 6). Based on cross plotted Zr and TiO_2 values, both wells almost entirely fall within the felsic igneous provenance zone. For Ni values, Beconsall-1Z has an average of 72.47 ± 14.35 ppm, whereas Preese Hall-1 has an average of 74.26 ± 51.52 ppm which also indicates that there is no significant difference between wells (two sample T-tests). Binary plots of TiO_2 and Ni indicate that no values plot within the mafic zone. Both cores, based on Ni and TiO_2 values, plot as 'texturally/ mineralogically mature sediment, mudstones and sandstone' provenances, near to the felsic zone (Figure 18 and Table 5).

Upper Bowland Shale Formation Comparison

		DF1	DF2	TiO2 (%)	Zr (ppm)	Ni (ppm)	Mo EF	U EF	P EF	As EF	V EF	Cr EF	Zn EF	Ni EF	Fe EF	S EF	Co EF	Mn EF	Mo (ppm)	TOC (%)	Pr/Ph	PI
Becconsall-1Z	Min	0.23	-5.48	0.18	36.19	54.2	5.25	3.24	0.02	1.44	0.19	1.14	0.95	0.00016	0.88	0.0010	1.65	0.29	4.10	2.14	0.90	0.17
	Max	8.61	2.55	0.60	99.80	121.1	28.07	17.15	15.70	6.14	46.38	14.85	4.01	0.00059	2.78	0.0033	4.47	12.29	48.40	4.52	1.83	0.36
	Average	2.72	-2.43	0.42	70.69	72.5	17.31	8.54	1.28	3.32	4.20	2.06	1.76	0.00028	1.40	0.0019	2.58	1.00	24.55	3.20	1.26	0.26
	StDev	1.68	1.80	0.10	17.17	14.4	5.64	2.94	2.47	1.24	7.51	2.16	0.64	0.00010	0.31	0.0005	0.71	1.80	9.29	0.53	0.24	0.05
Preese Hall-1	Min	1.72	-2.88	0.15	40.90	12.6	0.69	0.88	0.03	0.72	0.80	1.12	0.25	0.00013	0.62	0.0007	0.87	0.09	1.40	0.36	1.26	0.08
	Max	20.81	13.35	0.69	133.10	205.8	64.13	18.10	6.95	16.96	14.61	5.26	4.16	0.00079	9.70	0.0037	26.41	9.54	88.80	5.75	1.77	0.49
	Average	7.99	2.51	0.44	75.73	74.3	18.83	7.34	1.12	3.14	3.75	1.93	1.38	0.00029	1.38	0.0016	2.92	0.92	26.10	2.51	1.48	0.24
	StDev	4.73	3.97	0.13	23.21	51.5	14.60	4.14	1.23	2.57	3.13	0.70	0.89	0.00015	1.35	0.0007	4.00	1.65	22.87	1.42	0.20	0.09

Table 5: Trace metal and organic geochemistry of the upper Bowland Shale Formation. (StDev = Standard Deviation).

Two Sample T-test Measuring the Statistical Difference Between Becconsall-1Z and Preese Hall-1			
Proxy	Significance	Confidence Interval	P Value
GR API	Significant	95%	0.000
Total Clay Mineral	Significant	95%	0.000
Total Carbonate	Significant	95%	0.000
TiO ₂	Insignificant	95%	0.381
Zr	Insignificant	95%	0.256
Ni	Insignificant	95%	0.778
Mo	Insignificant	95%	0.683
Mo EF	Insignificant	95%	0.530
U EF	Insignificant	95%	0.126
V EF	Insignificant	95%	0.717
Zn EF	Significant	95%	0.031
Ni EF	Insignificant	95%	0.778
Mn EF	Insignificant	95%	0.832
Co EF	Insignificant	95%	0.593
TOC	Significant	95%	0.004
Pr/Ph	Insignificant	95%	0.264

Table 6: Two sample T-test results showing statistical differences between Becconsall-1Z and Preese Hall-1. Core availability limits statistical interpretations, therefore these results are used with caution.

Deposition and Eogenesis

Elemental enrichment factors (EF) were used to identify differences in sediment deposition, eogenesis and bottom water redox conditions (Figure 20). The Mo EF values are similar in both cores, however averages in Becconsall-1Z are lower (17.31 ± 5.64) compared to Preese Hall-1 (18.83 ± 14.60) and two sample T-tests indicate that the differences between Mo EF values in Becconsall-1Z and Preese Hall-1 are not significant (95 % CI). Similarly, U EF values are not significantly different (two sample T-tests) between the two cores with an average for Becconsall-1Z of 8.54 ± 2.94 and an average for Preese Hall-1 of 7.34 ± 4.14 . In both wells, nearly all Mo EF values indicate that the basin was near to the weak restriction zone (Figure 19). Mo values were not significantly different (two sample T-tests) between the two wells and range from 4.10 – 48.40 ppm for Becconsall-1Z with an average of 24.55 ± 9.29 ppm versus 26.10 ± 22.87 ppm for Preese Hall-1 (Figure 21).

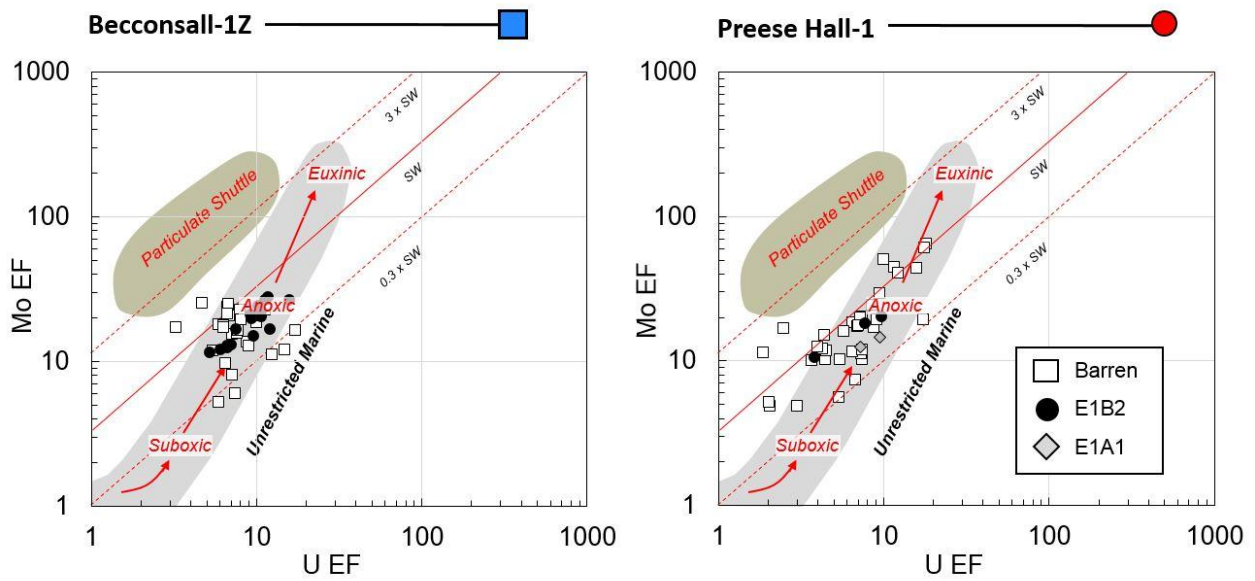


Figure 19: Molybdenum and Uranium trace metal enrichment factors (EF) of the upper Bowland Shale Formation (Beconsall-1Z and Preese Hall-1) using previous annotations of redox states (e.g. Riley et al. 2019).

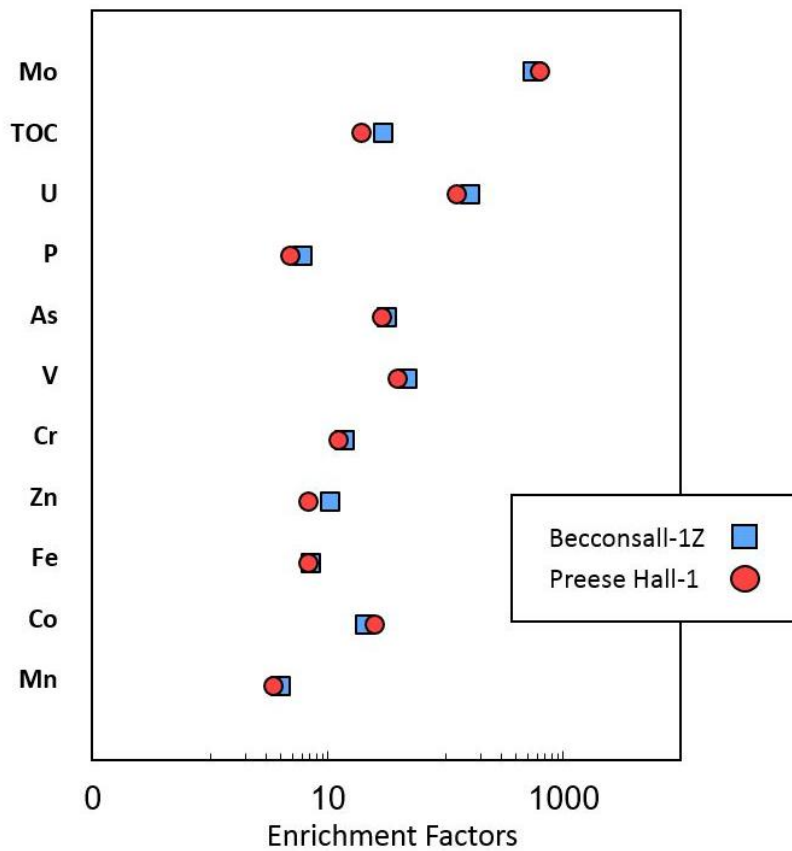


Figure 20: Average enrichment factors (EF) in Beconsall-1Z and Preese Hall-1.

No single trace metal proxy can be used to identify anoxia, therefore vanadium (V) is used to verify. Vanadium is typically incorporated in the sediment through adsorption onto particle surfaces in low oxygen (Wehrli and Stumm 1988). The V EF values do not differ significantly (two sample T-test) between Preese Hall-1 with an average of 3.14 ± 2.57 , and Beconsall-1Z with an average of 4.20 ± 7.51 . Nickel (Ni), zinc (Zn) and cobalt (Co) are also redox sensitive (Tribovillard et al. 2006), but their cycles are complex (e.g. Craigie 2018). The Ni EF values are $2.8 \times 10^{-4} \pm 1.0 \times 10^{-4}$ for Beconsall-1Z and $2.9 \times 10^{-4} \pm 1.5 \times 10^{-4}$. Zn EF average values are 1.76 ± 0.64 for Beconsall-1Z and 1.38 ± 0.89 for Preese Hall-1. Co EF average values are 2.64 ± 0.71 for Beconsall-1Z and 2.58 ± 0.71 for Preese Hall-1. The abundance of redox sensitive trace metal Mn is typically linked to clay mineral, carbonate and pyrite abundance (Craigie 2018). Average Mn EF values for Beconsall-1Z are 1.00 ± 1.80 and 0.92 ± 1.65 for Preese Hall-1. Regarding enrichments factors of Zn, Ni, Mn and Co, two sample T-tests indicate that differences between Beconsall-1Z and Preese Hall-1 is significant only for Zn (95 % CI).

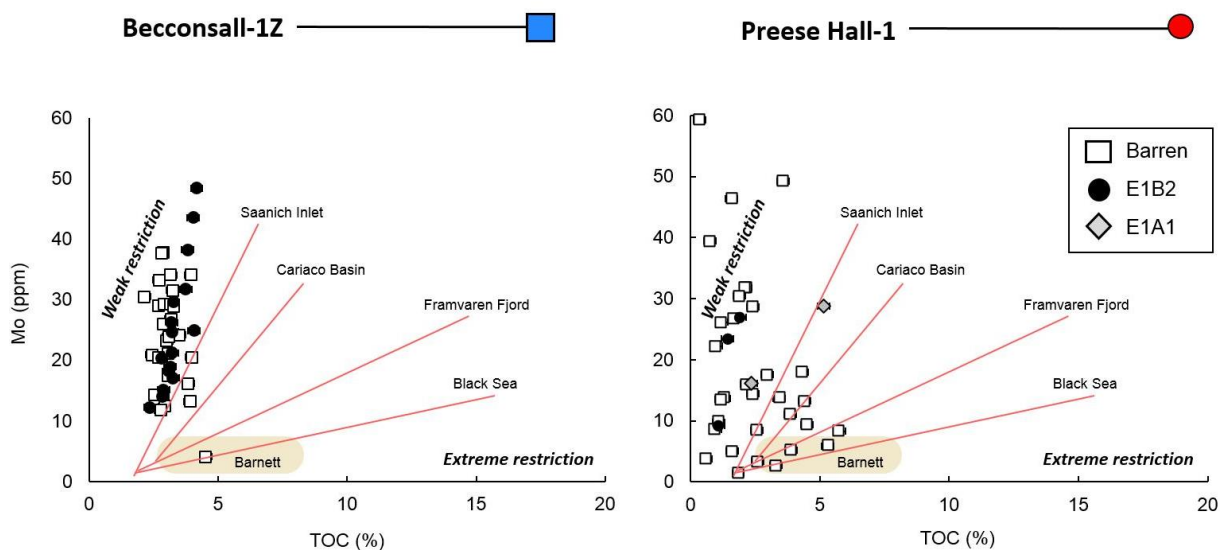


Figure 21: Molybdenum (ppm) and TOC (%) of the upper Bowland Shale Formation (Beconsall-1Z and Preese Hall-1) after Riley et al. (2019).

Organic Geochemistry

Pyrolysis records the production index (PI) to document the thermal maturity of OM in Preese Hall-1 and Beconsall-1Z. In both cores, all samples are > 0.08 with PI in Preese Hall-1 ranging from 0.08 – 0.49 and ranging from 0.17 – 0.36 in Beconsall-1Z (Table 5). Additionally, during molecular analysis preparation, EOM does not exceed 11 mg. This restricted the use of molecular proxies beyond Pr/Ph analyses. Both Figure 21 and Figure 22 show that the average TOC is lower for Beconsall-1Z (1.26 ± 0.24 %) than for Preese Hall-1 (3.13 ± 0.53 %). Two sample T-tests indicate that there are significant differences in TOC between Beconsall-1Z and Preese Hall-1 (95 % CI).

Pristane/phytane (Pr/Ph) values in Beconsall-1Z are 1.26 ± 0.24 for Beconsall-1Z and 1.48 ± 0.20 for Preese Hall-1. Two sample T-tests indicate that Pr/Ph do not significantly differ between Beconsall-1Z and Preese Hall-1 (Figure 22).

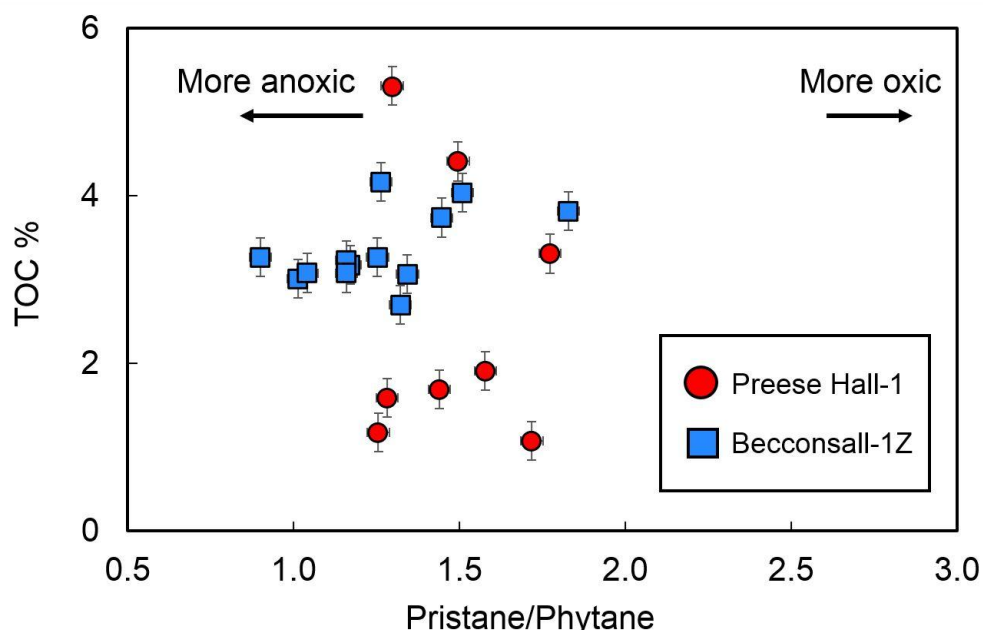


Figure 22: Pristane/phytane versus TOC (%) from the upper Bowland Shale Formation wells Beconsall-1Z and Preese Hall-1.

Discussion

Lithology and Provenance

Up to 6 times thicker in Preese Hall-1 relative to Beconsall-1Z, the upper Bowland Shale Formation successions most likely reflect an increase in the sediment supply (turbidite and hemi-pelagic settling) and/or accommodation space in the central Bowland Basin (Figure 2). The sedimentology in Preese Hall-1 and Beconsall-1Z therefore supports previous interpretations that infill was typically north-derived (Clarke et al. 2018; Cliff et al. 1991; Collinson et al. 1988; Drewery et al. 1987; Gilligan 1920; Lawrence et al. 1987; Leeder 1988a; Reading 1964). Based on this interpretation, Preese Hall-1 is more proximal to the primary sedimentary source compared to Beconsall-1Z (e.g. Clarke et al. 2018). However, it is uncertain how much sediment was sourced from the Central Lancashire High relative to the primary sediment source to the north (Figure 2). The closer proximity to the northern primary source likely caused increased sediment supply to the north sub-basin. In contrast, Beconsall-1Z was closer to the Central Lancashire High, located on the palaeoshoreline to the south (Fraser and Gawthorpe 2003; Smith et al. 2005; Waters et al. 2009). For example, gravity maps (Clarke et al. 2018) suggest increased palaeobathymetry towards the central sub-basin indicating that the water depth at Beconsall-1Z was shallower than Preese Hall-1, possibly due to the Beconsall-Ashnott High. This difference in palaeobathymetry may explain observed differences in the thickness of the sedimentary package. Additionally, it is possible that the Beconsall-Ashnott High promoted bypass of turbidites near Beconsall-1Z. Alternatively, this palaeotopographic high may have promoted erosion of mudstones at Beconsall-1Z, accounting for a thinner package towards the south. Therefore, more evidence, in the form of additional cores, is needed to interpret the possibility of unconformities related to bypass and/or erosion.

Geochemical provenance proxies suggest that Bowland Basin prodeltaic sediments were of felsic igneous, intermediate igneous and/or quartzose

sedimentary origin (Figure 18). DF1 and DF2 were not as clear in identifying the provenance of the sediment as the TiO₂ and Zr cross plots. This is most likely due to the large number of elements used in DF and because each element and compound is affected by burial depth differently (Wintsch and Kvale 1994). However, both methods support interpretations of a sandstone-derived origin that was more similar in geochemistry to felsic igneous rocks. Furthermore, the geochemistry is indicative of felsic-derived quartz-rich sediment, similar to the proximal and stratigraphically overlying Millstone Grit Formation (Figure 23). Therefore, this study supports a sedimentological link between the distal prodeltaic upper Bowland Shale Formation and proximal quartzo-feldspathic Millstone Grit Group, as previously proposed using sedimentology (Clarke et al. 2018; Cliff et al. 1991; Collinson et al. 1988; Drewery et al. 1987; Gilligan 1920; Lawrence et al. 1987; Leeder 1988a; Reading 1964).

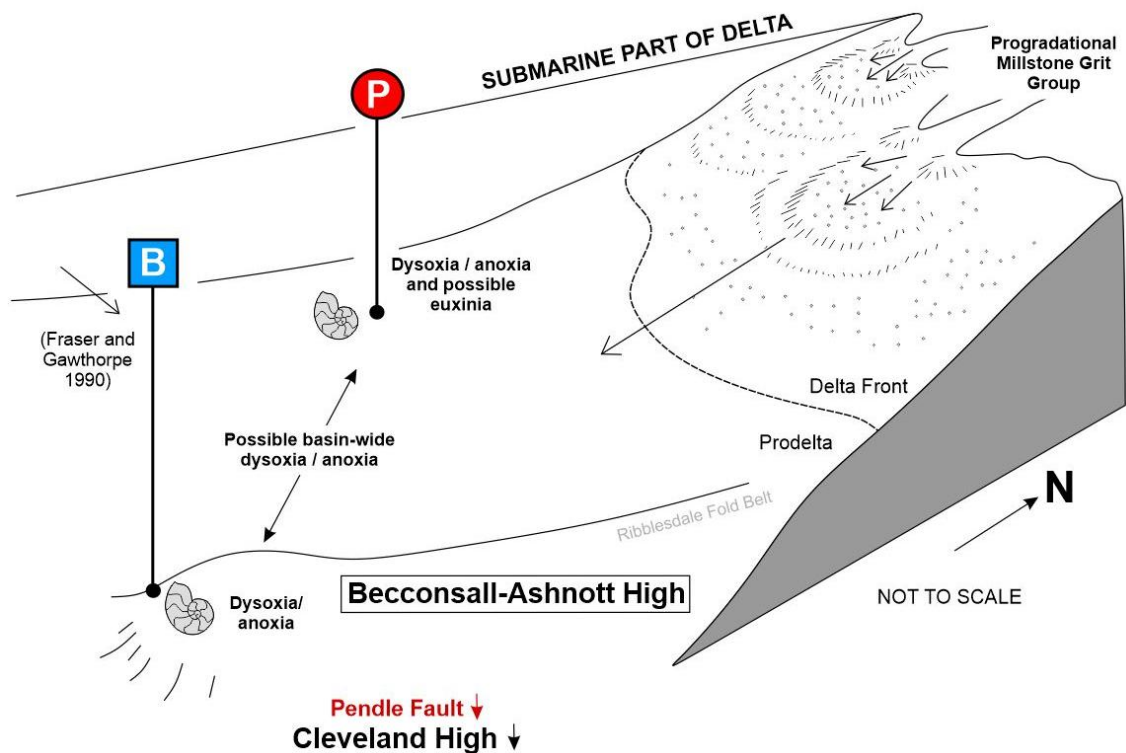


Figure 23: Summary diagram of the Upper Mississippian Bowland Basin. (B = Becconsall-1Z, P = Preese Hall-1).

Intermediate igneous (or similar) contributions in the Beconsall-1Z cross plotted DF1 and 2 (Figure 18) may be outliers. These clustered data-points border the felsic igneous provenance zone and may reflect subtle differences in sedimentation through time rather than changes in provenance. For example, both DF1 and 2 use K in their formula (Roser and Korsch 1988), however the mobility and abundance of K is affected by diagenesis (Wintsch and Kvale 1994) and this is linked to the diagenetic alteration of clay minerals (Howard 1981). Despite these uncertainties, cross plots of other provenance proxies (TiO_2 and Ni as well as TiO_2 and Zr) support interpretations of a provenance similar in geochemistry to felsic igneous rocks.

Deposition and Eogenesis

We use geochemistry to investigate the depositional and eogenetic processes of the upper Bowland Shale. This is achieved by using stratigraphic (gamma well log data) and biostratigraphic (marine band) markers at the base and top of the upper Bowland Shale Formation in previous studies (Clarke et al. 2018). However, core material is limited in this unexplored basin and marine band correlations are restricted to marine band E₁B₂ (Figure 16; Clarke et al. 2018). For this reason, time series comparisons and chronostratigraphic charts are difficult. Therefore, time equivalent marine bands are used to guide geochemical interpretations in this study and the cross-basin deposition and early diagenesis of the upper Bowland Shale (Upper Mississippian), from the centre to the margins of the Bowland Basin, is compared as a package.

Similarities between Beconsall-1Z and Preese Hall-1 average Pr/Ph values (1.26 and 1.48, respectively), Mo EF (17.3 and 18.8) and U EF (8.5 and 7.3) as well as observed insignificance (two sample T-test) suggest that there was little difference in the degree of anoxia across the basin. This suggests that bottom waters of the Bowland Basin were anoxic basin-wide during the deposition of the upper Bowland Shale Formation (Figure 23). However, cross plots of upper Bowland Shale Mo EF and U EF (Figure 19) suggest that bottom waters of the central Bowland Basin (Preese Hall-

1) may have also been more anoxic, relative to the southern Bowland Basin (Beaconsall-1Z). It is possible that the difference in bottom water conditions could support interpretations of increased water depth at Preese Hall-1, relative to Beaconsall-1Z, which resulted in a thicker sedimentary package at Preese Hall-1. Time equivalent beds in Preese Hall-1 and Beaconsall-1Z (marine band E₁B₂) suggest that the basin was similarly anoxic during marine band deposition/ goniatite preservation. However, the limited core material and uncertainty related to time equivalence in barren sediment prevents final geochemical interpretations of time equivalent stratigraphy spatially, across the basin. It is certain, however, that U EF are not associated with Mo EF (Figure 19) which can be typical of low oxygen bottom waters (Algeo and Tribovillard 2009). In this scenario, non-correlations of Mo EF and U EF are typically likely linked to differences in the mechanisms of element transportation from water to sediment (Algeo and Tribovillard 2009). For example, the water to sediment transportation of U is reliant on organometallic ligands whereas Mo is reliant on thiomolybdate shuttles (Algeo and Tribovillard 2009). In the upper Bowland Shale, however, the exact mechanisms that drive water-sediment transportation are not certain.

Trace metal enrichments and depletions, quantified by enrichment factors (Brumsack 2006a), are used in this study to interpret the bottom water conditions and provenance of the upper Bowland Shale Formation, relative to "average shale" (Wedepohl et al. 1991; Wedepohl 1969-1978). However, Van der Weijden (2002) suggests that these values provide important information, but highlights possible false equivalencies in the wide application of average shale comparisons. Qualitative comparisons with Mo EF and U EF cross plots, compared to standards outlined in Algeo and Tribovillard (2009), indicate that Preese Hall-1 experienced euxinia. The euxinia experienced by Preese Hall-1 was correlated to the increases in TOC measured to the central sub-basin (Figure 21), which infers increased potential for hydrocarbon preservation in the central Bowland Basin compared to the basin margin.

Bowland Basin organic geochemistry (e.g. Pr/Ph) can be compared to that of previous studies on the same formation in the Widmerpool Gulf (e.g. Gross et al. 2015). This study observes Pr/Ph values that predominantly fall between 1 and 2, similar to the Widmerpool Gulf where this signal is interpreted to represent dysoxia (Gross et al. 2015). However, because Pr/Ph values are not always indicative of bottom water conditions (Ten Haven et al. 1987) and the trace metal geochemistry suggests basin-wide anoxia, Pr/Ph values (all <2) in Preese Hall-1 and Becconall-1Z (Figure 19 and Figure 20) are not finally conclusive but may indicate fluctuations between low or absent dissolved seawater oxygen during the deposition of the upper Bowland Shale Formation.

Additionally, time-equivalent sediments in the Gainsborough Trough and Fort Worth Basin have been previously used as UK (Gross et al. 2015) and USA (Wright 2016; Yang et al. 2016) geochemical analogues, respectively, to the Bowland Basin. Therefore, this study compares the geochemistry of these palaeoceanographic analogies to the upper Bowland Shale Formation. The observed positive correlations of Mo and TOC suggests that Mo reduction and OM burial are related, consistent with geochemical results for the Gainsborough Trough (Figure 2). This is similar to the Bowland Basin, however, the Bowland Basin may be more anoxic and/or euxinic towards the centre. This subtle difference may reflect increases in Bowland Basin restriction, relative to the Gainsborough Trough. However, it is possible that these minor differences most likely reflect Mo enrichment and OM contribution and/or preservation, rather than differences in connectivity. This latter interpretation accounts for outlying anomalous results (e.g. possible outlier of Mo 4.52 ppm in Figure 21).

This palaeoceanographic study uses nested sampling to account for limited core material. Therefore, statistical results should be treated with caution. Furthermore, limited biostratigraphic indicators (Chapter 5; Waters 2009; Clarke et al. 2018) prevents time series plots beyond that of E₁B₂.

The new data from this study presents an opportunity to compare the upper Bowland Shale Formation to other Mississippian hydrocarbon source

rocks, such as the Barnett Shale, with respect to geochemistry (Wright 2016; Yang et al. 2016) and as a shale gas target (Andrews 2013b). This is despite palaeogeographic differences, where the Fort Worth Basin was likely more distal in relation to the Carboniferous Bowland Basin (Blakey 2008) but the geochemistry of Fort Worth infers extreme basin restriction (Rowe et al. 2008).

This study has interpreted the Bowland Basin to have been weakly restricted during upper Bowland Shale Formation deposition, however, based on comparisons with Rowe et al. (2008), the Fort Worth Basin was near to extreme basin restriction. Therefore, future studies that analogue the Fort Worth and upper Bowland Shale Formation must account for differences in basin restriction.

The upper Bowland Shale Formation is only partially cored at both locations (Beaconsall-1Z and Preese Hall-1). Therefore, comparisons of palaeoceanographic changes throughout the entire formation is not possible in this study. Based on the new data in this study, it is clear that the upper Bowland Shale Formation was deposited in anoxia in Beaconsall-1Z and Preese Hall-1, at the margin and centre of the Bowland Basin respectively. This was suitable for hydrocarbon preservation during deposition and eogenesis and promoted maximum TOC contents of 4.52 % in Beaconsall-1Z and 5.75 in Preese Hall-1 (averages exceed 2 in each well) which are desirable for hydrocarbon exploration. Hydrocarbon exploration is recommended to target the north and/or central Bowland Basin where the mudstone target formation is up to 6 times thicker than at the basin margin.

Conclusions

1. This study used sedimentology, inorganic geochemistry and mineralogy to show that the upper Bowland Shale Formation was sourced from a northern quartzo-feldspathic primary provenance. Mudstone geochemistry is indicative of a felsic igneous, intermediate and/or quartzose sedimentary provenance, most likely related to the proximal Millstone Grit Group which outcrops throughout North Wales and Warwickshire (Waters et al. 2009).
2. Sediments at Preese Hall-1 were proximal to primary sedimentary supply, resulting in increased sediment supply relative to accommodation space. Local differences in sedimentation rate within the basin may reflect differences in basinal topography and palaeobathymetry (Beaconsall-Ashnott High).
3. Trace metal and organic geochemical data (e.g. U, Mo enrichment factors, Pr/Ph ratios and Mo-TOC cross plots) suggested that anoxia and/or dysoxia persisted basin-wide. These interpretations are comparable to previous studies of the time-equivalent sections from the Widmerpool Gulf and Gainsborough Trough (Riley et al. 2018) suggesting that these UK basins were likely connected during the Upper Mississippian.
4. Increased TOC and possible anoxia and/or euxinia towards the central basin reflect a likely increase in hydrocarbon generation potential towards Preese Hall-1. A thicker sedimentary package here, relative to Beaconsall-1Z, suggests that the central Bowland may be a more favourable shale gas target than the southern part of the basin.
5. We broadly compare the palaeoceanography of Mississippian Bowland Basin deposits to that of the Fort Worth Basin (Mississippian Barnett Shale) and suggest that the Fort Worth Basin was more restricted than the Bowland Basin at the time of deposition. Future work should investigate the applicability of previous upper Bowland-Barnett Shale comparisons (Andrews 2013b).

6. Average shale standards (Wedepohl et al. 1991; Wedepohl 1969-1978) should be used with caution during geochemical analyses of UK Carboniferous source rocks. However, trace metal enrichment factors (e.g. U and Mo) are reliable cross-core comparison proxies. Future studies should aim to extensively compare enrichment factors in the upper Bowland Shale to that of well-explored source rocks to minimise subsurface risk during exploration.

Chapter 7. Selecting an Analogue for the Bowland Shale Formation using Geochemistry.

Abstract

The resource estimation of unexplored shale gas targets with limited core and outcrop material has high uncertainty and associated economic risk. One way to minimise uncertainty and decrease risk during petroleum exploration is to compare data from the target formation to that of a better understood, well explored formation that is closely analogous. Analogue comparisons should be broadly similar to the investigated unexplored target in composition as well as basin morphology and, preferably, time of deposition. However, the relative importance of basin morphology to the time of deposition is not previously studied. We investigate the relatively unexplored Mississippian Bowland Shale Formation in the Bowland Basin (Lancashire, UK) because this current target for unconventional exploration has limited core (from wells Preese Hall-1 and Beconsall-1Z) and outcrop material, increasing reliance upon analogue comparisons. The geochemical composition (X-ray fluorescence) of the upper Bowland Shale is analysed and computationally compared (Gaussian Mixture Model) to the elemental abundances of two other Mississippian formations (Bakken Shale and Barnett Shale) and one succession broadly similar in basin morphology (Marcellus Shale) digitised from previous studies. We conclude that analogue comparisons are most effective when depositional processes are prioritised over basin morphology and time similarities. Furthermore, the Barnett Shale is an effective analogue comparison to the Bowland Shale Formation. The Gaussian Mixture Model most readily groups the elemental compositions of the Barnett and Bowland shales, for example in redox sensitive trace metal abundances (i.e. Mo and U enrichment factors). This is most likely because they experienced similar depositional and/or early diagenetic processes (e.g. similar ocean redox states).

Introduction

Mudstones are an important source of petroleum that significantly contribute to the onshore energy mix (Arthur et al. 2009). Reliance on these “unconventional” systems will continue to grow as Europe transitions away from coal-powered electricity generation (Campbell et al. 2013; EU 2011; Wiseall et al. 2018) using the engineering technique called hydraulic fracturing. The success of this method in the USA (or US) precedes attempts to utilise resources in the UK (USEIA 2011). For this reason, the literature (e.g. Andrews 2013) as well as social and news media, compare US shale gas plays (e.g. Barnett, Marcellus etc.) to current targets in north-west UK, such as the Bowland Shale Formation in the Bowland Basin. Comparisons between target formations are typical in the US, achieved by comparing their mineralogy and geochemistry (Leventhal 1991). We compare the mineralogy and geochemistry of the Bowland Shale Formation to US shale gas formations to select the most accurate analogue.

Selecting a suitable analogue comparison is essential to the reduction of subsurface uncertainty during petroleum exploration and appraisal. The reliance upon analogue data is high in basins with limited available core and outcrop data (e.g. Nwaobi and Anandarajah 2018), such as in the upper Bowland Shale Formation, an informal subdivision of the Bowland Shale Formation which is a promising target for hydrocarbon production (Aitkenhead 1992; Clarke et al. 2018; Hennissen and Gent 2019).

In the upper Bowland Shale, geological and geochemical data are limited and the reliance upon analogues, models and literature-derived data is high (Andrews 2013a; Andrews 2013b; Clarke et al. 2018; Wiseall et al. 2018). Therefore, it is important that the most accurate analogues are used to inform subsurface interpretations, such as gas in-place estimates (Andrews 2013b; Harrison et al. 2019; Whitelaw et al. 2019). However, it is difficult or unachievable to analogise every characteristic of an existing petroleum system to another (Singh et al. 2008). This is especially difficult in the upper Bowland Shale because it is relatively unexplored. The upper

Bowland Shale has indistinct amorphous OM in abundance and it is much thicker than many other shale gas plays at 499 m in the centre of the Bowland Basin (Preese Hall-1) and 84 m at the southern margin (Beaconsall-1Z; Clarke et al. 2018).

Previous studies suggest that formations that are similar in time, such as the Mississippian Barnett Shale and Bakken Shale, could be used as analogues to each other and the upper Bowland Shale (Andrews 2013b; He et al. 2016). Additionally, informal attempts to analogise the Bowland and Marcellus basins are typically based on similarities in palaeogeography and basin morphology (e.g. Andrews 2013). These comparisons are confined to the available data. However, as in Figure 24, there are complications to these basin morphological and time series analogies because the Bowland Basin only crudely shares similarities in basin morphology with the Marcellus and the upper Bowland Shale Formation is not similar in depositional environment to the Barnett or Bakken (e.g. Figure 24; Blakey 2008).

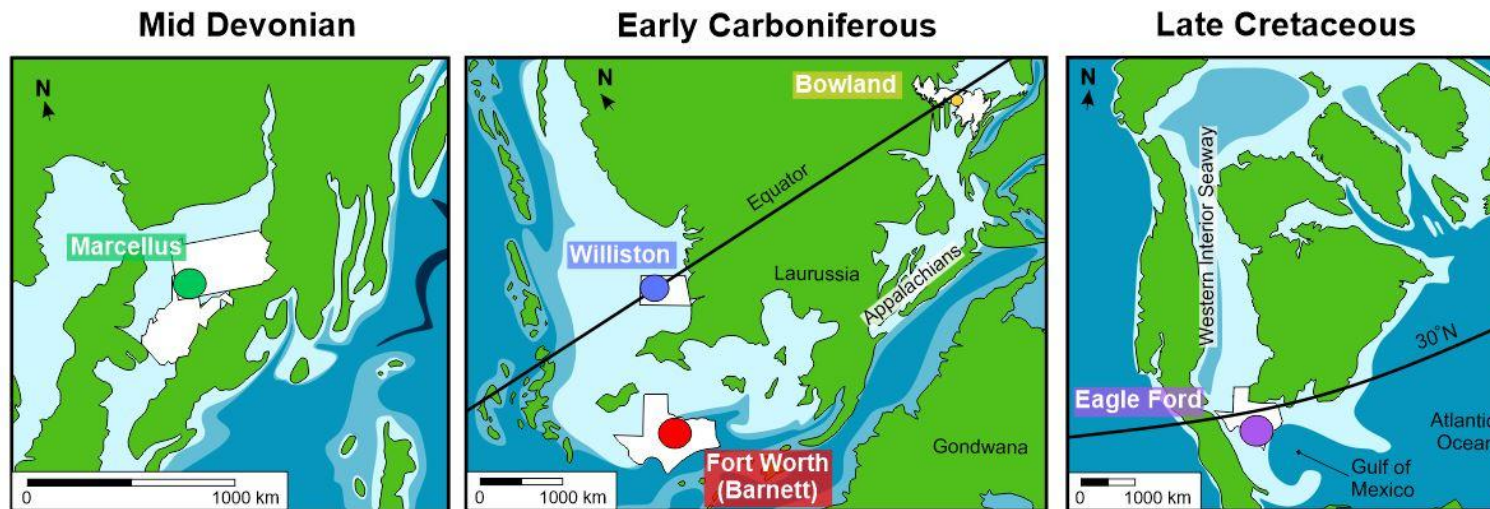
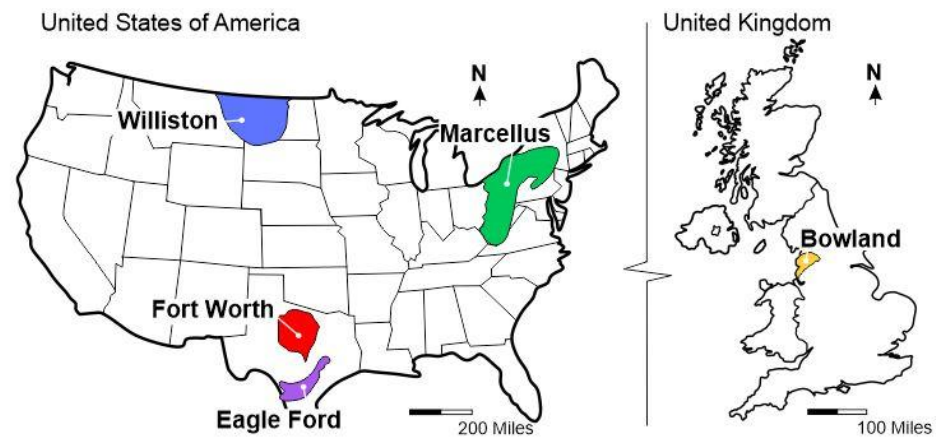


Figure 24: Modern maps of the USA and UK with positions of major shale gas targets (top). Palaeogeographic maps of studied basins (bottom). Adapted from Blakey (2008).

The challenge of selecting a suitable analogue for the upper Bowland Shale is related to the fact that shale petroleum plays in general are complex and varied. For example, the differences in the OM type across a basin and between basins can differ significantly in origin/provenance. For example the Marcellus Shale is typically type II-III and the Barnett Shale is predominantly type II (Bruner and Smosna 2011). Additionally, OM can be altered by thermal and/or biological degradation (Jarvie et al. 2005). Therefore, this study investigates the similarities and differences in mineralogical and trace metal abundances across different formations. Although mineralogy and trace metal geochemistry can be influenced by processes of provenance and diagenesis, they are typically better constrained than organic geochemical proxies (Craigie 2018; Degens 1967).

Trace metal geochemistry is important because high abundances of redox sensitive elements (e.g. U, Mo and V) are associated with abundances in OM and source rock "sweet spots" with high petroleum yield (e.g. Schlanger and Jenkyns 1976). This link between redox sensitive trace metal abundances and OM is clear in fossiliferous highstands, sometimes called marine bands, where high gamma and associated U are typically associated with zones of increased organic carbon (Clarke et al. 2018). However, redox sensitive trace metal abundances (e.g. U and Mo) can be influenced by sedimentary provenance and detrital input, obscuring bottom water palaeoceanographic interpretations (Craigie 2018). Therefore, we also investigate the provenance to early diagenetic story of the upper Bowland Shale and the analogue comparisons.

The upper Bowland Shale provenance and redox proxies (XRF) are compared to those of the Barnett and Bakken Shales (similar depositional time) as well as the Marcellus Shale (similar in basin morphology). The Eagle Ford Shale is used as a control as its depositional time and basin morphology differed from the Bowland Shale and Bowland Basin, respectively (Andrews 2013b; Hsu and Nelson 2002). We identify the best suitable palaeoceanographic analogue for the upper Bowland Shale

Formation from a suite of 4 other formations. A combination of geochemistry and 2D multivariate computational models are used to select a suitable analogue for the upper Bowland Shale.

Geological Settings

Bowland Shale Formation

See Geological History.

Barnett Shale Formation

The Barnett Shale Formation (Barnett) was deposited during the Mississippian in the Fort Worth Basin of north and central Texas (see Montgomery et al. 2005 and Pollastro et al. 2007 for comprehensive geological history). Similar to the Bowland Shale, the Fort Worth Basin formed during major thrust-fold deformation associated with Rheic Ocean closure and the formation of Pangaea (e.g. Montgomery et al. 2005). Sediments deposited in the basin consist of five lithofacies including black shale, lime grainstone, calcareous black shale, dolomitic black shale and phosphatic black shale (Henk 2005; Henk et al. 2000; Hickey and Henk 2006; Loucks and Ruppel 2007). Poor sorting in the lime grainstones are suggested to be associated with gravity flows (Rowe et al. 2012). Some authors suggest that Upper Pennsylvanian and Permian strata were eroded before minor Cretaceous sediment deposition (Henry 1982; Walper 1977).

The Barnett Shale consists of c. 1800 to 2100 m of marine-deposited carbonates and mudstones (Montgomery et al. 2005). For comparison, X-ray fluorescence (XRF) data from Rowe et al. 2012 is used for this study and was originally collected from the 1-Blakely drill core, Wise County, Texas, USA (see Loucks and Ruppel 2007; Rowe et al. 2012; Rowe et al. 2008). This Barnett Shale study succession is 36 m thick.

Bakken Formation

The Lower Mississippian Bakken Shale Formation (Bakken) is a fissile, non-calcareous organic rich, black marine mudstone succession deposited in the Williston Basin (e.g. Gerhard et al. 1982). This elliptical intra-

cratonic basin spans North Dakota, South Dakota, Montana, Manitoba and south east Saskatchewan (Murphy 2014). Tectonic structures in the Williston Basin are typically subtle (Gerhard et al. 1982). Basin subsidence began during the Cambrian, however major sediment infilling started during the Ordovician (Pollastro et al. 2013).

Despite the success of the Bakken Shale as a petroleum source rock, the maximum thickness of the Bakken Shale is 49 m (LeFever 2008). The Bakken Formation consists of three members including the Lower Shale Member, the Middle Sandstone Member and the Upper Shale Member (Murphy 2014) and each member is laterally continuous (Hester and Schmoker 1985; Meissner 1978; Smith and Bustin 1996, 2000; Webster 1982, 1987).

XRF data from the production target Lower Shale Member, western and north-western North Dakota, from Murphy 2014 was selected for statistical comparison. This Bakken Shale study succession is 7.55 m.

Marcellus

The Marcellus Shale Formation (Marcellus) was deposited during the Middle Devonian in the Appalachian Basin, south west Pennsylvania (e.g. Lash and Blood 2014). The basin was elongate and trended north east-south west at c. 30° south latitude (Scotese and McKerrow 1990) and formed due to subsidence related to thrust-loads associated with the Acadian oblique collision of Avalonian microplate and Laurentia (Ettensohn 1985, 1987; Faill et al. 1985; Ferrill and Thomas 1988; Rast and Skehan 1993; Scotese and McKerrow 1990). Blakey (2013) infers that the nearby Marcellus and Appalachian Basin were connected to the Rheic (global) Ocean to the southwest, creating an environment suitable for marine mudstone deposition. For a comprehensive history of the Marcellus Formation, see Ver Straeten et al. (1994).

The Marcellus Formation thickens to the east and consists of clastic marine and terrestrial sediments (Lash and Blood 2014). It is divided into two members, the (lower) Union Spring Member and (upper) Oatka Creek

Member (Ettensohn 1985; Faill et al. 1985; Friedman and Johnson 1966; Lash and Blood 2014). The succession used in this study is 5.72 m thick including both the Oatka Creek (2.29 m) and Union Springs members (2.92 m) from Lash and Blood (2014).

Eagle Ford Formation

The Upper Cretaceous Eagle Ford Group (Eagle Ford) is a mudstone dominated, carbonate rich petroleum source rock (e.g. Shultz 2015). The Eagle Ford succession is thickest in South Texas, in the Maverick Basin, and it thins at the San Marcos Arch (Denne et al. 2014). The San Marcos Arch separates the Eagle Ford into two depositional regimes, namely a siliciclastic dominated succession to the north east and a carbonate dominated succession to the south west (Denne et al. 2014). Sediments were deposited on the Central Texas Platform shelf (Dawson 1997) in a stratified water column and anoxic bottom waters (Denne et al. 2014; Lock and Peschier 2006).

The Eagle Ford Shale is typically divided into upper and lower successions. Denne et al. (2014) suggests that the Lower Eagle Ford Shale sediments were typically deposited in low oxygen and/or euxinic conditions, however the Upper Eagle Ford Shale had increased oxygen levels and less free sulphur. Upper and Lower Eagle Ford Shale geochemical data are analysed, using trace metal data from the south western carbonate dominated system (see Shultz 2015).

Methods

These analogue comparisons used XRD, XRF and GMM techniques. See Methodology.

Collected and analysed XRF and XRD data from upper Bowland Shale cores (Beaconsall-1Z and Preese Hall-1) was compared to that of the Barnett Shale (digitised from Rowe et al. 2012), Bakken Shale (Murphy 2014), Marcellus Shale (digitized from Lash and Blood 2014) and Eagle Ford Shale (Shultz 2015).

Automatic processing was used to automate p-values to investigate the significance of elemental relationships (95 % CI) using the MATLAB corr function, which is a Pearson correlation coefficient. Element-element relationships were analysed using intersecting cells that were significant (green), insignificant (red) or significant but manually interpreted as weakly correlated (orange). R symbols refer to negative correlations.

Results

Mineralogical Composition

Mineralogical analyses are used to characterise the sediment composition. Figure 25 compares the relative total mineral abundance of the upper Bowland, Barnett, Bakken, Marcellus and Eagle Ford. It shows that the Eagle Ford (Passey et al. 2010) is mineralogically distinct from all other formations used in this study because it is less quartz rich than the Barnett, Bakken, Marcellus and upper Bowland. With the exception of the Eagle Ford, each formation can be classified as "quartz dominated". Figure 25 shows that relative total quartz abundances differ between the Barnett (30 - 90 %), Eagle Ford (30 - 40 %), Bakken (50-80 %) and Marcellus (35 - 75 %) as well as between wells Beconsall-1Z (39 - 84 %) and Preese Hall-1 (31 - 61 %) in the upper Bowland Shale.

Relative total clay mineral contents ("total clay") are variable between the formations (Figure 25). For example, the abundances of total clay differ between Barnett (10 - 70 %), Eagle Ford (7 - 60 %), Bakken (20 - 50 %) and Marcellus (25 - 65 %) as well as between the two wells in the upper Bowland Shale, Beconsall-1Z (27 - 65 %) and Preese Hall-1 (10 - 25 %). This shows that the Barnett has the largest range of relative total clay mineral content, compared to the other formations. The Eagle Ford has the highest relative total carbonate abundance (Figure 25), ranging from 20 - 83 %. This differs from all other formations because they each typically have minimum carbonate abundances of 0 or near 0. The ranges of relative total carbonate differ between the Barnett (0 - 63 %), Bakken (0 - 22 %) and Marcellus (0 - 25 %) with distinct differences between

upper Bowland Shale wells Beconsall-1Z (0 - 17 %) and the more carbonate-dominant Preese Hall-1 (17 - 69 %).

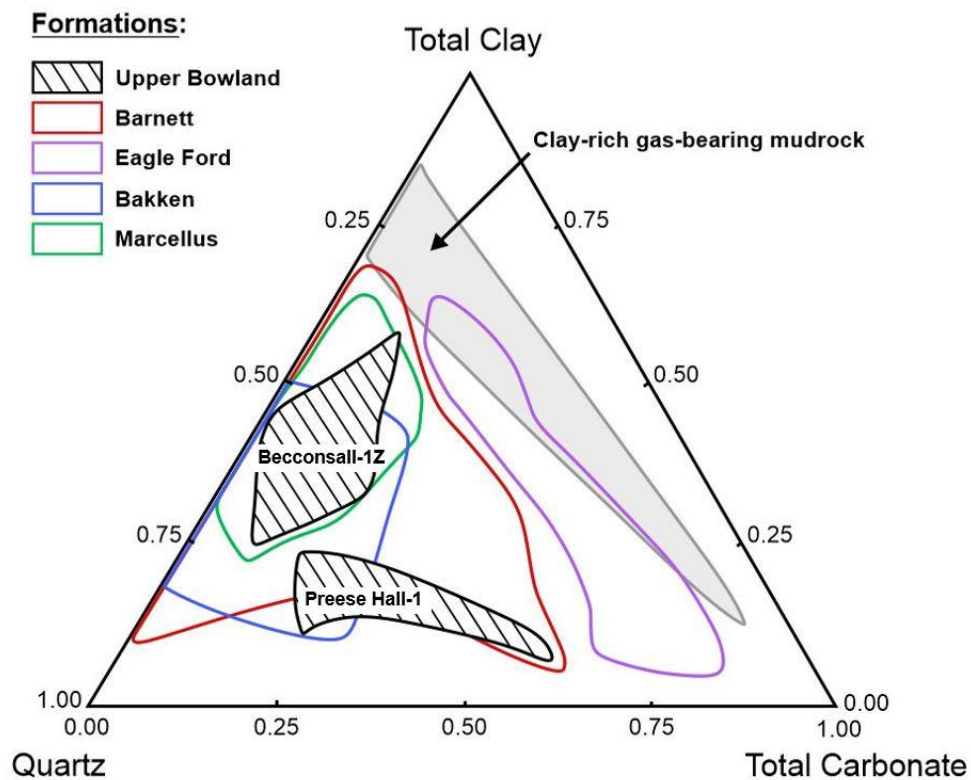


Figure 25: Ternary plot showing the mineralogy of upper Bowland (Beconsall-1 and Preese Hall-1), Barnett, Bakken, Marcellus and Eagle Ford formations.

Geochemical Composition (XRF)

The geochemical composition of each studied formation is based on elemental data. Table 7 displays the minimum, maximum, average and standard deviation (StDev) of key elements for each formation including collected and analysed upper Bowland data. Table 7 and Figure 26 show that the upper Bowland Shale has the highest average trace metal values for Fe (32355 ppm), Mn (346.1 ppm), Si (273381 ppm) and S (22695 ppm). The Bakken has highest average elemental values for Zn (371 ppm), Mo (317.7 ppm), Cu (83.8 ppm), Zr (102.3 ppm), V (654.5 ppm), K (31225 ppm), Rb (115.0 ppm), Ti (2831 ppm), Al (47403 ppm), Ni (336.0 ppm) and Ca (32088 ppm). The Marcellus has the highest average value for U (65.7 ppm).

Table 7 shows that the Eagle Ford has the lowest average values for Fe (11307 ppm), Si (86371 ppm), Zr (31.6 ppm), K (3446 ppm), Rb (23.1 ppm), Ti (834.8 ppm), Al (15472 ppm), Ni (51.6 ppm), S (8086 ppm) and Ca (269000 ppm). The Barnett has the lowest average elemental values for Zn (29.1 ppm), Mo (5.8 ppm), Mn (165.4 ppm), Cu (29.6 ppm), V (117.1 ppm) and U (6.3 ppm).

Averages of enrichment factors (EF) in Figure 26 are used to observe elemental abundances relative to average shale (Brumsack 2006b; Wedepohl et al. 1991; Wedepohl 1969-1978). Figure 26 shows that the Bakken has the highest average elemental EF of Mo (215.7) and V (8.9). The Eagle Ford has the highest average elemental EF of Zn (11.6), Fe (3.8), Mn (3.6), Cu (12.7), Si (3.3), Zr (1.6), K (11305.1), Ti (1.6), S (40.35) and Ca (390.5). The Marcellus has highest average elemental enrichments of U (48.3).

The upper Bowland Shale Formation has lowest average EF values for K (1.0) and S (0.3). The Bakken has the lowest average EF values for Ti (1.2) and Ca (6.9) and the Marcellus has the lowest average EF of Fe (0.7). The Barnett is least enriched in Zn (0.7), Mo (4.7), Mn (0.5), Cu (1.6), Si (1.6), Zr (0.9), V (1.9) and U (6.3) averages. In terms of elemental ranges, K EF average values have the largest range (i.e. 11305

in the Eagle Ford's and 1 in the upper Bowland). Average Ti EF values have the smallest elemental range of EF averages (Eagle Ford's 1.6 to Bakken's 1.2). The Eagle Ford has high Ca relative bulk averages and high average EF (390.5). However, the upper Bowland Shale has low relative Ca abundances (5.8 ppm) and a relatively higher averages of Ca EF (12.4).

Upper Bowland Shale Formation (Combined Beconsall-1Z and Preese Hall-1)

Element (ppm)	P	Zn	Fe	Mo	Mn	Cu	Si	Th	Zr	V	K	As	Rb	Ti	Al	U	Na	Ni	S	Ca
Min	4	8.0	7867	1.4	44.2	1.4	93118	0.6	36.2	7.7	758	0.6	6.5	870.7	5627	0.9	0.0	12.6	2735	126000
Max	3457	238.6	75678	88.8	3905.0	184.8	339388	10.7	133.1	1948.0	23231	206.1	122.7	4156.9	89394	36.9	10707	205.8	66450	2058000
Average	426	79.1	32355	25.3	346.1	58.7	273381	5.0	73.2	245.8	12293	23.4	65.0	2556.4	46889	11.6	1340	73.4	22695	733632
StDev	595	48.6	12203	17.4	543.1	29.6	48014	2.2	20.4	279.2	4621	23.0	22.6	704.3	15973	6.9	2148	37.6	10938	376052

Bakken Formation

Min	475	8.0	4991	3.0	118.0	11.0	82731	4.0	47.0	0.0	7838	6.0	36.0	1311.0	15018	1.0	3217.0	14.0	4301	9284
Max	1131	3612.0	41909	626.0	1033.0	372.0	320615	13.0	274.0	1373.0	44051	100.0	174.0	3903.0	68529	73.0	5124.0	656.0	27856	278956
Average	765	371.0	28395	317.7	223.1	83.8	261902	9.2	102.3	654.5	31225	44.5	115.0	2831.6	47403	47.0	4523.3	336.0	19907	32088
StDev	128	779.2	9462	152.3	178.9	69.4	48025	2.2	45.8	355.6	7922	23.9	34.9	743.4	12393	19.8	480.3	149.5	5229	56936

Eagle Ford Formation

Min	202	28.0	7670	6.0	147.0	25.0	24400	2.0	8.0	31.0	869	4.0	8.0	204.0	549	1.0	2320.0	20.0	3320	207000
Max	1012	164.0	24380	96.0	290.0	61.0	169700	5.0	73.0	521.0	7891	28.0	48.0	1735.0	33200	18.0	3830.0	111.0	15180	360000
Average	550	82.4	11307	33.4	166.6	36.6	86371	3.1	31.6	175.1	3446	12.2	23.1	834.8	15472	9.6	2948.6	51.6	8086	269000
StDev	293	42.1	4304	29.0	36.2	10.7	40788	1.0	21.9	138.2	1897	7.1	11.1	436.6	9911	6.9	419.1	26.4	3310	46774

Marcellus Formation

Min	-	-	3271	37.4	-	-	-	5.4	-	-	-	-	-	-	13710	24.6	-	-	-	-
Max	-	-	36866	275.4	-	-	-	40.2	-	-	-	-	-	-	72857	117.4	-	-	-	-
Average	-	-	17814	126.5	-	-	-	17.0	-	-	-	-	-	-	46684	65.7	-	-	-	-
StDev	-	-	9725	81.2	-	-	-	11.6	-	-	-	-	-	-	13433	24.4	-	-	-	-

Barnett Formation

Min	265	0.7	8381	0.5	50.0	0.7	45549	1.5	6.9	19.6	136	-	-	522.4	7782	0.1	-	2.1	2356	20032
Max	20770	65.2	36663	49.5	396.8	64.9	349687	12.8	150.1	279.2	20868	-	-	5015.6	92481	34.4	-	173.8	24058	321773
Average	4394	29.1	21243	5.8	165.4	29.6	201212	6.4	73.7	117.1	11330	-	-	2678.2	47017	8.2	-	83.6	12746	132963
StDev	4676	15.0	7228	5.9	67.8	15.5	76212	2.4	34.7	44.5	4807	-	-	1141.5	20400	6.3	-	36.1	4727	88770

Table 7: Elemental results for upper Bowland, Bakken, Barnett, Marcellus and Eagle Ford formations.

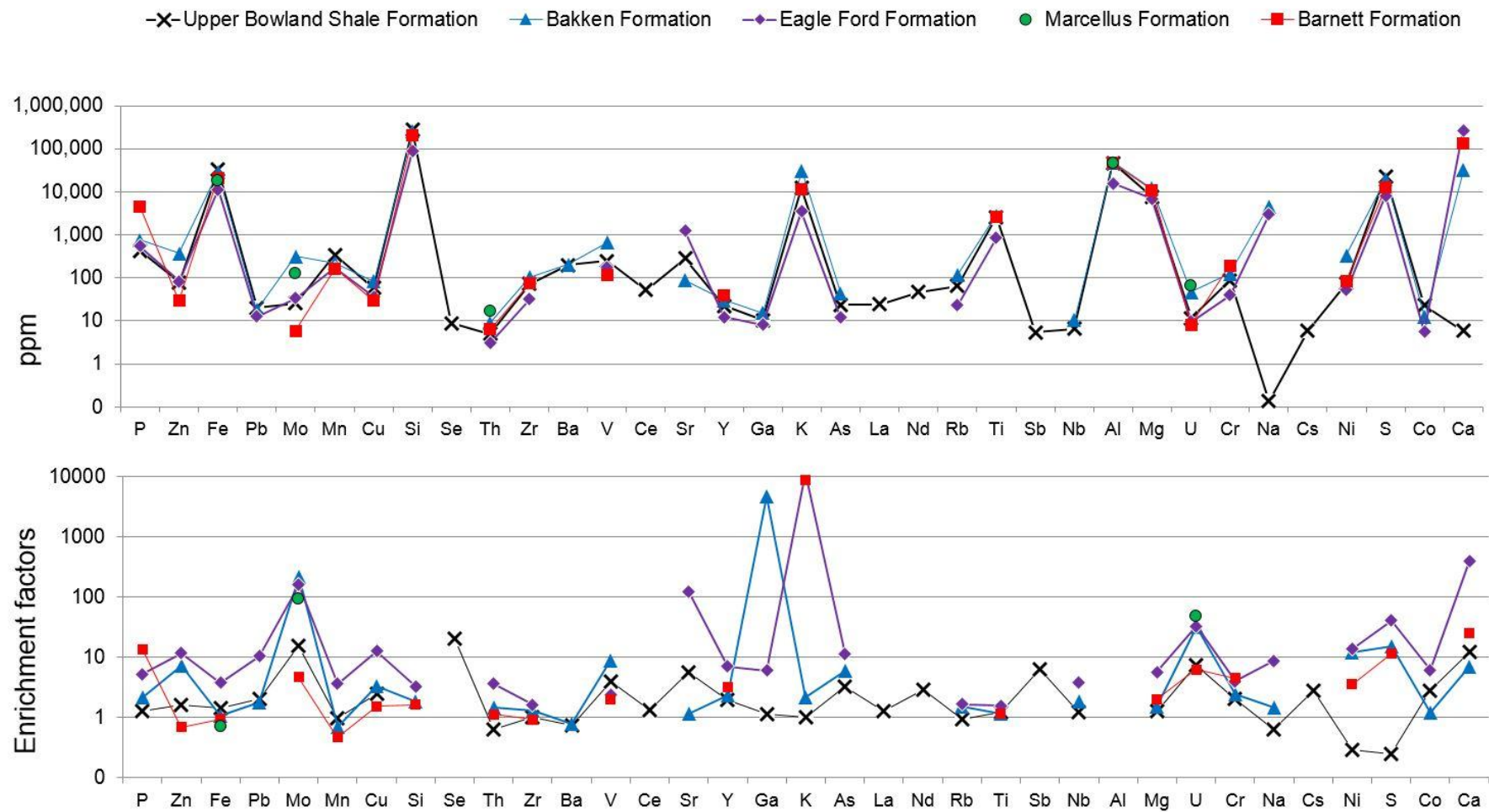


Figure 26: Elemental geochemistry of the upper Bowland, Bakken, Eagle Ford, Marcellus and Barnett formations.

Element associations are investigated using correlation graphs (Figure 27). Limited open access data from the Marcellus prevents a comprehensive assessment of Mo, Th, Fe and U relationships with other elements. However, regarding the other study formations, the Bakken has the most numerous significant element-element interactions. The Eagle Ford has the least numerous significant element-element interactions of the chosen elements. In the Bakken, Barnett, upper Bowland and Eagle Ford, relationships between provenance proxy Zr and redox sensitive element Mo are insignificant and/or interpreted as having no correlation (Figure 27). This is also true for elements Ni, U and V. Similarly, the Bakken, Barnett, upper Bowland and Eagle Ford show no significant relationships between elements Si (linked to clay minerals and quartz) and Mo as well as between elements Si and U. Additionally, these formations show that Fe and S correlate with significance (Figure 27).

TiO₂ and Ni cross plots (Figure 28) are typically used to investigate the provenance of mudstones. Figure 28 shows that all formations similarly plot under sedimentary mudstones and siltstones near to the felsic zone. The Bakken has the largest range of Ni values (14 to 297 ppm) whereas the Eagle Ford has the smallest range (20 to 111 ppm). The Eagle Ford has lowest average TiO₂ values (0.08 %), however average TiO₂ values for the Barnett (0.45 %), Bakken (0.47 %) as well as for the upper Bowland at Beconsall-1Z (0.42) and Preese Hall-1 (0.44) which are similar. Table 7 and Figure 28 show that Zr and TiO₂ cross plot predominantly within the felsic igneous provenance zone. One Eagle Ford sample and one Barnett sample plot within the mafic igneous zone.

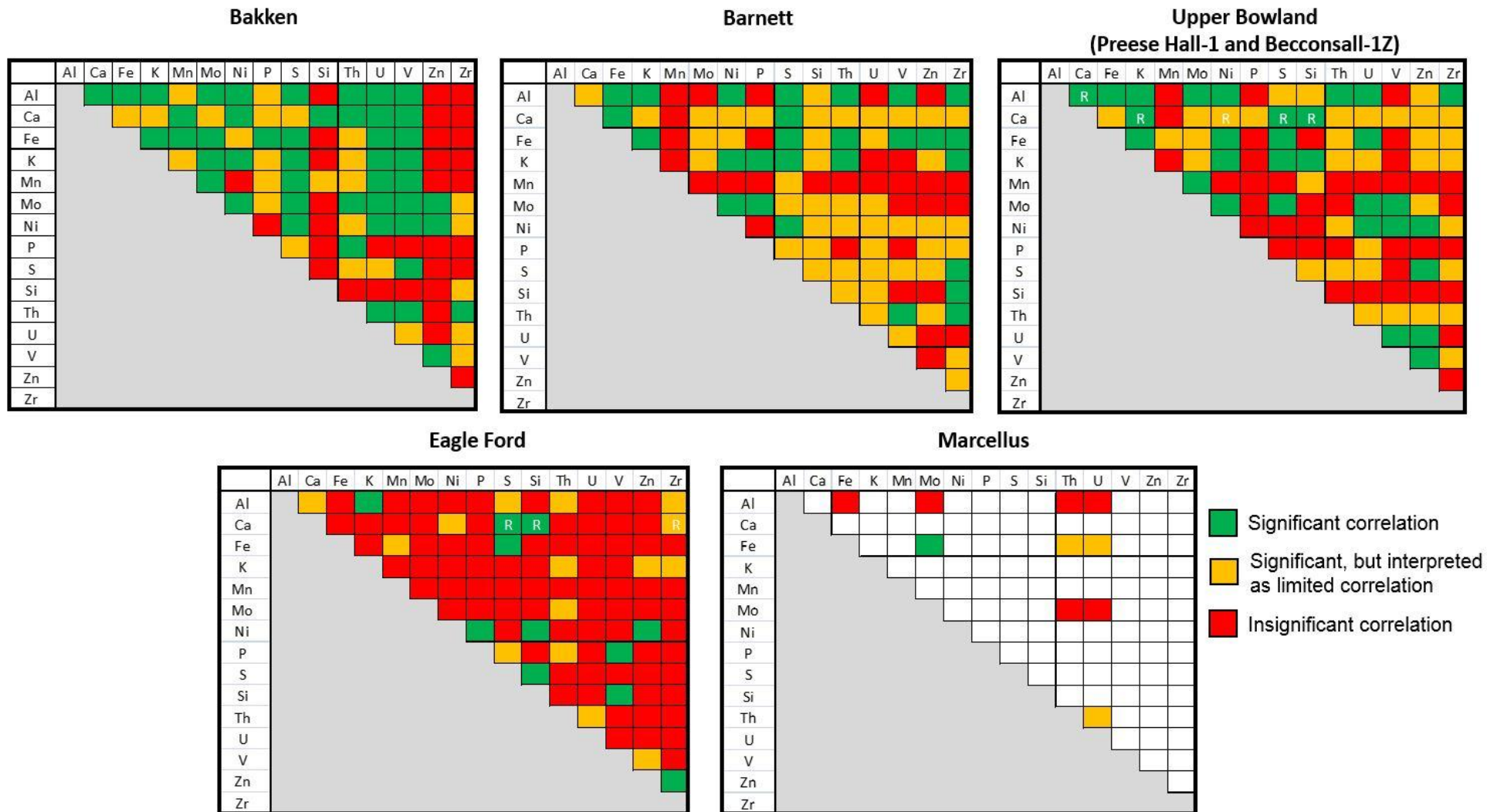


Figure 27: Correlation diagrams showing element-element associations / relationships.

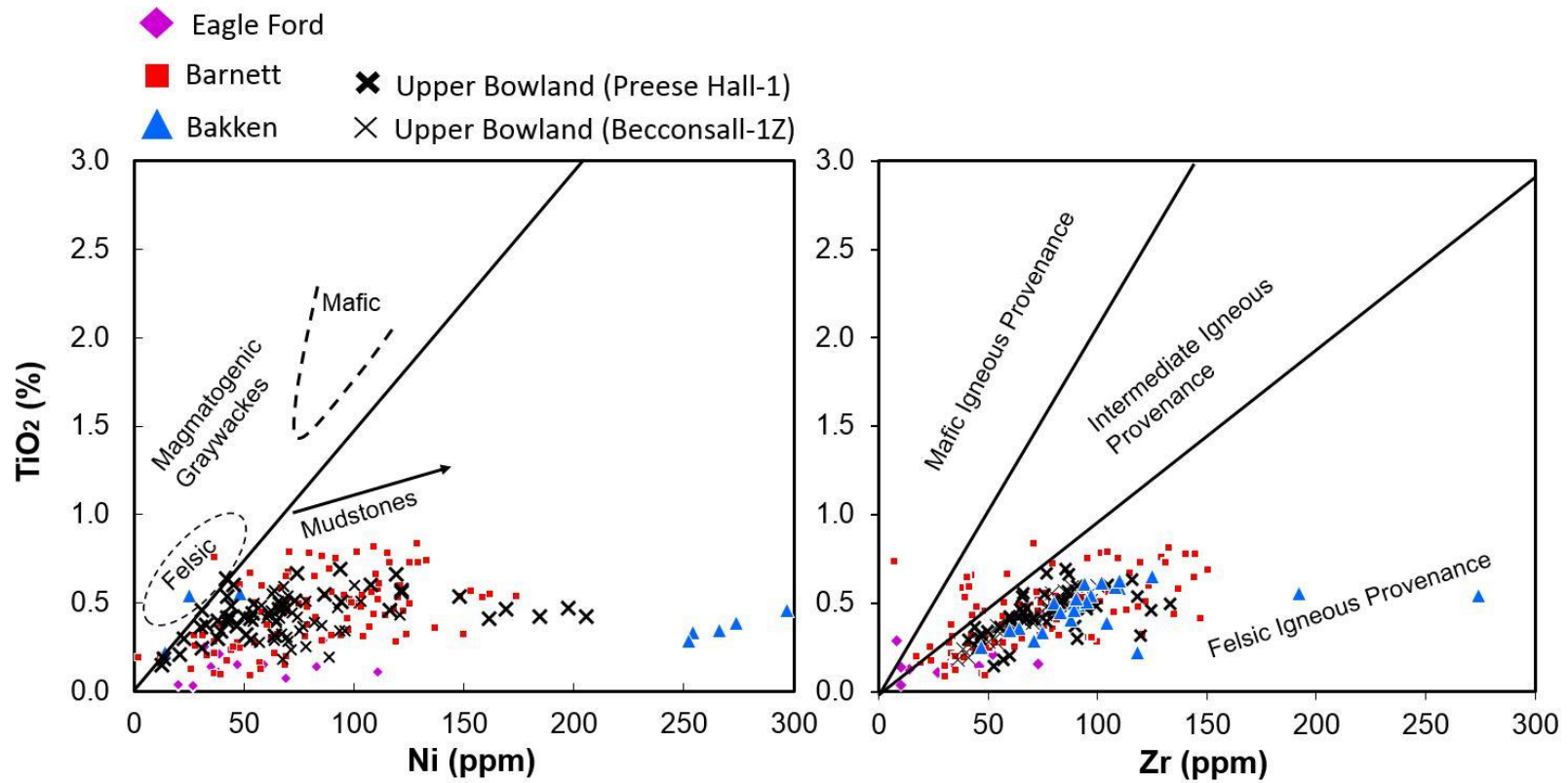


Figure 28: Binary plots using provenance proxies TiO₂ and Ni (left, after Floyd et al. 1989) as well as TiO₂ and Zr (right, after Hayashi et al. 1997) of the upper Bowland (Beaconsall-1Z and Preese Hall-1), Barnett, Eagle Ford, Bakken and Marcellus.

SiO₂ and Zr are typically cross plotted to identify the provenance of silica. Figure 29 shows that the Eagle Ford typically sits closest to the origin, near to a terrestrial linear trend (Ratcliffe et al. 2012b). The Barnett typically has a wide spread and scattered dataset that lie near both to the terrestrial and biogenic trendlines. The Bakken and upper Bowland are typically nearer to the biogenic trendline than other formations. However, there are differences between the trends of upper Bowland Shale Formation wells Beconsall-1Z (following the biogenic trendline, similar to Bakken) and Preese Hall-1 (positive correlation in between biogenic and terrestrial trendlines). Table 7 and Figure 29 shows that the ranges in Zr abundance differ between the upper Bowland (96.9 ppm), Bakken (227.0 ppm), Eagle Ford (65 ppm) and Barnett (143.2 ppm). There are differences between the ranges of upper Bowland wells Beconsall-1Z (60.9 ppm) and Preese Hall-1 (92.2 ppm). Ranges also differ for SiO₂ between the Bakken (52.4 %), Eagle Ford (28.4 %) and Barnett (65.1 %) as well as between Beconsall-1Z (26.9 %) and Preese Hall-1 (51.9 %).

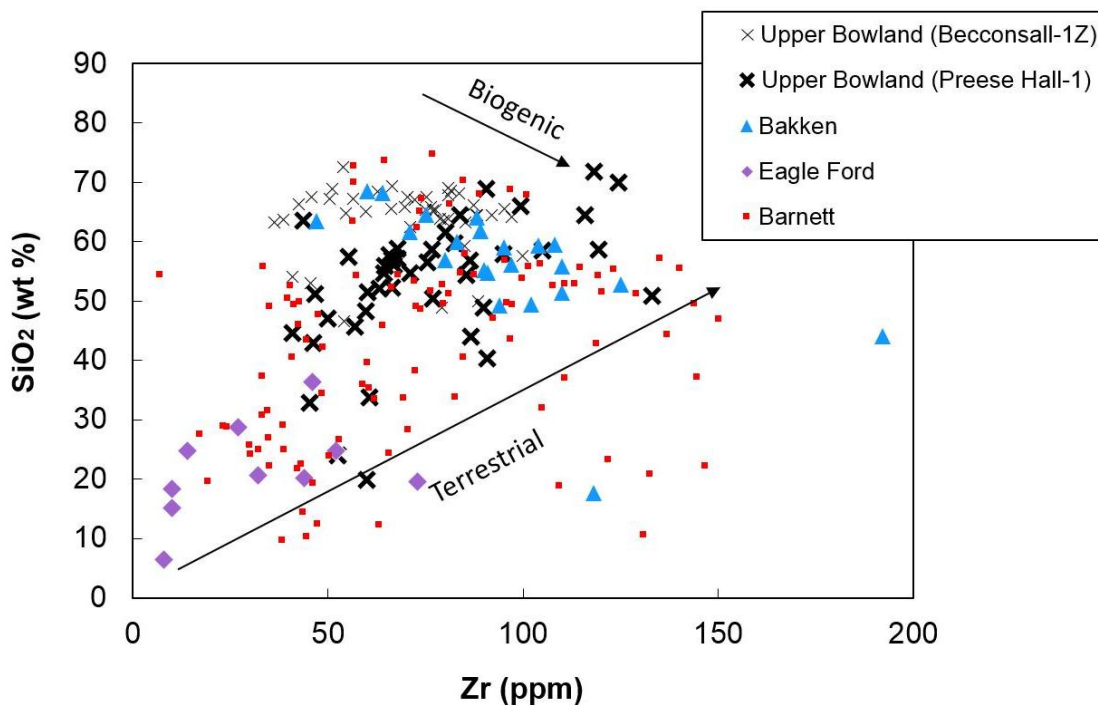


Figure 29: Binary plot of Zr and SiO₂ of the upper Bowland, Barnett, Eagle Ford, Bakken and Marcellus. Trends of biogenic and terrestrial silica adapted from Ratcliffe et al. (2012b)

Cross plots using enrichment factors of Mo and U are typically used to analyse bottom water palaeoredox conditions. Figure 30 shows a cross plot of Mo EF and U EF of the different formations. Additionally, Figure 30 has been grouped manually using interpretive observations, such as similarities in trend. These redox sensitive element abundances typically plot closer to the origin than the other formations. Average Mo EF in the Barnett are 4.7, ranging from 24.7 to 0.5. Averages for U EF in the Barnett are 6.3 and range from 22.9 to 0.1 (Table 7; Figure 30).

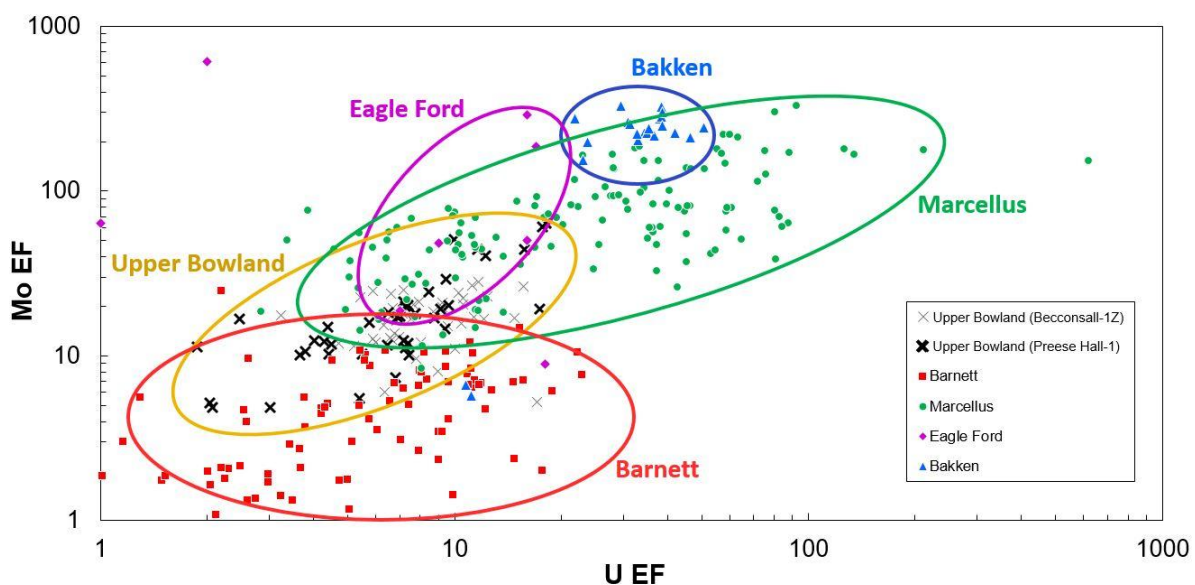


Figure 30: Mo and U enrichment factors (EF) of the upper Bowland (Beaconsall-1Z and Preese Hall-1), Barnett, Eagle Ford, Bakken and Marcellus.

Beaconsall-1Z in the upper Bowland has an average Mo EF of 17.3 and values range from 28.1 to 5.3. Beaconsall-1Z U EF have an average of 8.5 and range from 17.15 to 8.54. Preese Hall-1 Mo EF values have an average of 18.8 and range from 64.1 to 0.7. Preese Hall-1 U EF values average at 7.3 and range from 18.1 to 0.9. In the Bakken, Mo EF values average at 215.7 and range from 5.8 to 329.5. Bakken U EF averages at 31.4 and ranges from 50.7 to 0.7. Eagle Ford Mo EF have an average of 159.1 and values range from 607.2 to 8.9. U EF values in the Eagle Ford have an average of 32.7 and range from 117.5 to 1.9. In the Marcellus, averages for Mo EF are 92.0 and values range from 236.7 to 0.3. U EF

values in the Marcellus have an average of 48.3 and range from 89.8 to 0.3 (Table 7; Figure 30).

Computational Comparisons of Bottom Water Palaeoredox and Provenance proxies

Figure 31, Figure 32 and Figure 33 show cross plots of trace metal abundance (top) as well as two models that manually and computationally group data using a non-optimal (left) and optimal (right) function, respectively. For each figure, these hypothetical groups are called “Shale Formation *n*”. Comparisons between cross plots are described qualitatively.

Figure 31 shows similarities between the Ln(UEF) and Ln(MoEF) cross plot and the non-optimised model (left). When this cross plot is programmed to computationally divide formations into 6 groups, the Bakken can typically be represented as isolated cluster Shale Formation 3. The Bakken has a distinct grouping in the non-optimised model. The Marcellus is less clearly grouped as the Bakken in a non-optimised model but shares similarities with Shale Formation 2. Both wells in the upper Bowland Shale Formation are grouped and this formation typically shares similarities with Shale Formation 4, however, the spread of upper Bowland Shale Formation Ln(MoEF) and Ln(UEF) could be classified as Shale Formation’s 1 and 5. Eagle Ford data have no clear designated hypothetical Shale Formation in both non-optimised and optimised runs. The wide range of Barnett data are not constrained to a particular, non-optimised, Shale Formation. However, the lower values of Barnett Ln(MoEF) and Ln(UEF) are typically well captured as Shale Formation 6.

When Ln(UEF) and Ln(MoEF) data from the different formations are run optimally (Figure 31), the model computationally calculates that the most suitable number of groupings is 3. In this model (right), the Shale Formation divisions encapsulate more data points for each Shale Formation than in the non-optimised model. Run optimally, Shale Formation 1 typically groups the upper Bowland (Beaconsall-1Z and Preese Hall-1) and most Eagle Ford points. Shale Formation 2 groups the

Barnett most clearly but includes some Eagle Ford and Bakken data. Divisions between the Shale Formations do not depict the original Ln(UEF) and Ln(MoEF) data in this model, particularly between Shale Formation's 1 and 3. Shale Formation 2 typically groups Bakken, Marcellus and Eagle Ford data.

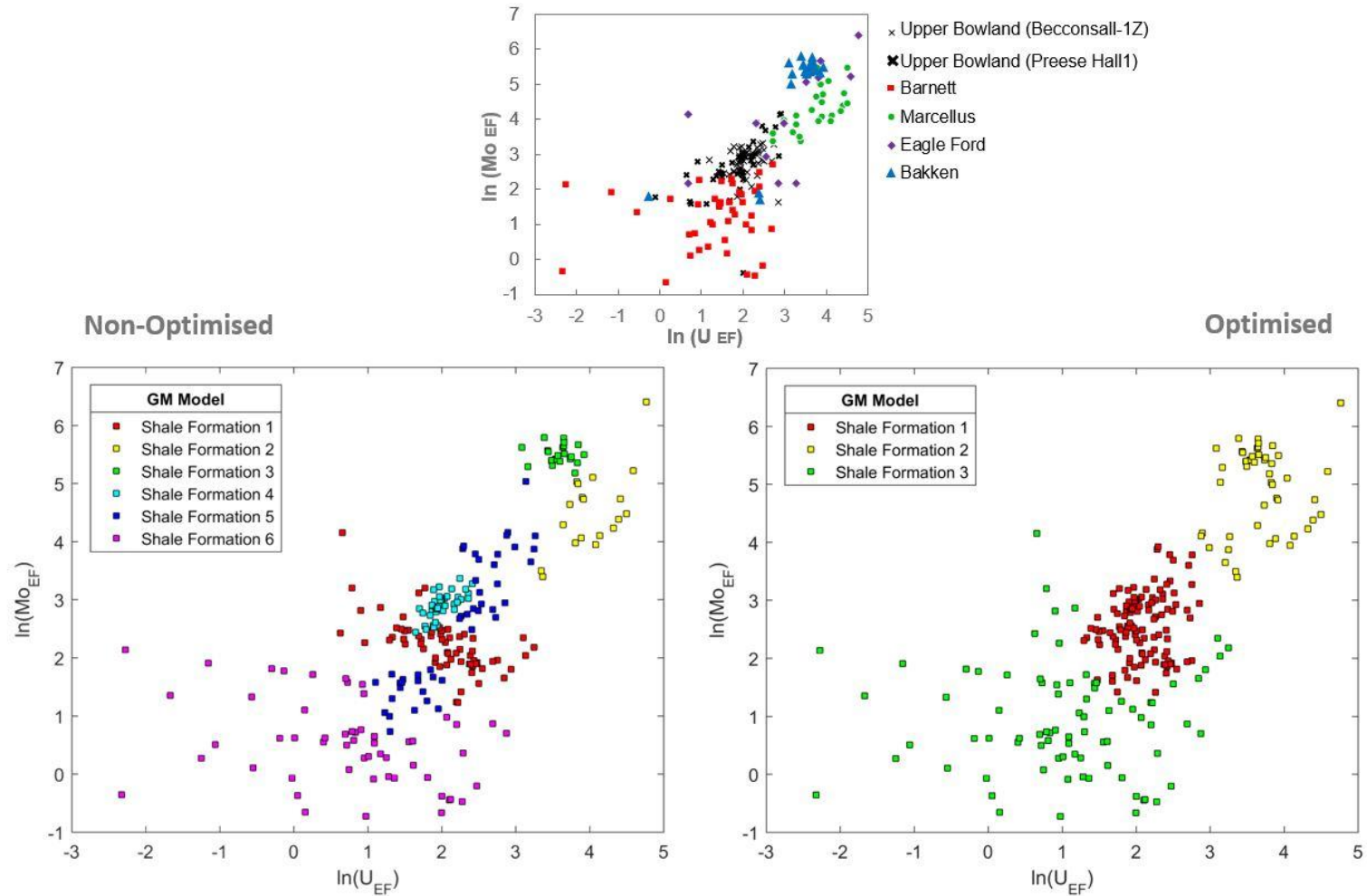


Figure 31: Cross plotted $\ln(U_{EF})$ and $\ln(Mo_{EF})$ (top). These data are run as a non-optimised 2D multivariate model, grouping into 6 hypothetical formations titled “Shale Formation n” (left). The optimised model (right) groups the original data into a computationally-derived number of hypothetical formations. (EF = Enrichment Factor).

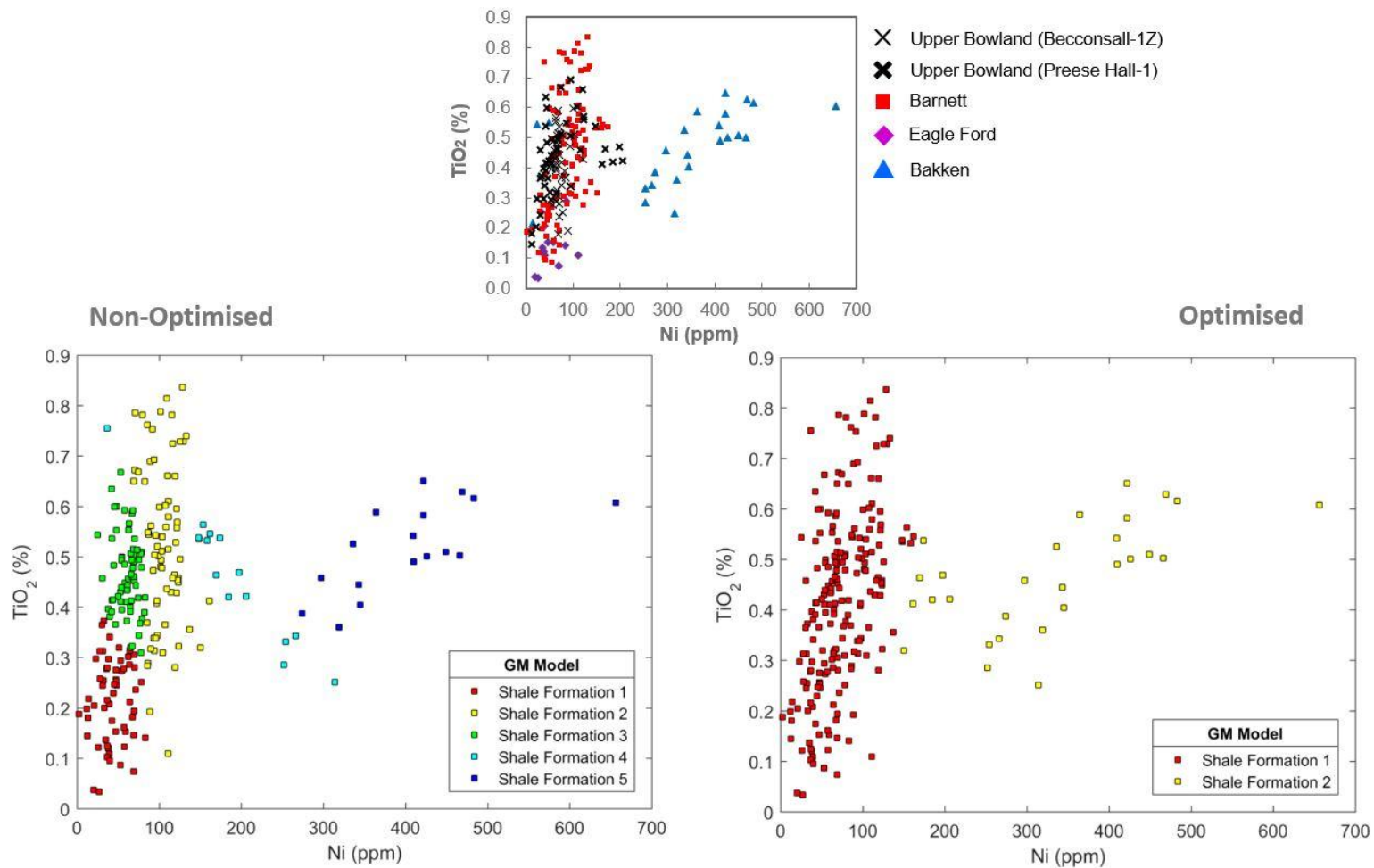


Figure 32: Cross plotted TiO_2 (%) and Ni (ppm). These data are run through a non-optimised (left) and optimised (right) 2D multivariate model.

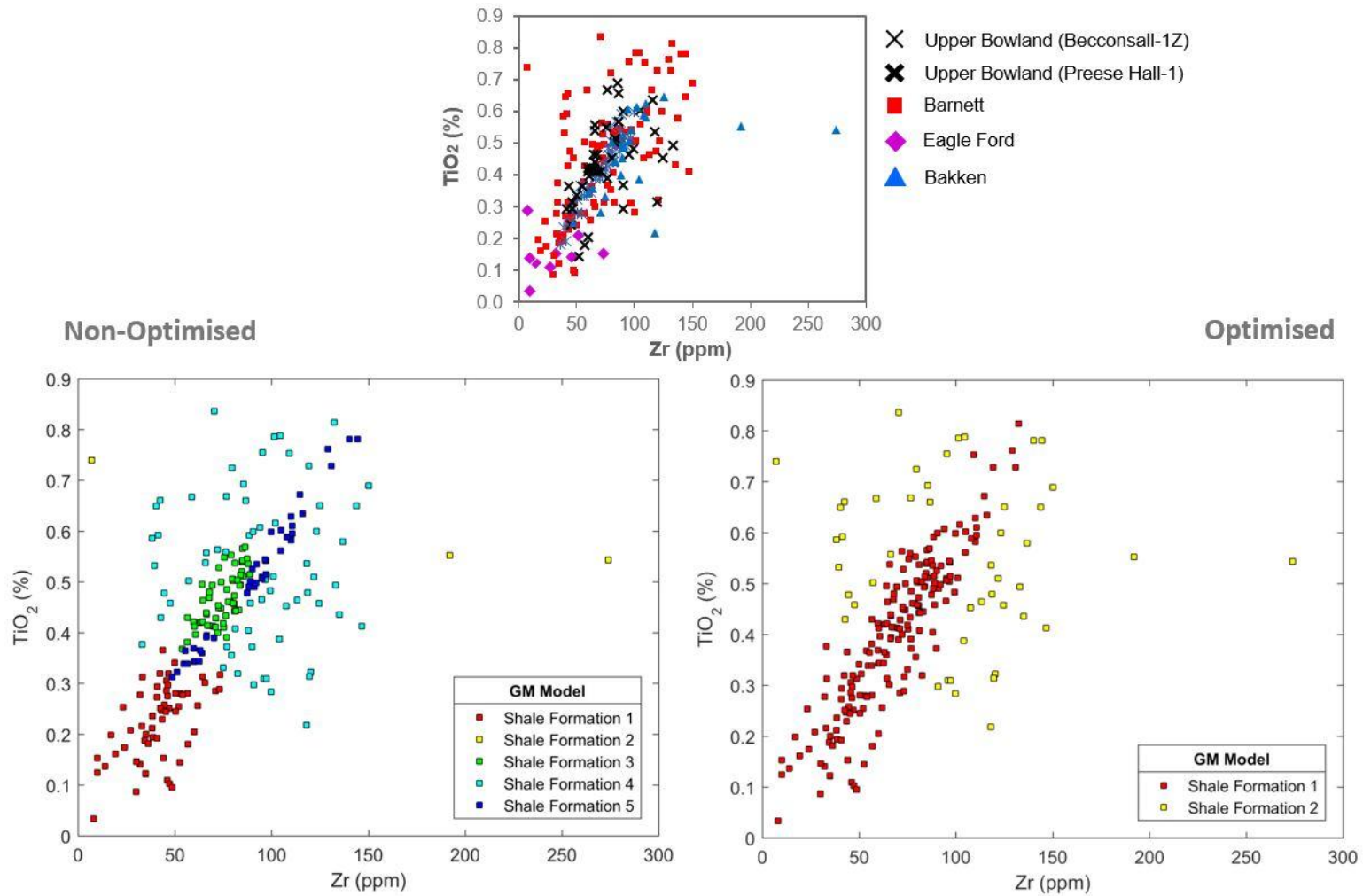


Figure 33: Cross plotted TiO₂ (%) and Zr (ppm). These data are run through a non-optimised (left) and optimised (right) 2D multivariate model.

Similarly, Figure 32 shows that both non-optimised and optimised models do not identify distinct differences in Ni and TiO₂ abundances between the upper Bowland, Barnett, Eagle Ford and Bakken. However, Shale Formation 5 only incorporates Bakken data because the model recognises that the Bakken exhibits a clear and different trend to the rest of the formations. The Marcellus is not used in this figure due to limitations of open access data. However, Shale Formation grouping separations from the non-optimised model do not match trends in the original cross plot (top). This is particularly true for the Barnett, upper Bowland and Eagle Ford, but less so for the Bakken. When optimised (right), Figure 32 shows that the model identifies 2 groups. This model typically separates the Bakken (including just a few points from the upper Bowland and Barnett) from all other formations.

Figure 33 and Figure 28 show that all formations have a positive correlation between Zr and TiO₂ (excluding Marcellus). This model's non-optimised divisions do not reflect the original formations. However, Shale Formations 4 and 5 do represent the spread of data known to be the original Zr and TiO₂ trends in the Barnett. However, as in all models, the Eagle Ford is not recognised as a distinguishable cluster. This model also recognises that the central cluster of points can be divided into Shale Formation 3 and Shale Formation 5. This is reflected in the original cross plot of TiO₂ and Zr (top of Figure 33), where Shale Formation 5 most resembles Bakken data and the upper Bowland is best captured by Shale Formation 3. However, the spread of the upper Bowland data is not captured in this model, particularly in Preese Hall-1. Regarding the upper Bowland, Beconsall-1Z and Preese Hall-1 are grouped as one Shale Formation in both non-optimised and optimised models. Optimised runs of Zr and TiO₂ data show that the model identifies two distinct groups. This optimised model typically does not reflect the original data (top of Figure 33).

Discussion

Analogue studies are important to the future of UK and worldwide frontier exploration because limited core material in unexplored basins drives reliance upon existing data (e.g. Nwaobi and Anandarajah 2018). Trace metal and palaeoceanographic data are important because predicting the depth and extent of abundant redox sensitive trace metals (e.g. U and V) is a key method in the identification of source rock “sweet spots” (Clarke et al. 2018; Craigie 2018; Jones and Manning 1994). However, this study is the first to investigate the most suitable palaeoceanographic analogue to the upper Bowland, a relatively unexplored UK petroleum target. Geochemistry is used in this study to select the most suitable palaeoceanographic analogue to the upper Bowland. It is important to discuss the similarities and limitations of each formation to assess their applicability.

The Bakken Shale versus the upper Bowland Shale Formation

The Bakken is investigated as an analogue to the upper Bowland because they were both deposited during the Mississippian.

Mineralogically, the Bakken is similar to upper Bowland wells Preese Hall-1 and Beconsall-1Z (Figure 25), however the Bakken is the most unlike any other formation in both redox sensitive trace metal abundances and in provenance proxies. This is best illustrated in Figure 30 and Figure 32 where the Bakken is identified as a separate “Shale Formation” in Mo-U EF and TiO₂-Ni models. Redox sensitive trace metal enrichment is linked to ocean euxinia and/or anoxia (Scott et al. 2017). The Bakken was deposited in comparatively more extreme anoxic and/or euxinic bottom water conditions, relative to the upper Bowland. This interpretation is supported by the relative extreme abundance of V and Ni as well as V EF compared to the other formations. Furthermore, Mo and U are both similarly interpreted as being unrelated to Zr using Figure 27, suggesting that, as in all the formations studied, Mo and U abundances are not linked to detrital input but are instead associated with bottom water redox conditions. This current study therefore supports the use of correlation

diagrams in previous studies (Craigie 2018) used previously to identify element associations.

The Bakken and upper Bowland share similarities in biogenic silica abundances in the upper Bowland and Bakken as in well as the detrital proxies Zr-TiO₂ cross plots (Figure 29).

The increased biogenic silica abundance in the Bakken, observed in this study, supports previous studies that suggest that Bakken silica is sourced from abundant deposits of Radiolaria (Sonnenberg et al. 2011). This abundance is relatively high compared to the other formations, such as the Barnett (e.g. Loucks and Ruppel 2007). However, some authors recognise clear abundances of terrestrial/detrital silica in the Bakken (Nandy et al. 2015) which are not observed in this study. Therefore, all mineralogical and trace metal data used in this current study suggest that the Bakken was sourced from a similar provenance type to the upper Bowland. However, as with the Marcellus, the bottom water conditions at the time of deposition were more reducing (Chermak and Schreiber 2014; Scott et al. 2017) in the Bakken relative to the upper Bowland. Therefore, the Bakken is not a suitable palaeoceanographic analogue to the upper Bowland.

The Barnett Shale versus the upper Bowland Shale Formation

The Barnett Shale Formation is investigated as an analogue to the upper Bowland Shale Formation because they were both deposited during the Mississippian.

The Barnett, similar to the Bakken, closely resembles that of the upper Bowland as a quartz dominated formation (Figure 25). The trace metal composition of the Barnett is typically similar to that of the upper Bowland in provenance proxy abundance (e.g. Figure 28) as well as in redox sensitive trace metal abundances, such as V, Fe, Mo and U (Figure 30 and Figure 26). Additionally, cross plots of Barnett and upper Bowland Mo and U EF are the most similar (Figure 30) suggesting that ocean conditions were similarly low in oxygen at the time of deposition and/or eogenesis.

Computational models support this interpretation. For example, in Figure 31, both the non-optimised and optimised models typically group Barnett and upper Bowland data separately, but the borders of these groups are not representative of the true upper Bowland and Barnett. The Barnett is the most similar in bottom water redox conditions to the upper Bowland as well as in provenance geochemistry and in major trace metal abundance (Figure 34). Exceptions to their similarity include biogenic silica abundance (Figure 29). This suggests that the geochemistry of the upper Bowland and Barnett can be differentiated into two separate formations using only geochemistry (without sedimentology). However, both formations share the most similarities in ocean redox states when compared to the other formations in this study. Therefore, these qualitative and computational comparisons suggest that the Barnett is the most suitable palaeoceanographic analogue to the upper Bowland.

The Marcellus Shale versus the upper Bowland Shale Formation

The Marcellus is investigated as an analogue to the upper Bowland Shale Formation because they share similar characteristics in basin morphology and have been previously analogised in the literature (Andrews 2013b).

The Marcellus is used in this study despite limited data to, in part, highlight gaps in open access sources. Therefore, caution should be taken when interpreting and comparing these data to the upper Bowland. Of the available data, Figure 30 shows that Marcellus Mo and U enrichments are much higher than the upper Bowland (Figure 26 and Figure 30), suggesting that water column stratification was elevated and/or more sustained in the Marcellus relative to the upper Bowland, using standards proposed in Tribovillard et al. (2012). For example, Marcellus Mo and U EF infer maintained anoxia-euxinia (supporting interpretations from Wendt et al. 2015) whereas the upper Bowland is more indicative of an anoxic environment (Chapter 6). Computational optimised and non-optimised 2D multivariate models support this qualitatively interpreted difference because the majority of Marcellus Mo and U data (Figure 31) are identified as a separate hypothetical "Shale Formation" to the upper Bowland. Open

access data gaps highlight the relative uncertainty in geochemical processes and further limits the applicability of upper Bowland-Marcellus comparisons. However, the available data show that redox sensitive trace metal trends, ranges, abundances and enrichments are not analogous to the upper Bowland.

The Eagle Ford Shale versus the upper Bowland Shale Formation

The geochemistry of the Eagle Ford is used as a control in this study because it is not similar to the upper Bowland in either basin morphology or time of deposition.

The Eagle Ford is most mineralogically different to all other formations because it is carbonate rich (Figure 25) and therefore abundant in elemental Ca (Table 7 and Figure 26). This characteristic is established in the literature (Cash 2016; Hsu and Nelson 2002). The Eagle Ford is most enriched in Ca (Figure 26), linked to low abundances of Al, K, Ti and Si (elements typically associated with clay minerals) (e.g. Craigie 2018). Figure 26, Figure 30 and Figure 31 suggest that, compared to the other formations in this study, Eagle Ford mineralogy and heavy metal abundances (e.g. low Zr), is not distinctly different in redox sensitive trace metal abundance (Mo, U, V and Mn). This is most likely because the elements in this Eagle Ford succession have limited associations to other elements (Figure 27). This suggests that these redox sensitive trace metals are not related to mineralogy or heavy mineral input. The Eagle Ford does not share enough geochemical similarity to act as an appropriate analogue to the upper Bowland. For example, Figure 31 shows ambiguity in grouping the Eagle Ford, however the model does identify some similarities with the upper Bowland and Eagle Ford in Mo and U enrichment. This suggests that, although the upper Bowland and Eagle Ford differ in mineralogy and in the majority of elemental abundances, they share some similarities in trace metal reduction and oxygen levels. The literature supports interpretations of similar anoxia in the upper Bowland (Chapter 6) and Eagle Ford (Ratcliffe et al. 2012a) during deposition.

Alternatively, optimised models in Figure 31 identify the upper Bowland as a separate group ("Shale Formation 1"). Therefore, it is possible to interpret the upper Bowland as separate to all other formations in terms of elemental geochemistry. This highlights the challenges linked to the use of analogues in general because it is rare/unattainable that two formations are identical. However, the aim of this study is to identify the best suitable analogue for the upper Bowland. Therefore, in this scenario, the Barnett is the most geochemically analogous.

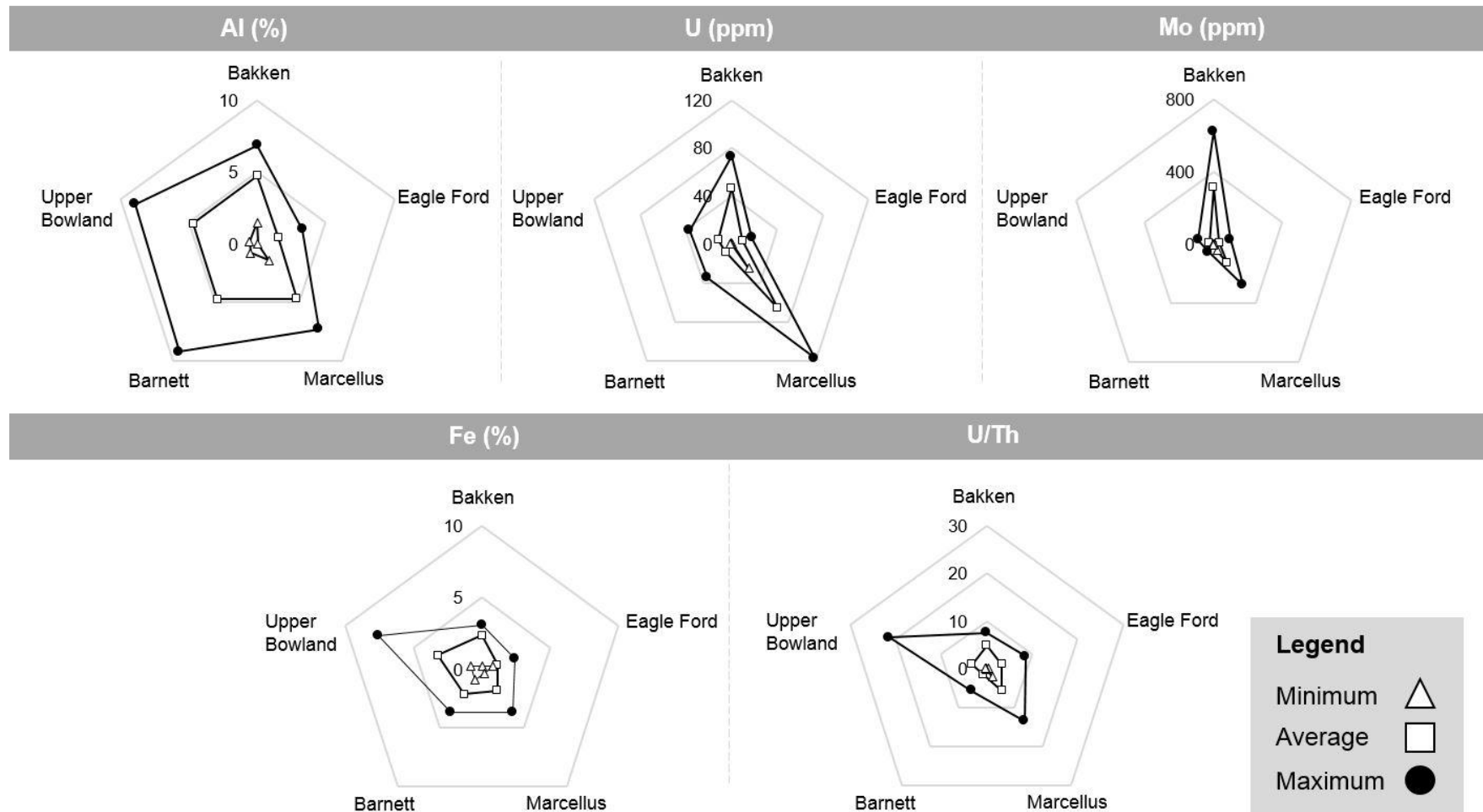


Figure 34: Summary of key elements illustrating similarities between the Upper Bowland and Barnett (e.g. Al and U abundances) as well as their differences (e.g. U/Th).

Challenges Associated with Further Comparison

This study could not compare every worldwide formation to the upper Bowland because of limited open access data availability. Therefore, there may be other, more suitable palaeoceanographic analogues that are not yet available or studied. For example, Clarke et al. (2018) suggests that the Wolfcamp Formation in the Midland Basin is morphologically similar to the Bowland Basin (e.g. formation thickness). Other challenges include the uncertainty of upscaling interpretations to all wells drilled through each formation. This was not possible in this study because of restrictions linked to open access XRF data, particularly in the Marcellus. However, we interpret the data and models used in this study to be applicable if used with caution. For example, models in Figure 31, Figure 32 and Figure 33 group both upper Bowland cores (Beconsall-1Z and Preese Hall-1) as one "Shale Formation" suggesting that the model accurately recognises the geochemical similarities of two cores within the same formation.

Additionally, all optimised models group data into fewer groups than the non-optimised (manually selected) for each cross plot. This suggests that, despite geochemical differences between formations, they each share some geochemical similarities.

It is important to acknowledge that this study uses the best available geochemical data for each succession and therefore the average sampling resolution differs between the Bakken (average 0.3 m), upper Bowland (c. 0.4 m), Barnett (c. 0.4 m), Eagle Ford (c. 7 m) and Marcellus (c. 0.3 m) formations. Differences in elemental data sampling resolutions will affect interpretation (Craigie 2018). However, the ranges of trace metal data used in this study (e.g. Mo and U EF) largely differs between each succession and supports previously established trends, such as the Ca rich Eagle Ford (Pommer and Milliken 2015) and Mo rich Bakken (Scott et al. 2017). Therefore, it is likely that the observed geochemical differences between each formation are a true reflection of the palaeoceanographic comparison. This is best illustrated by the Bakken and Barnett formations

which have similar sample resolutions but are clearly different in redox sensitive trace element geochemistry (Figure 26 and Figure 30).

Palaeogeography versus Time

It is important to discuss the relative importance of palaeogeography to time and their relevance to source rock analogue studies to guide future analogue selections.

We interpret the Barnett to be the most analogous to the upper Bowland with regards to bottom water redox states and palaeoceanography. The Barnett and Bakken formations were both deposited during the Mississippian, the same geological time series as the upper Bowland. However, the Barnett is more geochemically similar to the upper Bowland whereas the Bakken could be interpreted as the most different with regards to ocean oxygen levels. Therefore, we support previous studies that compare the geochemistry of source rocks from different depositional time series (e.g. Brumsack 2006). Therefore, the comparison of similar time series is not a necessary requirement for an analogue study using trace metals. Additionally, this study supports the use of modern analogue studies (Brumsack 2006a; Griffiths et al. 2018; Schulz et al. 2005), provided that their depositional processes and/or bottom water conditions are similar to their ancient counterparts. However, this interpretation does not extend to organic/isotopic geochemistry because these techniques are more reliant upon changes in palaeobiogeochemistry over time (Berner et al. 2000; Peters-Kottig et al. 2006; Peters et al. 2005).

We suggest that regional source rock analogue comparisons should prioritise selection based on similarities in depositional setting and the processes related to palaeoceanography. Additionally, local controls on water column stratification are also important considerations, for example OM burial (Canfield 1994; Katz 2005; Tyson 1987). However, this study interprets the Marcellus as an unsuitable analogue to the upper Bowland, and therefore similarities in basin morphology may not always be a useful indication of a suitable analogue.

Conclusions

1. The Barnett Shale is identified to be the best palaeoceanographic analogue for the upper Bowland Shale Formation, based on similarities in mineralogy, bottom water redox conditions, trace metal abundances and enrichment factors.
2. We show how similarities in mineralogy do not necessarily reflect similarities in depositional and/or eogenetic processes. In the upper Bowland, Barnett and Bakken, redox sensitive trace metal abundances are the most useful when comparing the geochemical differences between these similarly quartz dominated source rocks.
3. Two-dimensional multivariate models are useful to the geochemical comparison of source rocks. However, future work should aim to develop qualitative comparisons into quantified observations of similarities/differences. We show that it is important to understand the element-element relationships before running these models.
4. The success of the Bakken as a petroleum target is interpreted, contextualised and compared to other US shale plays as well as to the upper Bowland. The high hydrocarbon yield of the Bakken (Scott et al. 2017) is linked to high OM burial related to increased and/or sustained water column stratification at the time of deposition and/or eogenesis. This palaeoceanographic characteristic is distinct from even the other major US formations.
5. Similarities in depositional time are not the most important control on palaeoceanographic analogue reliability with regards to trace metal geochemistry. The Bakken (Carboniferous) does not share palaeoceanographic similarities with the upper Bowland (Carboniferous). The Barnett (also Carboniferous) is most applicable as a palaeoceanographic analogue to the upper Bowland. Therefore, this study supports the use of modern analogue studies providing their depositional and early diagenetic environments are similar to their ancient counterparts.

Chapter 8. Discussion

We address five key themes in this thesis: (i) the integration of sequence stratigraphy and geochemistry (ii) the benefits and challenges of outcrops and analogues (iii) well correlation (iv) sweet spot discrimination in unexplored basins and (v) sweet spot discrimination in the Bowland Shale Formation.

The Integration of Sequence Stratigraphy and Geochemistry

The integration of sequence stratigraphy and geochemistry is a fundamental challenge in petroleum exploration and geoscience in general (Craigie 2018; LaGrange et al. 2020). Recent studies have recognised the importance of integrating large-scale sequence stratigraphic processes with geochemistry (e.g. Birgenheier et al. 2017; Egenhoff and Fishman 2013; Li and Schieber 2020; Taylor and Macquaker 2014; Wilson and Schieber 2015) and the unique difficulties specific to mudstone successions, such as subtle compositional variability (LaGrange et al. 2020). The integration of multi-scale techniques and concepts is crucial in deciphering local from regional processes (Craigie 2018; LaGrange et al. 2020), which can improve the accuracy of upscaled interpretations. Additionally, previous work has identified the importance of marine bands as the potential key to help develop sequence stratigraphic models (e.g. Davies and Elliott 1996; Martinsen et al. 1995) and some previous studies have used geochemistry to understand marine band formation processes (Bloxam and Thomas 1968, Horn 1960; Riley 1993). However, few studies have used marine bands as a means of integrating sequence stratigraphy and geochemistry (Gross et al. 2015) as this current thesis does. Additionally, previous studies (e.g. Gross et al. 2015; La Grange 2020), unlike our current study, have not focussed on the Bowland Basin or analysed marine bands at high resolution (10 cm sampling intervals). Other authors (Gross et al. 2015; LaGrange et al. 2020) have aimed to synthesise mudstone sequence stratigraphy and geochemistry using different analytical techniques (predominantly inorganic and organic,

respectively) but with similar overall approaches. LaGrange et al. (2020) suggests that their multi-scale integration was limited by their use of one technique (elemental analyses). Gross et al. (2015) predominantly studied the organic geochemistry of mudstone depositional cycles, similarly limiting their model's potential. However, in this current study, we have used a multi-proxy and multi-disciplinary approach. Although this can be time consuming and expensive, we identify geochemical differences between systems tracts using a combination of biostratigraphy (*Tumulites pseudobilingue*) as well as inorganic and organic proxies. For example, we identify elevated XRF-derived Mo/U at the base of the falling stage systems tract (e.g. averages of 1.7, 2 and 2.7 in zones 1, 2 and 3 respectively in Beconsall-1Z) and elevated pyrolysis-derived OSI (averages of 18.3, 23.7 and 18 in zones 1, 2 and 3 respectively in Beconsall-1Z) in a highstand. Therefore, our data support interpretations from Tribovillard et al. (2006) which suggest that Mo/U ratio is crucial to the identification of key stratigraphic boundaries. In the case of Mo/U and other similar ratios (e.g. Mo/Al; Craigie 2018), some redox proxies may be more easily interpreted with respect to large scale depositional processes (e.g. Tribovillard et al. 2006). However, other stratigraphic proxies, such as elevated OSI in a highstand, may have less clear controls when upscaled (linked to hydrocarbon generation and/or retention).

This study may be the first to use a multi-disciplinary and multi-technique approach designed to understand the limitations of the sequence stratigraphic-geochemical integration of UK Carboniferous rocks.

Therefore, specific literature comparisons are limited. It is possible that the challenges related to sequence stratigraphic-geochemical integration may stem from how each different technique separately approaches uncertainty. For example, regional sequence stratigraphic subsurface mapping typically embraces uncertainty (Martinsen et al. 1995) whereas geochemical techniques typically emphasise caution with explicit reference to quantifiable error (e.g. Craigie 2018). We suggest that this problem could be minimised by the introduction of expressed error in sequence

stratigraphy, which might be achieved by testing the limits of established sequence stratigraphic models. However, it is currently difficult to reconcile the two methods without expressing qualitative caution (e.g. LaGrange et al. 2020).

In every chapter, this thesis analyses large scale processes (outcrop or core sedimentology and biostratigraphy) prior to geochemical interpretations, suggested previously by Craigie (2018). Future studies concerning the integration of sequence stratigraphy and geochemistry during mineral or petroleum exploration will benefit from adopting this approach by determining regional controls on sedimentology prior to geochemical analysis.

The Benefits and Challenges of Outcrops and Analogues

In a relatively unexplored basin with minimal core material and well log data, outcrop analyses and data from analogous plays are crucial resources. The upper Bowland Shale Formation is used in this project as a case study to investigate the effectiveness of outcrop and analogue comparisons, in part because it is a relatively unexplored basin with limited outcrop exposure with no clear ancient analogue (Andrews 2013; Clarke et al. 2018).

We support previous suggestions (Leythaeuser 1973) that the organic geochemistry of a mudstone can be obscured by chemical, physical and biological weathering and that the best samples for geochemical analyses are taken from streams (Emmings et al. 2017). We also agree with Emmings et al. (2017) with regards to elevated OI, T_{max} and low HI in outcrops, interpreted to be linked to weathering. However, it is difficult to discern weathering signals from that of thermal maturity effects without using shallow drill-cores. Therefore, this current project supports previous interpretations made by Leythaeuser (1973) that recommend caution during outcrop organic geochemical analyses. Additionally, for this upper Bowland outcrop and core comparison, similar and laterally extensive depositional environments were selected (marine bands). However, other unavoidable pitfalls of outcrop analyses include uncertainties related to

lateral continuity (Slatt et al. 1992). For example, the upper Bowland Shale outcrop at LMC is c. 60 km from the Preese Hall-1 production well. Therefore, it is possible that in a natural and dynamic depositional system, the geochemistry of a different, outcrop location is not the same as material from subsurface cores. Outcrop analyses, and the pitfalls of weathering and depositional differences relative to core, will remain an important aspect to source rock characterization in the Bowland (Emmings et al. 2017). Therefore, future work should aim to sample streams or shallow cores (Emmings et al. 2017).

Analogue studies are an established strategy for minimising subsurface risk in unconventional targets (Craigie 2018; Schulz et al. 2015). However, selecting a suitable analogue for a formation with minimal subsurface data is difficult. We show that computational modelling of trace metal geochemistry (Figure 38; Figure 39; Figure 40) is an effective method in selecting a suitable palaeoceanographic analogue. However, although it is most effective to select an analogue with identical characteristics (e.g. basin geometry, palaeogeography, palaeoceanography and time equivalent), the geological record is limited. Therefore, we suggest that a useful palaeoceanographic analogue prioritises depositional environment over time-equivalence when investigating elemental geochemistry. Additionally, we support the use of modern and ancient analogues (Schulz et al. 2015), provided that the depositional environment is similar. Therefore, we support the use of “average shale” comparisons (Wedepohl et al. 1991; Wedepohl 1969-1978), which is used as an analogue throughout this thesis, supported by the compositional similarities of all studied formations (Figure 33). However, this thesis agrees with Van der Weijden (2002), that the extensive use and over-interpretation of enrichment factors and average shale comparisons should be used with caution.

Future geochemical studies of unexplored basins should integrate computational models that express uncertainty (e.g. Stephen et al. 2001)

with outcrop and analogue data to more accurately interpret subsurface petroleum targets.

Well Correlation

The uncertainty linked to subsurface well correlation is a global challenge (e.g. Nsianya 2013; Preston et al. 1998; Alvarez 2018) and therefore is not unique to the Bowland Shale. However, this formation was selected as the subject of our study because it is a good example of an actively explored unconventional target with limited well correlation due to subtle compositional variability (Clarke et al. 2018).

Biostratigraphy is an established method of guiding wells, when drilling, worldwide (Moslow et al. 2018) as well as in the upper Bowland Shale (Clarke et al. 2018). Additionally, well correlation risk can be minimised using geochemical and petrophysical stratigraphic indicators of U, ^{40}K and/or Th enrichment to increase confidence of biostratigraphic observations (Clarke et al. 2018; Fadiya 2014). Additionally, Craigie (2018) summarises a range of possible trace metal proxies for mudstone well correlation, from redox sensitive Mo/Al to heavy metal input proxies like Zr/Al, and these ratios were applied to our study. Craigie (2018) does not investigate the Bowland Shale Formation and we suggest that the Bowland is a particularly difficult formation to correlate using chemostratigraphy and two sample T-tests (limited proxies showing statistical significance; Figure 14). We suggest that this primarily reflects the previously recognised sedimentological uniformity of the Bowland Shale Formation in comparison to other previously studied and more heterogeneous mudstone formations, such as the Barnett Shale (Andrews 2013). Craigie (2018) expresses the importance of trace metal proxies such as Ti/Al, Zr/Al and Th/K (detrital and/or heavy metal input proxies). However, these do not change significantly up succession in either Becconsall-1Z or Preese Hall-1 across a marine band using a two-sample T-test (Figure 14). This also differs from previously investigated time equivalent beds in the County Clare Basin (Davies and Elliott 1996) where these proxies show distinct changes within a marine band, relative to the

rocks above and below. However, in this current study, we suggest that the future production of any chemostratigraphic correlation scheme should, if in a similar scenario, turn to focus on redox sensitive proxies (e.g. Mo/U), which we show can differ significantly up succession across a marine band using a two sample T-test. Additionally, the novel use of other techniques such as organic geochemistry as well correlation proxies was borne out of the limitations posed by burial depth and exceptionally subtle compositional differences up succession (mudstone-dominated formation; Figure 8 and Figure 20).

We show how the Bowland Shale's burial depth >5000 m (Andrews 2013a) may have obscured well correlation organic geochemical proxies causing near-origin clustering in a pseudo-van Krevelen (Figure 5) as seen in previous work (Emmings et al. 2017). However, we further suggest that the applicability of molecular analyses is further limited by low EOM (<2 mg in Beconsall-1Z and Preese Hall-1) and low abundances of key molecular proxies (e.g. Pristane/n-C₁₇ <2 and Phytane/n-C₁₈ ≤1 in all studied cores and outcrops). In these circumstances, we suggest that future studies may benefit from a multi-disciplinary approach (e.g. elevated OSI; Figure 15). However, it has previously been suggested that the integration of different chemostratigraphic datasets can lead to further challenges because chemozone boundaries do not always 'fit' or integrate exactly (Craigie 2018). It is possible that our dataset reflects this interpretation, for example, in both cores the maximum values of Mo/U and OSI feature in different zones (Zone 3 and Zone 2, respectively). However, although we show that these two proxies are useful for marine band identification, they represent different processes such as water column stratification (Tribovillard et al. 2006) and hydrocarbon retention and/or generation, respectively. Crucially, the limitations of each technique used in this Bowland Shale study may also limit the confidence of multi-technique integration and it is likely that multi-proxy integration will challenge future geochemical studies. However, we suggest that the

increased confidence and benefits of a multi-disciplinary approach to well correlation outweighs the challenges linked with dataset integration.

Sweet Spot Discrimination in an Unexplored Basin

Well correlation is academically useful to stratigraphic navigation (e.g. Alvarez 2018; Nsianya 2013; Preston et al. 1998), but it is also essential to play fairway analyses and sweet spot discrimination (e.g. Skupio and De Alemar Barberes et al. 2017; Zhou et al. 2019). Sweet spot discrimination is related to well correlation because the directional drilling of unconventional targets involves following a hydrocarbon enriched zone and then creating a complex fracture network (e.g. Zahid et al. 2007). However, unlike the previous sub-section on well correlation, this sub-section addresses the identification, appraisal and production of a hydrocarbon sweet spot in an unexplored basin. Most modern unconventional plays, for example in the United States, aim to further exploit existing fields and in some cases have a wealth of data to inform future exploration (Cipolla et al. 2010). Many US fields are in the production stage of development (Cipolla et al. 2020). However, worldwide, there are new unconventional targets with limited previous exploration, such as in China and South America (e.g. Hammes 2019; Jiang et al. 2019; Lennon 2019). Therefore, data acquired from the Bowland Shale frontier target could be used as an analogue for other unexplored shale gas targets.

Major challenges facing frontier target exploration include the increased risk related to limited data/material in unexplored conventional (e.g. Craigie 2018) and unconventional plays (Clarke et al. 2018; Martini et al. 2019). These scenarios can also lead to potentially high reward (Ali 2019). However, 'more data' is not always an option in frontier exploration, due to the increased expense and time-consuming nature of extra coring. In this Bowland Shale study, we use a multi-disciplinary approach to increase confidence in interpretations (multi-scale inorganic and organic techniques). However, this may not be suitable for all future studies aiming to analyse the geochemistry of a potential sweet spot. For

example, as in the case of GC/MS or GC/FID versus gamma ray logs or XRF analyses, some techniques can be more expensive than others. However, whilst techniques like gamma are generally considered to be more unanimously applicable to subsurface exploration than, for example molecular analyses, the usefulness of techniques like molecular analyses can profoundly increase confidence of interpretations (Adams and Gasparini 2013). We therefore suggest that future work on sweet spot discrimination in an unexplored basin will benefit from a comprehensive balance sheet that weighs the negatives of a costly multi-disciplinary approach against the benefits of increased confidence during sweet spot discrimination.

A balance sheet of this kind must also account for other considerations such as the applicability of various techniques to a specific target formation and basin. For example, in our Bowland study, burial depths of >5000 m (Andrews 2013a) present limitations upon the applicability of molecular analyses (e.g. EOM <2 mg; peak integration attainable from just 44 % of all 15 g samples). Additionally, our study supports previous interpretations that show the limitations of OM pyrolysis (Emmings et al. 2017) on weathered outcrops. However, we also suggest that the 'trade off' between techniques is not so clear because some techniques may be more reliant upon the prior use of others, such as GC/MS and RockEval pyrolysis respectively (e.g. Killops and Killops 2013; Peters et al. 2005). One further benefit of adopting a multi-disciplinary approach towards sweet spot discrimination is in the increased likelihood of novel discoveries. For example, we show how OSI proxies can be used to increase confidence during well correlation, whereas they have previously been used to estimate the quantities of 'gas versus oil' (Jarvie 2012).

Additionally, we support the use of cross-disciplinary conservative error to increase confidence of interpretations by adopting error calculations derived from biochemistry and mathematics (Holmes and Buhr 2007). Our approach supports the interpretations of other authors who recommend the essential use of conservative errors in all geochemical studies

(Anderson 1976; Craigie 2018; Ingamells 1974; Killops and Killops 2013). However, ultimately, in exploration these data and errors must be used to inform large scale interpretations (LaGrange et al. 2020). Therefore, we also support previous studies (e.g. Craigie 2018; Killops and Killops 2013; Tinnin et al. 2014; Zhou et al. 2008) that suggest the future of exploration and sweet spot discrimination in unexplored basins relies heavily on accurate and minimised error, basin-wide, for example by integrating datasets and/or using high-precision techniques and methods.

Sweet Spot Discrimination in the Bowland Shale Formation

The Bowland Shale Formation has been suggested in previous studies to be a target for shale gas and therefore it is more than a useful analogue for other frontier formations and basins (Andrews et al. 2013; Clarke et al. 2018).

The wildcat production well Preese Hall-1, exploration well Beconsall-1Z (e.g. Clarke et al. 2018) and more recent production wells at the Preston New Road site in Lancashire (currently confidential) have been used in part to minimise subsurface risk during production (Clarke et al. 2018; Cuadrilla 2019a; Cuadrilla 2019b). Therefore, this current academic Bowland project is limited to the study of outcrops, Beconsall-1Z and Preese Hall-1 which correlate marine band E₁B₂. Despite limited outcrop and core material, this project aims to maximise confidence during sweet spot discrimination in the Bowland and compliments previous unconventional studies that recommend a high resolution approach (e.g. Craigie 2018). Additionally, just as these data from the Bowland Shale can be used to minimise risk in other modern and future frontier targets, previously explored formations can be used as analogues for sweet spot discrimination in the Bowland Shale Formation. For example, the Barnett has been previously used as an analogue for the Bowland in previous studies (e.g. Andrews 2013; Murphy 2014; Rowe et al. 2012; Shulz 2015) and our GM models (Figure 38 and Figure 39) further support this analogy by showing that Bowland trace metal geochemistry (e.g. Mo and U

abundance) is more similar to the Barnett than many other major economically produced US plays, such as the Bakken and Eagle Ford.

Economically producible sweet spots are preferably: (i) hydrocarbon-enriched as a bed or member and (ii) laterally continuous (e.g. Craigie 2018; Islam 2014).

In many US unconventional plays, the highstand is prioritised as the sweet spot in part because it is sufficiently enriched in TOC (Strickland et al. 2011). However, in the upper Bowland, maximum TOC values lie within Zone 1 in both cores (4.5 % in Beconsall-1Z and 5.3 % in Preese Hall-1). Therefore, Beconsall-1Z and Preese Hall-1 in isolation do not provide enough evidence to suggest that marine band E₁B₂ is more enriched in organic carbon than zones 1 or 3. However, US analogues suggest that highstands are more suitable targets during play fairway production, for example in the Bakken (Sarg 2011). This apparent difference between Bowland marine bands and the US highstands may be due to specific differences linked to sampling error, well position and thermal maturation. For example, we suggest that Bowland OM is difficult to analyse in both outcrop and core due to high thermal maturity (e.g. average T_{max} 458.6 °C in Beconsall-1Z, 470.0 °C in Preese Hall-1 and 441.1 °C in LMC2). The extreme burial depth of upper Bowland Shale marine bands most likely promoted increased OM thermal degradation relative to the many studied US analogues which have undergone less burial. For example, the Bakken has been buried to less than <3000 m (Kent et al. 1994) whereas the upper Bowland Shale has been buried >5000 m (Andrews 2013a). Therefore, it is possible that Bowland Shale marine bands are relatively more enriched in hydrocarbons than zones 1 and 3, but in areas of the basin that have been less deeply buried and undergone less thermal maturation.

Clarke et al. (2018) previously used seismic interpretation and biostratigraphy (marine band E₁B₂) to suggest that laterally extensive beds in the Bowland Shale Formation extend > 15 km. Our Bowland Shale study further supports this interpretation by using geochemistry to

identify the location of marine band E₁B₂ in Preese Hall-1 and Beconsall-1Z. Additionally, we show that the palaeoenvironment of the Bowland Shale Formation was anoxic at the basin margins (Mo EF ranging from 0.69 – 64.13 with an average of 18.83 in Preese Hall-1) and in the central basin (Mo EF ranging from 5.25 – 28.07 with an average of 17.31 in Beconsall-1Z). This interpretation is further supported through the use of organic geochemistry (Pr/Ph <2 in both cores), suggesting that the conditions for OM preservation and carbon burial were basin wide. This geochemical lateral continuity is a desirable characteristic for any unconventional hydrocarbon target and therefore we agree with previous studies (Clarke et al. 2018) that aim to investigate the upper Bowland Shale Formation for shale gas.

Is the upper Bowland Shale a Suitable Target for Petroleum?

This thesis highlights the benefits of core material and the uncertainties associated with limited subsurface data. Despite uncertainties associated with limited cores, thicknesses in Beconsall-1Z (south basin) and Preese Hall-1 (central basin) were recorded to be 84 m and 499 m, respectively. This is c. 2 -14 times thicker than the Barnett Shale and c. 2 - 10 times thicker than the Bakken Formation successions that are studied as time equivalent analogues (e.g. Sarg 2011). It is possible that numerous stratigraphic layers could be exploited for gas in the UK and for this reason the central Bowland Basin is likely a more desirable target for shale gas production than the southern margin.

We show that the upper Bowland Shale Formation has little mineralogical and geochemical heterogeneity, for example TOC standard deviations record 0.53 % in Beconsall-1Z and from 1.42 % in Preese Hall-1 with averages of 3.20 % and 2.51% respectively. Therefore, average TOC abundances are >2 % basin wide which is informally desirable as a petroleum target (e.g. Clarke et al. 2018; Reading 2009). Similarly, organic geochemistry, such as average Pr/Ph values of 1.26 in Beconsall-1Z and 1.48 in Preese Hall-1, as well as trace metal (average Mo EF of 17.31 in Beconsall-1Z and 18.83 in Preese Hall-1) infer sustained basin-

wide anoxia at the time of deposition. This likely drove basin wide OM preservation, which is needed in a laterally extensive source rock (Katz 2005). However, anoxia and associated OM burial in the Bowland Basin is not comparable to the size and extreme OM burial of some other shale gas targets, such as the Bakken (Sarg 2011).

Many factors outside of geochemistry determine the success of a petroleum play, however accurate geochemical analyses are essential (Craigie 2018). For example, oil based drilling fluids can limit the accuracy of organic geochemical analyses (Wenger et al. 2004), through the suppression of T_{max} (Carvajal-Ortiz and Gentzis 2015). However, oil based muds were not used in the drilling of Beconsall-1Z or Preese Hall-1 (Clarke et al. 2018), therefore the organic geochemistry of previous studies as well as in this thesis are representative of natural processes. Our organic geochemical analyses (e.g. PI >0.16 in both cores) suggest that petroleum in the upper Bowland is most likely thermally mature and gas dominated with some condensate. This supports previous work by Clarke et al. (2018) which record T_{max} values of 459 and 470 °C in Beconsall-1Z and Preese Hall-1, respectively. We suggest that T_{max} ranges from 450 to >470 °C and OM is gas-prone. However, previous authors debate the abundance of free gas (Clarke et al. 2018) relative to adsorbed gas (Whitelaw et al. 2019), which can have consequences for reserve estimates.

The true producible gas volumes of any shale gas target, including the upper Bowland, are not known until post-production. However, we show how geochemistry is a powerful contributor to minimising subsurface and economic risk associated with petroleum exploration and appraisal. Future work on the upper Bowland and other unexplored formations should embrace the effectiveness of geochemistry, especially when integrated with petrophysics, geomechanics, geophysics, computational models and sedimentology.

Chapter 9. Conclusions

- Time-efficient techniques such as biostratigraphy, gamma ray well logs, XRF and Rock-Eval are recommended for stratigraphic navigation on well-site. The reliability of upper Bowland directional drilling and well correlation can be improved using proxies of trace metal geochemistry (Mo/U) and organic geochemistry (OSI), derived from XRF and Rock-Eval pyrolysis respectively. Complex molecular geochemical analyses of deeply buried, thermally mature and over-mature Carboniferous successions are limited by low EOM (<2 mg), restricting their use as a correlation proxy. However, in this scenario, molecular analyses are useful for palaeoceanographic interpretations of OM and to contextualise the processes controlling trace metal reduction.
- Palaeoceanographic interpretations of the upper Bowland Shale Formation are best achieved using a combination of petrographic, trace metal, mineralogical and organic geochemical analyses from well and core. The upper Bowland Shale Formation is a thick succession (84 m thick in Beconsall-1Z and 499 m thick in Preese Hall-1) of quartz-rich feldspathic mudstone similar in geochemistry to the ensuing delta to the north (Millstone Grit Group). During Upper Mississippian hemi-pelagic prodeltaic deposition and eogenesis, the Bowland Basin was anoxic in the centre and towards the basin margins.
- High TOC content in the north (maximum 5.75 %) relative to the south (maximum 4.52 %) suggests that OM productivity / preservation was greater towards the central Bowland Basin. The central Bowland Basin is likely a preferred target location for shale gas production. Additionally, the sedimentary package is six times thicker in the centre (Preese Hall-1) relative to the southern basin margin (Beconsall-1Z) which is desirable for economic shale gas production of numerous stratigraphic layers.

- Outcrop and analogue studies are necessary in relatively unexplored basins to supplement all available well and core data. However, in mature and overmature outcrops and core, the complexity and highly variability organic compounds are rarely analogous, and the effects of thermal maturity are difficult to discern from weathering effects. This can obscure palaeoceanographic interpretations.
- A suitable analogue study should prioritise depositional setting over time equivalence. For example, the upper Bowland Shale Formation was deposited during the Mississippian, like the Bakken and Barnett shales. However, despite their similar mineralogy and provenance, the Bakken is not similar to the upper Bowland in trace metal geochemistry, but the Barnett is. The Barnett, despite differences in global location at the time of deposition, is the most applicable ancient palaeoceanographic analogue for the upper Bowland Shale Formation.
- Future work should investigate the fundamental controls on amorphous OM with regards provenance, deposition and eogenesis which is abundant in the upper Bowland Shale and many other shale gas targets (Curtis et al. 2012; Emmings et al. 2019b; Hennissen et al. 2017).

Suggestions for Future Work

- The integration of sequence stratigraphy and geochemistry is a fundamental uncertainty in geoscience that we address throughout this thesis and has been expressed in previous work (e.g. Craigie 2018). Future work should extrapolate our interpretations of marine band geochemistry and test the limits of the wider application of subsurface elemental and organic geochemical correlation. We suggest starting with a geochemical comparison of marine band E₁B₂ in other Mississippian basins (e.g. Gainsborough Trough and / or County Clare). For example, previous work on Carboniferous marine bands in County Clare (e.g. Davies and Elliott 1996) could be further explored using proxies proposed in this current study (e.g. relatively

high Mo/U and OSI above and within the marine band, respectively). It is possible that rocks with less complex or mature burial histories will be less challenging to correlate using marine bands. For example, we have studied the thermally degraded OM of Bowland Shale marine bands subjected to >5000 m burial depth (Andrews 2013a), but further study of less mature rocks may introduce even more marine band correlation proxies.

- In this current study, we found that Pr/Ph ratios are <2 basin wide; TOC and Mo cross-plots show the Bowland Basin was weakly restricted during upper Bowland deposition which is further supported by U EF and Mo EF cross-plots which suggest the Bowland Basin was anoxic, basin-wide. Future projects should investigate interpretations, proposed in this current study, that the location between Preese Hall-1 and Beconsall-1Z is likely a suitable environment for trace metal reduction and organic carbon burial. If so, it is important to investigate the potential for oil and gas recovery in this location.
- The upper and lower Bowland Shale are current targets for natural gas (Clarke et al. 2018) and geochemistry is one important factor throughout continual resource estimation. However, future work should analyse other related geological features of the Bowland Shale. For example, in this current study, the term "sweet spot" delineates a laterally extensive bed enriched in hydrocarbons. However, economic sweet spot discrimination relies also on suitable geomechanical parameters such as stiffness, but the geomechanical properties of the subsurface Bowland Shale are currently uncertain. Further knowledge of how Bowland Basin hydrocarbon sweet spots (marine bands) respond to the hydraulic fracturing process would be crucial as the Bowland Shale enters the production development stage (Clarke et al. 2018).
- Craigie (2018) explains how a geochemical project's requirements can target the type of elemental analyses needed, such as Inductively Coupled Plasma Mass Spectrometry (ICP-MS) versus

XRF. In this current study, we suggest that XRF for on-site chemostratigraphic analyses would prove useful during sweet spot discrimination and play fairway analyses. However, future work should analyse the relative effectiveness of ICP-MS, ICP-Optical Emission Spectrometry (ICP-OES), hand-held XRF or core scanning with respect to time efficiency and accuracy in deeply buried unconventional plays. Beyond elemental analyses, gamma, mineralogical and pyrolysis methods should be prioritised on well-site for multi-proxy geochemical analyses and improved accuracy (Clarke et al. 2018; Craigie 2018).

- We recommend the use and presentation of element-element correlation diagrams, shown in Chapter 7 of this current study, to avoid misinterpretations of elemental abundances in all future chemostratigraphic studies. For example, if Mo and Zr show a positive correlation, then it is likely that Mo abundances are linked to heavy mineral input, rather than sediment-water interface redox reactions. Previously adopted alternatives to this include principal component analyses (e.g. Emmings 2017) which, although useful, can sometimes obscure interpretations of causation and correlation for the reader. Other authors (Craigie 2018) express the usefulness of element-element correlation prior to elemental analyses without displaying it. We recommend that the display of these grids in future work (e.g. main body or appendix) would prove useful.
- Molecular techniques are limited by thermal maturation in mature rocks buried >5000 m (e.g. Chapter 4). In this current study, we suggest that molecular analyses in the Bowland Shale be treated with caution and future molecular analysis should use large samples (>15 g) to account for low EOM (<2 mg). However, previous studies (Gross et al. 2015) have successfully analysed the OM of Bowland Shale Formation marine bands, though at low resolution and outside of the natural gas target. Our aim to directly understand the industrially explored source rock proved usefully applicable in a

natural gas context; however this approach limited our scope for molecular analyses.

- Geochemical analyses are more time efficient with computer science and more contextualised with sedimentology (e.g. Craigie 2018). As well as saving time, multi-proxy, cross-disciplinary approaches used alongside geochemical analyses are more accurate in comparison to geochemistry used in isolation (Craigie 2018). Therefore, we recommend the use of cross-disciplinary approaches for the most time-efficient and accurate results. Understanding the relationship between micro and macro scale interpretations is currently a universal fundamental uncertainty linked to all aspects of geoscience. It is essential that these uncertainties are minimised through the integration of multiple skill-sets.

References

- ADAMS, J.A. & GASPARINI, P., 2013. *Gamma-ray spectrometry of rocks*. Elsevier.
- AITKENHEAD, N. 1992. Geology of the Country around Garstang.
- ALGEO, T.J., SCHWARK, L. & HOWER, J.C. 2004. High-resolution geochemistry and sequence stratigraphy of the Hushpuckney Shale (Swope Formation, eastern Kansas): implications for climato-environmental dynamics of the Late Pennsylvanian Midcontinent Seaway. *Chemical Geology*, **206**, 259-288.
- ALGEO, T.J. & TRIBOVILLARD, N. 2009. Environmental analysis of paleoceanographic systems based on molybdenum–uranium covariation. *Chemical Geology*, **268**, 211-225.
- ALI, F.O., 2019. *High-Risk High-Reward: Hydrocarbon exploration in frontier markets—a safety roulette?* (Master's thesis, University of Stavanger, Norway).
- ALVAREZ, J.S., 2018. Regional chemostratigraphy and mechanical stratigraphy of the Barnett Shale, Fort Worth Basin, Texas. *UMI thesis*.
- ANDERSON, G.M., 1976. Error propagation by the Monte Carlo method in geochemical calculations. *Geochimica et Cosmochimica Acta*, **40**(12), pp.1533-1538.
- ANDREWS, I.J. 2013a. Appendix E: Thermal modelling of the Pennine Basin, central Britain. *DECC*.
- ANDREWS, I.J. 2013b. The Carboniferous Bowland Shale gas study: geology and resource estimation. *British Geological Survey for Department of Energy and Climate Change, London, UK*.
- ANDREWS, I.J. 2013c. Appendices A, B, C, E: The Carboniferous Bowland Shale gas study. *British Geological Survey for Department of Energy and Climate Change, London, UK*.
- ARTHUR, J.D., BOHM, B. & LAYNE, M. 2009. Hydraulic fracturing considerations for natural gas wells of the Marcellus Shale.

- ARTHURTON, R.S. 1983. The skipton rock fault--an Hercynian wrench fault associated with the Skipton Anticline, northwest England. *Geological Journal*, **18**, 105-114.
- ARTHURTON, R.S. 1984. The Ribblesdale fold belt, NW England—a Dinantian-early Namurian dextral shear zone. *Geological Society, London, Special Publications*, **14**, 131-138.
- ARTHURTON, R.S., JOHNSON, E.W. and MUNDY, D.J.C., 1988. Geology of the country around Settle.
- BAGNOUD-VELÁSQUEZ, M., SPANGENBERG, J., POIRÉ, D.G. & PERAL, L.G. 2013. Stable isotope (S, C) chemostratigraphy and hydrocarbon biomarkers in the Ediacaran upper section of Sierras Bayas Group, Argentina. *Precambrian Research*, **231**, 388-400.
- BECK, M., DELLWIG, O., SCHNETGER, B. & BRUMSACK, H.-J. 2008. Cycling of trace metals (Mn, Fe, Mo, U, V, Cr) in deep pore waters of intertidal flat sediments. *Geochimica et Cosmochimica Acta*, **72**, 2822-2840.
- BEHAR, F., BEAUMONT, V. & PENTEADO, D.B. 2001. Rock Eval 6 Technology: Performance and Development. *Oil and Gas Science and Technology*, **56**, 111-134.
- BERNER, R., PETSCH, S., LAKE, J., BEERLING, D., POPP, B., LANE, R., LAWS, E., WESTLEY, M., CASSAR, N. & WOODWARD, F. 2000. Isotope fractionation and atmospheric oxygen: implications for Phanerozoic O₂ evolution. *Science*, **287**, 1630-1633.
- BHATTACHARYA, J.P. 1993. The expression and interpretation of marine flooding surfaces and erosional surfaces in core; examples from the Upper Cretaceous Dunvegan Formation, Alberta foreland basin, Canada. *Sequence stratigraphy and facies associations*, 125-160.
- BIRGENHEIER, L.P., HORTON, B., MCCAULEY, A.D., JOHNSON, C.L. and KENNEDY, A., 2017. A depositional model for offshore deposits of the lower Blue Gate Member, Mancos Shale, Uinta Basin, Utah, USA. *Sedimentology*, **64**(5), pp.1402-1438.
- BISAT, W.S. 1922. Yorkshire Naturalists at Clitheroe. *Naturalist*, 225-226.
- BISAT, W.S. 1924. The Carboniferous Goniaticites of the North of England and their zones. *Yorkshire Geological Society*, **20**, 40-124.

- BJØRLYKKE, K., AAGAARD, P., EGEBERG, P.K. & SIMMONS, S.P. 1995. Geochemical constraints from formation water analyses from the North Sea and the Gulf Coast Basins on quartz, feldspar and illite precipitation in reservoir rocks. *Geological Society, London, Special Publications*, **86**, 33-50.
- BLAKEY, R.C. 2008. Gondwana paleogeography from assembly to breakup—A 500 my odyssey. *Geological Society of America Special Papers*, **441**, 1-28.
- BLOXAM, T.W. & THOMAS, R.L. 1968. Palaeontological and geochemical facies in the *Gastrioceras subcrenatum* marine-band and associated rocks from the North Crop of the South Wales Coalfield. *Quarterly Journal of the Geological Society*, **124**, 239-277.
- BOWEN, H.J.M. 1979. Environmental chemistry of the elements. Academic Press.
- BRANDON, A., RILEY, N.J., WILSON, A.A. & ELLISON, R.A. 1995. Three new early Namurian (E1c-E2a) marine bands in central and northern England, UK, and their bearing on correlations with the Askrigg Block. *Proceedings of the Yorkshire Geological and Polytechnic Society*. Geological Society of London, 333-355.
- BRUMSACK, H.-J. 2006a. The trace metal content of recent organic carbon-rich sediments: implications for Cretaceous black shale formation. *Palaeogeography, Palaeoclimatology, Palaeoecology*, **232**, 344-361.
- BRUMSACK, H.J. 2006b. The trace metal content of recent organic carbon-rich sediments: Implications for Cretaceous black shale formation. *Palaeogeography, Palaeoclimatology, Palaeoecology*, **232**, 344-361, doi: 10.1016/j.palaeo.2005.05.011.
- BRUNER, K. & SMOSNA, R. 2011. A comparative study of the Mississippian Barnett shale, Fort Worth Basin, and Devonian Marcellus shale. *Appalachian Basin*, 106.
- CALVERT, S.E. and PEDERSEN, T.F., 1993. Geochemistry of recent oxic and anoxic marine sediments: implications for the geological record. *Marine geology*, *113*(1-2), pp.67-88.
- CAMBRIDGE, U.o. 2016. Crystallography Open Database.

- CAMPBELL, R.J., BROWN, P. & FOLGER, P.F. 2013. Prospects for coal in electric power and industry. Congressional Research Service.
- CANFIELD, D.E. 1994. Factors influencing organic carbon preservation in marine sediments. *Chemical Geology*, **114**, 315-329.
- CARVAJAL-ORTIZ, H. & GENTZIS, T. 2015. Critical considerations when assessing hydrocarbon plays using Rock-Eval pyrolysis and organic petrology data: data quality revisited. *International Journal of Coal Geology*, **152**, 113-122.
- CASH, R.J. 2016. *Acid fracturing carbonate-rich shale: a feasibility investigation of eagle ford formation*.
- CENTER., C.N.E.M. 1990. The Background concentrations of soil elements in China. Beijing: China Environmental Science Press.
- CENTER., C.N.E.M. 1994. The Atlas of Soil Environmental Background Value in the People's Republic of China. . *China Environmental Science Press: Beijing*, 1-195.
- CHERMAK, J.A. & SCHREIBER, M.E. 2014. Mineralogy and trace element geochemistry of gas shales in the United States: Environmental implications. *International Journal of Coal Geology*, **126**, 32-44.
- CHURCH, K.D. & GAWTHORPE, R.L. 1994. High resolution sequence stratigraphy of the late Namurian in the Widmerpool Gulf (East Midlands, UK). *Marine and Petroleum Geology*, **11**, 528-544.
- CIPOLLA, C.L., MACK, M.G. and MAXWELL, S.C., 2010, January. Reducing exploration and appraisal risk in low-permeability reservoirs using microseismic fracture mapping. In *Canadian Unconventional Resources and International Petroleum Conference*. Society of Petroleum Engineers.
- CLARKE, H., TURNER, P. & BUSTIN, R.M. 2014. Unlocking the resource potential of the Bowland Basin, NW England. *Society of Petroleum Engineers - European Unconventional Resources Conference and Exhibition 2014: Unlocking European Potential*, 908-918.
- CLARKE, H., TURNER, P., BUSTIN, R.M., RILEY, N. & BESLY, B. 2018. Shale gas resources of the Bowland Basin, NW England: a holistic study. *Petroleum Geoscience*, petgeo2017-2066.

- CLIFF, R., DREWERY, S. & LEEDER, M. 1991. Sourcelands for the Carboniferous Pennine river system: constraints from sedimentary evidence and U-Pb geochronology using zircon and monazite. *Geological Society, London, Special Publications*, **57**, 137-159.
- COCKS, L.R.M. & TORSVIK, T.H. 2006. European geography in a global context from the Vendian to the end of the Palaeozoic. *MEMOIRS-GEOLOGICAL SOCIETY OF LONDON*, **32**, 83.
- COLLINSON, J.D. 1968. Deltaic sedimentation units in the Upper Carboniferous of northern England. *Sedimentology*, **10**, 233-254.
- COLLINSON, J.D. 1969. The sedimentology of the Grindslow Shales and the Kinderscout Grit: a deltaic complex in the Namurian of northern England. *Journal of sedimentary research*, **39**.
- COLLINSON, J.D., BESLY, B.M. & KELLING, G. 1988. Controls on Namurian sedimentation in the Central Province basins of northern England. *Sedimentation in a Synorogenic Basin Complex: the Upper Carboniferous of Northwest Europe*. Blackie, Glasgow, **85**, 101.
- CORFIELD, S.M., GAWTHORPE, R.L., GAGE, M., FRASER, A.J. & BESLY, B.M. 1995. Inversion tectonics of the Variscan foreland of the British Isles. *Journal of the Geological Society*, **173**, 17-32.
- CORFIELD, S.M., GAWTHORPE, R.L., GAGE, M., FRASER, A.J. & BESLY, B.M. 1996. Inversion tectonics of the Variscan foreland of the British Isles. *Journal of the Geological Society*, **153**, 17-32.
- CRAIGIE, N. 2018. Principles of elemental chemostratigraphy. Springer.
- CRAIGIE, N.W. 2015. Applications of chemostratigraphy in Middle Jurassic unconventional reservoirs in eastern Saudi Arabia. *GeoArabia*, **20**, 79-110.
- CUADRILLA., 2019a, June. Preston New Road-1Z: LJ/06-09(z) HFP Report.
- CUADRILLA., 2019b, July. Hydraulic Fracture Plan PNR 2.
- CURTIS, C.D. 1964. Studies on the use of boron as a paleoenvironmental indicator. *Geochimica et Cosmochimica Acta*, **28**, 1125-1137.
- CURTIS, M.E., CARDOTT, B.J., SONDERGELD, C.H. & RAI, C.S. 2012. Development of organic porosity in the Woodford Shale with increasing thermal maturity. *International Journal of Coal Geology*, **103**, 26-31.

- DAVIES, S.J. & ELLIOTT, T. 1996. Spectral gamma ray characterization of high resolution sequence stratigraphy: examples from Upper Carboniferous fluvio-deltaic systems, County Clare, Ireland. *Geological Society, London, Special Publications*, **104**, 25-35.
- DAVIES, S.J. & MCLEAN, D. 1996. Spectral gamma-ray and palynological characterization of Kinderscoutian marine bands in the Namurian of the Pennine Basin. *Proceedings of the Yorkshire Geological Society*, **51**, 103-114.
- DAWSON, W.C. 1997. Limestone microfacies and sequence stratigraphy: Eagle Ford Group (Cenomanian-Turonian) north-central Texas outcrops.
- DE PATER, C.J.a.B., S. 2011. Geomechanical study of Bowland Shale seismicity. *Synthesis report. Cuadrilla Resources Ltd.*
- DEGENS, E.T. 1967. Diagenesis of organic matter. *Developments in Sedimentology*. Elsevier, 343-390.
- DENNE, R.A., HINOTE, R.E., BREYER, J.A., KOSANKE, T.H., LEES, J.A., ENGELHARDT-MOORE, N., SPAW, J.M. & TUR, N. 2014. The Cenomanian-Turonian Eagle Ford Group of South Texas: Insights on timing and paleoceanographic conditions from geochemistry and micropaleontologic analyses. *Palaeogeography, Palaeoclimatology, Palaeoecology*, **413**, 2-28.
- DREWERY, S., CLIFF, R. & LEEDER, M. 1987. Provenance of Carboniferous sandstones from U-Pb dating of detrital zircons. *Nature*, **325**, 50.
- DUNHAM, K.C. & WILSON, A.A. 1985. Geology of the Northern Pennine oilfield: Volume 2 Stainmore to Craven.
- DUSAR, M., PAPROTH, E., STREEL, M. & BLESS, M.J.M. 2000. Palaeogeographic and palaeoenvironmental characteristics of major marine incursions in northwestern Europe during the Westphalian C (Bolsovian). *Geologica Belgica*, **3**, 331-347.
- EARP, J.R., MAGRAW, D., POOLE, E.G., LAND, D.H. & WHITEMAN, A.J. 1961. Geology of the country around Clitheroe and Nelson. *Geological survey of Great Britain Memoir, England and Wales*, **69**, 346.
- EMERY, D. and MYERS, K. eds., 2009. *Sequence stratigraphy*. John Wiley & Sons.

- EGENHOFF, S.O. and FISHMAN, N.S., 2013. Traces in the dark—Sedimentary processes and facies gradients in the upper shale member of the Upper Devonian–Lower Mississippian Bakken Formation, Williston Basin, North Dakota, USA. *Journal of Sedimentary Research*, **83**(9), pp.803-824.
- EMMINGS, J.F., DAVIES, S.J., VANE, C.H., LENG, M.J., MOSS-HAYES, V., STEPHENSON, M.H. & JENKIN, G.R. 2017. Stream and slope weathering effects on organic-rich mudstone geochemistry and implications for hydrocarbon source rock assessment: A Bowland Shale case study. *Chemical Geology*, **471**, 74-91.
- EMMINGS, J.F., DAVIES, S.J., VANE, C.H., MOSS-HAYES, V. & STEPHENSON, M.H. 2019a. From marine bands to hybrid flows: Sedimentology of a Mississippian black shale. *Sedimentology*.
- EMMINGS, J.F., HENNISSSEN, J.A., STEPHENSON, M.H., POULTON, S.W., VANE, C.H., DAVIES, S.J., LENG, M.J., LAMB, A. & MOSS-HAYES, V. 2019b. Controls on amorphous organic matter type and sulphurization in a Mississippian black shale. *Review of Palaeobotany and Palynology*, **268**, 1-18.
- ESPITALIÉ, J. & BORDENAVE, M. 1993. Source rock parameters. *Applied petroleum geochemistry*, **2**.
- ESPITALIE, J., MADEC, M., TISSOT, B., MENNIG, J.J. & LEPLAT, P. 1977. Source rock characterization method for petroleum exploration. *Offshore Technology Conference*. Offshore Technology Conference.
- ESSER, H. 1991. Alltagshandeln und Verstehen: zum Verhältnis von erklärender und verstehender Soziologie am Beispiel von Alfred Schütz und "rational choice". Mohr.
- ETTENSohn, F.R. 1985. The Catskill delta complex and the Acadian orogeny: A model. *The Catskill Delta: Geological Society of America Special Paper*, **201**, 39-49.
- ETTENSohn, F.R. 1987. Rates of relative plate motion during the Acadian Orogeny based on the spatial distribution of black shales. *The Journal of Geology*, **95**, 572-582.
- EU. 2011. Energy Roadmap 2050. *Brussels, XXX COM (2011)*, **885**.

- FADIYA, S.L. 2014. Impact of wellsite biostratigraphy on exploration drilling in the deepwater offshore Nigeria. *Journal of African Earth Sciences*, **100**, 60-69.
- FAILL, R.T., WOODROW, D. & SEVON, W. 1985. The Acadian orogeny and the Catskill delta. *The Catskill Delta: Geological Society of America Special Paper*, **201**, 15-37.
- FARRIMOND, P., TAYLOR, A. & TELNÆS, N. 1998. Biomarker maturity parameters: the role of generation and thermal degradation. *Organic Geochemistry*, **29**, 1181-1197, doi: [http://dx.doi.org/10.1016/S0146-6380\(98\)00079-5](http://dx.doi.org/10.1016/S0146-6380(98)00079-5).
- FAUCHILLE, A.L., MA, L., RUTTER, E., CHANDLER, M., LEE, P.D. & TAYLOR, K.G. 2017. An enhanced understanding of the Basinal Bowland shale in Lancashire (UK), through microtextural and mineralogical observations. *Marine and Petroleum Geology*, **86**, 1374-1390.
- FERRILL, B.A. & THOMAS, W.A. 1988. Acadian dextral transpression and synorogenic sedimentary successions in the Appalachians. *Geology*, **16**, 604-608.
- FEWTRELL, M.D., SMITH, D.G., CLAYTON, G. & SEVASTOPULO, G.D. 1981a. Discussion on the recognition and division of the Tournaisian Series in Britain. *Journal of the Geological Society, London*, **137**, 61-63.
- FISHER, Q.J. & WIGNALL, P.B. 2001. Palaeoenvironmental controls on the uranium distribution in an Upper Carboniferous black shale (*Gastrioceras listeri* Marine Band) and associated strata; England. *Chemical Geology*, **175**, 605-621, doi: [http://dx.doi.org/10.1016/S0009-2541\(00\)00376-4](http://dx.doi.org/10.1016/S0009-2541(00)00376-4).
- FLOYD, P., SHAIL, R., LEVERIDGE, B. & FRANKE, W. 1991. Geochemistry and provenance of Rhenohercynian synorogenic sandstones: implications for tectonic environment discrimination. *Geological Society, London, Special Publications*, **57**, 173-188.
- FLOYD, P., WINCHESTER, J. & PARK, R. 1989. Geochemistry and tectonic setting of Lewisian clastic metasediments from the Early Proterozoic Loch Maree Group of Gairloch, NW Scotland. *Precambrian Research*, **45**, 203-214.

FRASER, A.J. & GAWTHORPE, R.L. 1990. Tectono-stratigraphic development and hydrocarbon habitat of the Carboniferous in northern England. *Geological Society, London, Special Publications*, **55**, 49-86.

FRASER, A.J. & GAWTHORPE, R.L. 2003. An atlas of Carboniferous basin evolution in northern England. Geological Society.

FRIEDMAN, G.M. & JOHNSON, K.G. 1966. The Devonian Catskill Deltaic Complex of New York, Type Example of a.

GAWTHORPE, R.L. & CLEMMY, H. 1987. Tectono-sedimentary evolution of the Bowland Basin, northern England, during the Dinantian. *Journal of the Geological Society of London*, **144**, 58-71.

GERHARD, L.C., ANDERSON, S.B., LEFEVER, J.A. & CARLSON, C.G. 1982. Geological development, origin, and energy mineral resources of Williston Basin, North Dakota. *AAPG Bulletin*, **66**, 989-1020.

GILLIGAN, A. 1920. The petrography of the Millstone Grit of Yorkshire. *Quart. Jour. Geol. Soc. London*, **70**, 251-294.

GOVINDARAJU, K. 1989. 1989 compilation of working values and sample description for 272 geostandards. *Geostandards Newsletter*, **13**, 1-113.

GOVINDARAJU, K. 1994. 1994 compilation of working values and sample description for 383 geostandards. *Geostandards Newsletter*, **18**, 1-158.

GRIFFITHS, J., WORDEN, R.H., WOOLDRIDGE, L.J., UTLEY, J.E., DULLER, R.A. & EDGE, R.L. 2018. Estuarine clay mineral distribution: Modern analogue for ancient sandstone reservoir quality prediction. *Sedimentology*.

GROSS, D., SACHSENHOFER, R.F., BECHTEL, A., PYTLAK, L., RUPPRECHT, B. & WEGERER, E. 2015. Organic geochemistry of Mississippian shales (Bowland Shale Formation) in central Britain: Implications for depositional environment, source rock and gas shale potential. *Marine and Petroleum Geology*, **59**, 1-21, doi: 10.1016/j.marpetgeo.2014.07.022.

GUION, P.D., GUTTERIDGE, P. & DAVIES, S.J. 2000. 14 Carboniferous sedimentation and volcanism on the Laurussian margin. *Geological history of Britain and Ireland*. Blackwell Science Oxford, 227-270.

HAMMES, U., 2019. EMD Shale Gas and Liquids Committee 2018 EMD Shale Gas and Liquids Committee Annual Report.

- HAMPSON, G.J., ELLIOTT, T. & DAVIES, S.J. 1997. The application of sequence stratigraphy to Upper Carboniferous fluvio-deltaic strata of the onshore UK and Ireland: implications for the southern North Sea. *Journal of the Geological Society*, **154**, 719-733.
- HANCOCK, N. & TAYLOR, A. 1978. Clay mineral diagenesis and oil migration in the Middle Jurassic Brent Sand Formation. *Journal of the Geological Society*, **135**, 69-72.
- HARRISON, B., OUEIDAT, T. & FALCONE, G. 2019. Choosing an Unconventional Play Analog for the Bowland Shale and Incorporating Onshore United Kingdom Operational Constraints in Potential Recovery Estimates. *SPE Europec featured at 81st EAGE Conference and Exhibition*. Society of Petroleum Engineers.
- HASHMY, K.H., DAVID, T., ABUEITA, S. & JONKERS, J. 2012. Shale Reservoirs: Improved Production from Stimulation of Sweet Spots. *SPE Asia Pacific Oil and Gas Conference and Exhibition*. Society of Petroleum Engineers.
- HAWKINS, K., DAVIES, S., MULLINS, G. & MACQUAKER, J. 2013. Miospore distribution and sedimentological facies distribution as an insight to changing terrestrial palaeoequatorial floral communities during a Pennsylvanian glacio-eustatic sea level cycle. *Review of Palaeobotany and Palynology*, **197**, 166-178.
- HAYASHI, K.-I., FUJISAWA, H., HOLLAND, H.D. & OHMOTO, H. 1997. Geochemistry of ~ 1.9 Ga sedimentary rocks from northeastern Labrador, Canada. *Geochimica et Cosmochimica Acta*, **61**, 4115-4137.
- HE, J., DING, W., ZHANG, J., LI, A., ZHAO, W. & DAI, P. 2016. Logging identification and characteristic analysis of marine–continental transitional organic-rich shale in the Carboniferous-Permian strata, Bohai Bay Basin. *Marine and Petroleum Geology*, **70**, 273-293.
- HEDGES, J.I. & KEIL, R.G. 1995. Sedimentary organic matter preservation: an assessment and speculative synthesis. *Marine chemistry*, **49**, 81-115.
- HENK, F. 2005. Lithofacies of the Barnett Shale Formation from outcrop to subsurface (abs.): Barnett Shale Symposium III. *Ellison Miles Geotechnology Institute: Texas Petroleum Technology Transfer Council, Texas Region, CD-ROM*.

- HENK, F., BREYER, J. & JARVIE, D. 2000. Lithofacies, petrology, and geochemistry of the Barnett Shale in conventional core and Barnett Shale outcrop geochemistry (abs.). *Barnett Shale Symposium, Fort Worth Texas: Oil Information Library of Fort Worth, Texas*.
- HENNISSEN, J.A. & GENT, C.M. 2019. Total organic carbon in the Bowland-Hodder Unit of the southern Widmerpool Gulf: a discussion. *Journal of Petroleum Science and Engineering*, **178**, 1194-1202.
- HENNISSEN, J.A.I., HOUGH, E., VANE, C.H., LENG, M.J., KEMP, S.J. & STEPHENSON, M.H. 2017. The prospectivity of a potential shale gas play: An example from the southern Pennine Basin (central England, UK). *Marine and Petroleum Geology*, **86**, 1047-1066, doi: <https://doi.org/10.1016/j.marpetgeo.2017.06.033>.
- HENRY, J.D. 1982. Stratigraphy of the Barnett Shale (Mississippian) and associated reefs in the northern Fort Worth Basin.
- HESTER, T. & SCHMOKER, J. 1985. Selected physical properties of the Bakken Formation. *North Dakota and Montana part of the Williston Basin: US Geological Survey oil and gas investigations chart*, **126**.
- HICKEY, J. & HENK, F. 2006. Barnett Shale, Fort Worth Basin: Lithofacies and implications (abs.): AAPG Southwest Section Meeting, Short Course, May 22, 2006, Midland, Texas.
- HIRD, C. & CLARKE, H. 2012. *Preese Hall-1 End of Well Report*. Cuadrilla Resources.
- HIRD, C., CLARKE, H. & WOOD, T. 2012. *Beaconsall-1 End Of Well Report*. Cuadrilla Resources.
- HODGE, T. 2003. The Saltfleetby Field, block L 47/16, licence PEDL 005, onshore UK. *Geological Society, London, Memoirs*, **20**, 911-919.
- HOLDSWORTH, B.K. & COLLINSON, J.D. 1988. Millstone Grit cyclicity revisited Sedimentation in a Synorogenic Basin Complex; the Upper Carboniferous of Northwest Europe. *Blackie and Son, London*, 132-152.
- HOLMES, D.T. & BUHR, K.A. 2007. Error propagation in calculated ratios. *Clinical biochemistry*, **40**, 728-734.

- HORN, M. 1960. Die Zone des Eumorphoceras pseudobilingue im Sauerland. *Fortschritte in der Geologie von Rheinland und Westfalen*, **3**, 303-342.
- HOUGH, E., VANE, C.H., SMITH, N.J.P. & MOSS-HAYES, V.L. 2014. The Bowland Shale in the Roosecote Borehole of the Lancaster Fells sub-Basin, Craven Basin, UK: a Potential UK Shale gas Play? *SPE/EAGE European Unconventional Resources Conference and Exhibition*.
- HOWARD, J.J. 1981. Lithium and potassium saturation of illite/smectite clays from interlaminated shales and sandstones. *Clays and Clay Minerals*, **29**, 136-142.
- HSU, S.-C. & NELSON, P.P. 2002. Characterization of eagle ford shale. *Engineering Geology*, **67**, 169-183.
- HUANG, W.-Y. & MEINSCHEN, W. 1979. Sterols as ecological indicators. *Geochimica et Cosmochimica Acta*, **43**, 739-745.
- HUDSON, R.G.S. 1944. The Carboniferous of the Broughton Anticline, Yorkshire. *Proceedings of the Yorkshire Geological Society* 25: 190-214.
- HUDSON, R.G.S. & TURNER, J.S. 1933. Correlation of Dinantian and Namurian in western Europe. *Leeds Philos. Lit. Soc. Proc.*, **2**, 407-482.
- HUNT, J.M. 1995. Petroleum geochemistry and geology.
- HUPPERT, J. 2013. Debates. *In: United Kingdom, House of Commons (ed.)*.
- HUYGHE, P., GUILBAUD, R., BERNET, M., GALY, A. & GAJUREL, A.P. 2011. Significance of the claymineral distribution in fluvial sediments of the Neogene to Recent Himalayan Foreland Basin (west-central Nepal). *Basin Research*, **23**, 332-345.
- ICDD. 2018. Minerals. *In: ICDD (ed.) Powder Diffraction File 4*.
- INGAMELLS, C.O., 1974. Control of geochemical error through sampling and subsampling diagrams. *Geochimica et Cosmochimica Acta*, 38(8), pp.1225-1237.
- ISBELL, J.L., MILLER, M.F., WOLFE, K.L. & LENAHER, P.A. 2003. Timing of late Paleozoic glaciation in Gondwana: Was glaciation responsible for the development of Northern Hemisphere cyclothem? *Special papers-geological society of America*, 5-24.

- ISLAM, M.R., 2014. *Unconventional gas reservoirs: evaluation, appraisal, and development*. Elsevier.
- JARVIE, D.M., HILL, R.J. & POLLASTRO, R.M. 2005. Assessment of the gas potential and yields from shales: The Barnett Shale model. *Oklahoma Geological Survey Circular*, **110**, 37-50.
- JARVIE, D.M., 2012. Shale resource systems for oil and gas: Part 2—Shale-oil resource systems.
- JIANG, T., JIN, Z., LIU, G., LIU, Q., GAO, B., LIU, Z., NIE, H., ZHAO, J., WANG, R., ZHU, T. and YANG, T., 2019. Source analysis of siliceous minerals and uranium in Early Cambrian shales, South China: Significance for shale gas exploration. *Marine and Petroleum Geology*, *102*, pp.101-108.
- JONES, B. & MANNING, D.A.C. 1994. Comparison of geochemical indices used for the interpretation of palaeoredox conditions in ancient mudstones. *Chemical Geology*, **111**, 111-129, doi: [https://doi.org/10.1016/0009-2541\(94\)90085-X](https://doi.org/10.1016/0009-2541(94)90085-X).
- KATZ, B.J. 2005. Controlling factors on source rock development—a review of productivity, preservation, and sedimentation rate.
- KAWAI, J., HAYASHI, K. and TANUMA, S., 1998. Extended X-ray emission fine structure of sodium. *Analyst*, *123*(4), pp.617-619.
- KENT, P. 1966. The structure of the concealed Carboniferous rocks of north-eastern England. *Proceedings of the Yorkshire Geological Society*, **35**, 323-352.
- KENT, D.M., CHRISTOPHER, J.E., MOSSOP, G. and SHETSEN, I., 1994. Geological history of the Williston Basin and Sweetgrass arch. *Geological Atlas of the Western Canada Sedimentary Basin. Canada: CSPG and Alberta Research Council*, pp.421-429.
- KILLOPS, S.D. & KILLOPS, V.J. 2013. Introduction to organic geochemistry. John Wiley & Sons.
- KOMBRINK, H., VAN OS, B.J.H., VAN DER ZWAN, C.J. & WONG, T.E. 2008. Geochemistry of marine and lacustrine bands in the Upper Carboniferous of the Netherlands. *Netherlands Journal of Geosciences*, **87**, 309-322.
- KÖNITZER, S.F., STEPHENSON, M.H., DAVIES, S.J., VANE, C.H. & LENG, M.J. 2016. Significance of sedimentary organic matter input for shale gas

generation potential of Mississippian Mudstones, Widmerpool Gulf, UK.

Review of Palaeobotany and Palynology, doi:

<http://dx.doi.org/10.1016/j.revpalbo.2015.10.003>.

KORN, D. & HORN, M. 1997. Subdivision of the basal Early Namurian (Early Carboniferous) in the Rhenish Massif (Germany). *Newsletters on Stratigraphy*, **35**, 115-126.

KUMPAN, T., BÁBEK, O., KALVODA, J., GRYGAR, T.M. & FRÝDA, J. 2014. Sea-level and environmental changes around the Devonian–Carboniferous boundary in the Namur–Dinant Basin (S Belgium, NE France): A multi-proxy stratigraphic analysis of carbonate ramp archives and its use in regional and interregional correlations. *Sedimentary Geology*, **311**, 43-59.

LAGRANGE, M.T., KONHAUSER, K.O., CATUNEANU, O., HARRIS, B.S., PLAYTER, T.L. and GINGRAS, M.K., 2020. Sequence stratigraphy in organic-rich marine mudstone successions using chemostratigraphic datasets. *Earth-Science Reviews*, p.103137.

LASH, G.G. & BLOOD, D.R. 2014. Organic matter accumulation, redox, and diagenetic history of the Marcellus Formation, southwestern Pennsylvania, Appalachian basin. *Marine and Petroleum Geology*, **57**, 244-263.

LAWRENCE, S., COSTER, P., IRELAND, R., BROOKS, J. & GLENNIE, K. 1987. Structural development and petroleum potential of the northern flanks of the Bowland Basin (Carboniferous), north-west England. *Petroleum Geology of North West Europe. Graham and Trotman, London*, **225**, 233.

LEEDER, M. 1988a. Recent developments in Carboniferous geology: a critical review with implications for the British Isles and NW Europe. *Proceedings of the Geologists' Association*, **99**, 73-100.

LEEDER, M.R. 1982. Upper Palaeozoic basins of the British Isles: Caledonide inheritance versus Hercynian plate margin processes. *Journal of the Geological Society of London*, **139**, 481-494.

LEEDER, M.R. 1988b. Recent developments in Carboniferous geology: a critical review with implications for the British Isles and NW Europe. *Proceedings of the Geologists' Association*, **99**, 73-100.

LEFEVER, J.A. 2008. Isopach of the Bakken Formation. North Dakota Geological Survey.

- LENNON, M., 2019. Estimating Chance for Success in Shale Gas Development Based on the Case of the United States.
- LEVENTHAL, J. 1991. Comparison of organic geochemistry and metal enrichment in two black shales: Cambrian Alum Shale of Sweden and Devonian Chattanooga Shale of United States. *Mineralium Deposita*, **26**, 104-112.
- LEYTHAEUSER, D. 1973. Effects of weathering on organic matter in shales. *Geochimica et Cosmochimica Acta*, **37**, 113-120.
- LI, Z. and SCHEIBER, J., 2020. Application of sequence stratigraphic concepts to the Upper Cretaceous Tununk Shale Member of the Mancos Shale Formation, south-central Utah: Parasequence styles in shelfal mudstone strata. *Sedimentology*, 67(1), pp.118-151.
- LIU, K., OSTADHASSAN, M., ZHOU, J., GENTZIS, T. & REZAAE, R. 2017. Nanoscale pore structure characterization of the Bakken shale in the USA. *Fuel*, **209**, 567-578.
- LOCK, B.E. & PESCHIER, L. 2006. Boquillas (Eagle Ford) upper slope sediments, west Texas: Outcrop analogs for potential shale reservoirs.
- LOPATIN, N., ZUBAIRAEV, S., KOS, I., EMETS, T., ROMANOV, E. & MALCHIKHINA, O. 2003. Unconventional oil accumulations in the Upper Jurassic Bazhenov Black Shale Formation, West Siberian Basin: a self-sourced reservoir system. *Journal of Petroleum Geology*, **26**, 225-244.
- LOUCKS, R.G. & RUPPEL, S.C. 2007. Mississippian Barnett Shale: Lithofacies and depositional setting of a deep-water shale-gas succession in the Fort Worth Basin, Texas. *AAPG Bulletin*, **91**, 579-601.
- MARTINI, F., ROGERS, E., BENNETT, S., DAVI, R., DOHERTY, J.T. and MONGAN, J., 2019. Integrated geophysical exploration in onshore frontier basins. *Geophysical Prospecting*, 67(6-Geophysical Instrumentation and Acquisition), pp.1664-1675.
- MARTINSEN, O.J. 1990. Fluvial, inertia-dominated deltaic deposition in the Namurian (Carboniferous) of northern England. *Sedimentology*, **37**, 1099-1113.
- MARTINSEN, O.J. 1993. Namurian (Late Carboniferous) Depositional Systems of the Craven-Area, Northern England: Implications for

Sequence-Stratigraphic Models. *Sequence stratigraphy and facies associations*, 247-281.

MARTINSEN, O.J., COLLINSON, J.D. & HOLDSWORTH, B.K. 1995. Millstone Grit cyclicity revisited, II: sequence stratigraphy and sedimentary responses to changes of relative sea-level. *Sedimentary Facies Analysis: A Tribute to the Research and Teaching of Harold G. Reading*, 305-327.

MAYNARD, J. 1981. Carbon isotopes as indicators of dispersal patterns in Devonian-Mississippian shales of the Appalachian Basin. *Geology*, **9**, 262-265.

MAYNARD, J. & LEEDER, M. 1992. On the periodicity and magnitude of Late Carboniferous glacio-eustatic sea-level changes. *Journal of the Geological Society*, **149**, 303-311.

MAYNARD, J.R. 1992. Sequence stratigraphy of the Upper Yeadonian of northern England. *Marine and Petroleum Geology*, **9**, 197-207, doi: [http://dx.doi.org/10.1016/0264-8172\(92\)90091-R](http://dx.doi.org/10.1016/0264-8172(92)90091-R).

MCGLADE, C., SPEIRS, J. & SORRELL, S. 2013. Methods of estimating shale gas resources—Comparison, evaluation and implications. *Energy*, **59**, 116-125.

MEISSNER, F. 1978. Patterns of source-rock maturity in nonmarine source-rocks of some typical western interior basins. *Nonmarine Tertiary and Upper Cretaceous source rocks and the occurrence of oil and gas in west-central US: Rocky Mountain Association of Geologists Continuing Education Lecture Series*, 1-37.

MONTGOMERY, S.L., JARVIE, D.M., BOWKER, K.A. & POLLASTRO, R.M. 2005. Mississippian Barnett Shale, Fort Worth basin, north-central Texas: Gas-shale play with multi-trillion cubic foot potential. *AAPG Bulletin*, **89**, 155-175.

MOSLOW, T.F., HAVERSLEW, B. & HENDERSON, C.M. 2018. Sedimentary facies, petrology, reservoir characteristics, conodont biostratigraphy and sequence stratigraphic framework of a continuous (395m) full diameter core of the Lower Triassic Montney Fm, northeastern British Columbia. *Bulletin of Canadian Petroleum Geology*, **66**, 259-287.

- MURPHY, B.R. 2014. Elemental chemostratigraphy of the Three Forks Formation, Williston Basin, North Dakota.
- MURRAY, D. 2015. Britain needs to get fracking. *The Spectator*. Spectator.
- MYERS, K.J. & WIGNALL, P.B. 1987. Understanding Jurassic organic-rich mudrocks—new concepts using gamma-ray spectrometry and palaeoecology: examples from the Kimmeridge Clay of Dorset and the Jet Rock of Yorkshire. *Marine clastic sedimentology*. Springer, 172-189.
- NANCE, W. & TAYLOR, S. 1977. Rare earth element patterns and crustal evolution—II. Archean sedimentary rocks from Kalgoorlie, Australia. *Geochimica et Cosmochimica Acta*, **41**, 225-231.
- NANDY, D., SONNENBERG, S.A. & HUMPHREY, J.D. 2015. Factors Controlling Organic-richness in Upper and Lower Bakken Shale, Williston Basin: An Application Inorganic Geochemistry, presented at AAPG Annual Convention & Exhibition. *Chemical Geology*, **232**, 12-32.
- NEWELL, A.J., VANE, C.H., SORENSEN, J.P.R., MOSS-HAYES, V. & GOODY, D.C. 2016. Long-term Holocene groundwater fluctuations in a chalk catchment: evidence from Rock-Eval pyrolysis of riparian peats. *Hydrological Processes* **30**, 4556-4567 doi: DOI: 10.1002/hyp.10903.
- NIKOLAEVA, S. 2013. New Viséan and Serpukhovian ammonoids from the Verkhnyaya Kardailovka section, eastern slope of the South Urals. *Paleontological Journal*, **47**, 386-399.
- NSIANYA, C.C., 2013. Chemostratigraphy Of The Mississippian-age Barnett Formation, Fort Worth Basin, Wise County, Texas USA.
- O'MARA, P.T. & TURNER, B.R. 1997. Westphalian B marine bands and their subsurface recognition using gamma-ray spectrometry. *Proceedings of the Yorkshire Geological Society*, **51**, 307-316.
- PAIKARAY, S., BANERJEE, S. & MUKHERJI, S. 2008. Geochemistry of shales from the Paleoproterozoic to Neoproterozoic Vindhyan Supergroup: Implications on provenance, tectonics and paleoweathering. *Journal of Asian Earth Sciences*, **32**, 34-48.
- PANALYTICAL. 2004. X'Pert Highscore Plus. PANalytical B. V., Almelo.
- PASSEY, Q.R., BOHACS, K., ESCH, W.L., KLIMENTIDIS, R. & SINHA, S. 2010. From oil-prone source rock to gas-producing shale reservoir-geologic and

petrophysical characterization of unconventional shale gas reservoirs. *International oil and gas conference and exhibition in China*. Society of Petroleum Engineers.

PETERS-KOTTIG, W., STRAUSS, H. & KERP, H. 2006. The land plant $\delta^{13}\text{C}$ record and plant evolution in the Late Palaeozoic. *Palaeogeography, Palaeoclimatology, Palaeoecology*, **240**, 237-252.

PETERS, K. 1986. Guidelines for evaluating petroleum source rock using programmed pyrolysis. *AAPG Bulletin*, **70**, 318-329.

PETERS, K., ROHRBACK, B. & KAPLAN, I. 1980. Laboratory-simulated thermal maturation of recent sediments. *Physics and Chemistry of the Earth*, **12**, 547-557.

PETERS, K.E., WALTERS, C.C. & MOLDOWAN, J.M. 2005. The Biomarker Guide Vol. 2. *Cambridge: Cambridge University Press*.

PETSCH, S., BERNER, R. & EGLINTON, T. 2000. A field study of the chemical weathering of ancient sedimentary organic matter. *Organic Geochemistry*, **31**, 475-487.

POLLASTRO, R.M., JARVIE, D.M., HILL, R.J. & ADAMS, C.W. 2007. Geologic framework of the Mississippian Barnett shale, Barnett-paleozoic total petroleum system, Bend arch–Fort Worth basin, Texas. *AAPG Bulletin*, **91**, 405-436.

POLLASTRO, R.M., ROBERTS, L.N. & COOK, T.A. 2013. Geologic assessment of technically recoverable oil in the Devonian and Mississippian Bakken Formation. US Geological Survey, Reston, Virginia.

POMMER, M. & MILLIKEN, K. 2015. Pore types and pore-size distributions across thermal maturity, Eagle Ford Formation, southern Texas. *AAPG Bulletin*, **99**, 1713-1744.

POSAMENTIER, H.W., JERVEY, M.T. & VAIL, P.R. 1988. Eustatic controls on clastic deposition I—conceptual framework.

POSAMENTIER, H.W. and VAIL, P.R., 1988. Eustatic controls on clastic deposition II—sequence and systems tract models.

POSAMENTIER, H.W. and ALLEN, G.P., 1999. *Siliciclastic sequence stratigraphy: concepts and applications* (Vol. 7, p. 210). Tulsa, Oklahoma: SEPM (Society for Sedimentary Geology).

- PRANGE, A. & KREMLING, K. 1985. Distribution of dissolved molybdenum, uranium and vanadium in Baltic Sea waters. *Marine chemistry*, **16**, 259-274.
- PRESS ASSOCIATION. 2014. Fracking 'good for the UK', says David Cameron. *The Guardian*.
- PRESTON, J., HARTLEY, A., HOLE, M., BUCK, S., BOND, J., MANGE, M. and STILL, J., 1998. Integrated whole-rock trace element geochemistry and heavy mineral chemistry studies; aids to the correlation of continental red-bed reservoirs in the Beryl Field, UK North Sea. *Petroleum Geoscience*, *4*(1), pp.7-16.
- RAMSBOTTOM, W.H.C. 1979. Rates of transgression and regression in the Carboniferous of NW Europe. *Quarterly Journal of the Geological Society of London*, **136**, 147-154.
- RAMSBOTTOM, W.H.C., CALVER, M.A., EAGAR, R.M.C., HODSON, F., HOLIDAY, D.W., STUBBLEFIELD, C.J. & WILSON, R.B. 1978. A correlation of Silesian rocks in the British Isles. *Geological Society Special Report*, **10**, 82.
- RAMSBOTTOM, W.H.C., RHYS, G.H. & SMITH, E.G. 1962. Boreholes in the Carboniferous rocks of the Ashover district, Derbyshire. *Bulletin of the Geological Survey of Great Britain*, **19**, 75-168.
- RAST, N. & SKEHAN, J.W. 1993. Mid-Paleozoic orogenesis in the North Atlantic: the Acadian orogeny. *The Acadian Orogeny: Recent Studies in New England, Maritime Canada and the Autochthonous Foreland*, 1-25.
- RATCLIFFE, K., WRIGHT, A. & SCHMIDT, K. 2012a. Application of inorganic whole-rock geochemistry to shale resource plays: an example from the Eagle Ford Shale Formation, Texas. *The Sedimentary Record*, **10**, 4-9.
- RATCLIFFE, K., WRIGHT, M. & SPAIN, D. 2012b. Unconventional methods for unconventional plays: using elemental data to understand shale resource plays.
- READ, J.F., OSLEGER, D., ELRICK, M., FRANSEEN, E.K., WATNEY, W.L., KENDALL, C. & ROSS, W. 1991. Two-dimensional modeling of carbonate ramp sequences and component cycles. *Sedimentary modeling: Computer simulations and methods for improved parameter definition: Kansas Geological Survey Bulletin*, **233**, 473-488.

- READING, H. 1964. A review of the factors affecting the sedimentation of the Millstone Grit (Namurian) in the Central Pennines. *Developments in Sedimentology*. Elsevier, 340-346.
- READING, H.G. ed., 2009. *Sedimentary environments: processes, facies and stratigraphy*. John Wiley & Sons.
- RILEY, D.A., PEARCE, T.J., MATHIA, E., RATCLIFFE, K. & MARTIN, J. 2018. The application of elemental geochemistry to UK onshore unconventional plays. *Geological Society, London, Petroleum Geology Conference series*. Geological Society of London, 585-594.
- RILEY, N. 1993. Dinantian (Lower Carboniferous) biostratigraphy and chronostratigraphy in the British Isles. *Journal of the Geological Society*, **150**, 427-446.
- RILEY, N.J., CLAQUE-LONG, J., HIGGINS, A.C., OWENS, B., SPEARS, A., TAYLOR, L. & VARKER, W.J. 1995. Geochronometry and geochemistry of the European Mid-Carboniferous boundary global stratotype proposal, Stonehead Beck, North Yorkshire, UK. *Annales de la Societe Geologique de Belgique*, **116**, 275-289.
- ROMERO-SARMIENTO, M.-F., ROUZAUD, J.-N., BERNARD, S., DELDICQUE, D., THOMAS, M. & LITCKE, R. 2014. Evolution of Barnett Shale organic carbon structure and nanostructure with increasing maturation. *Organic Geochemistry*, **71**, 7-16.
- ROSER, B. & KORSCH, R. 1988. Provenance signatures of sandstone-mudstone suites determined using discriminant function analysis of major-element data. *Chemical Geology*, **67**, 119-139.
- ROWE, H., HUGHES, N. & ROBINSON, K. 2012. The quantification and application of handheld energy-dispersive x-ray fluorescence (ED-XRF) in mudrock chemostratigraphy and geochemistry. *Chemical Geology*, **324**, 122-131.
- ROWE, H.D., LOUCKS, R.G., RUPPEL, S.C. & RIMMER, S.M. 2008. Mississippian Barnett Formation, Fort Worth Basin, Texas: Bulk geochemical inferences and Mo-TOC constraints on the severity of hydrographic restriction. *Chemical Geology*, **257**, 16-25, doi: <https://doi.org/10.1016/j.chemgeo.2008.08.006>.

SALAMEH, M.G. 2003. Can renewable and unconventional energy sources bridge the global energy gap in the 21st century? *Applied Energy*, **75**, 33-42.

SARG, J., 2011. *The Bakken-An unconventional petroleum and reservoir system*. Trustees Of The Colorado School Of Mines.

SCHLANGER, S. & JENKYNS, H. 1976. Cretaceous oceanic anoxic events: causes and consequences. *Geologie en mijnbouw*, **55**.

SCHULZ, H.-M., BECHTEL, A. & SACHSENHOFER, R. 2005. The birth of the Paratethys during the Early Oligocene: from Tethys to an ancient Black Sea analogue? *Global and Planetary Change*, **49**, 163-176.

SCOTESE, C.R. & MCKERROW, W.S. 1990. Revised world maps and introduction. *Geological Society, London, Memoirs*, **12**, 1-21.

SCOTT, C., SLACK, J.F. & KELLEY, K.D. 2017. The hyper-enrichment of V and Zn in black shales of the Late Devonian-Early Mississippian Bakken Formation (USA). *Chemical Geology*, **452**, 24-33.

SHANMUGAM, G. 1985. Significance of coniferous rain forests and related organic matter in generating commercial quantities of oil, Gippsland Basin, Australia. *AAPG Bulletin*, **69**, 1241-1254.

SHERWOOD LOLLAR, B., HIRSCHORN, S.K., CHARTRAND, M.M. and LACRAMPE-COULOUME, G., 2007. An approach for assessing total instrumental uncertainty in compound-specific carbon isotope analysis: implications for environmental remediation studies. *Analytical chemistry*, **79**(9), pp.3469-3475.

SHULTZ, J.M. 2015. *Pore Network Variation Identified Through NMR Analysis: Eagle Ford Group, South Texas, USA*.

SINGH, K., HOLDITCH, S.A. & AYERS, W.B. 2008. Basin analog investigations answer characterization challenges of unconventional gas potential in frontier basins. *Journal of Energy Resources Technology*, **130**, 043202.

SLATT, R.M., JORDAN, D.W., D'AGOSTINO, A.E. & GILLESPIE, R.H. 1992. Outcrop gamma-ray logging to improve understanding of subsurface well log correlations. *Geological Society, London, Special Publications*, **65**, 3-19.

- SLATT, R.M. & RODRIGUEZ, N.D. 2012. Comparative sequence stratigraphy and organic geochemistry of gas shales: Commonality or coincidence? *Journal of Natural Gas Science and Engineering*, **8**, 68-84.
- SLOWAKIEWICZ, M., TUCKER, M., VANE, C.H., HARDING, R., COLLINS, A. & PANCOST, R.D. 2015. Shale-gas potential of the mid-Carboniferous Bowland-Hodder unit in the Cleveland basin (Yorkshire), Central Britain. *Journal of Petroleum Geology*, **38**, 1-18.
- SMITH, A.C., KENDRICK, C.P., MOSS-HAYES, V.L., VANE, C.H. & LENG, M.J. 2017. Carbon isotope alteration during the thermal maturation of non-flowering plant species representative of those found within the geological record. *Rapid Communications in Mass Spectrometry*, **31**, 21-26.
- SMITH, M.G. & BUSTIN, R.M. 1996. Lithofacies and paleoenvironments of the upper Devonian and lower Mississippian Bakken Formation, Williston Basin. *Bulletin of Canadian Petroleum Geology*, **44**, 495-507.
- SMITH, M.G. & BUSTIN, R.M. 2000. Late Devonian and Early Mississippian Bakken and Exshaw black shale source rocks, Western Canada Sedimentary Basin: a sequence stratigraphic interpretation. *AAPG Bulletin*, **84**, 940-960.
- SMITH, N.J.P., KIRBY, G.A. & PHARAOH, T.C. 2005. Structure and evolution of the south-west Pennine Basin and adjacent area. *Subsurface Memoir of the British Geological Survey*.
- SONNENBERG, S.A., JIN, H. & SARG, J.F. 2011. PS Bakken Mudrocks of the Williston Basin, World Class Source Rocks. *AAPG Annu. Convent. Exhib.*
- SOULSBY, A. & KEMAL, A. 1988. Source rock maturity key to new plays. *Oil and Gas Journal*, **86**, 81-83.
- SPEARS, D.A. 1964a. The major element geochemistry of the Mansfield Marine Band in the Westphalian of Yorkshire. *Geochimica et Cosmochimica Acta*, **28**, 1679-1696.
- SPEARS, D.A. 1964b. The radioactivity of the Mansfield marine band, Yorkshire. *Geochimica et Cosmochimica Acta*, **28**, 673-681.
- SPEARS, D.A. & SEZGIN, H.I. 1985. Mineralogy and geochemistry of the Subcrenatum Marine Band and associated coal-bearing sediments, Langsett, South Yorkshire. *Journal of sedimentary research*, **55**, 570-578.

SKUPIO, R. and DE ALEMAR BARBERES, G., 2017. Spectrometric gamma radiation of shale cores applied to sweet spot discrimination in Eastern Pomerania, Poland. *Acta Geophysica*, 65(6), pp.1219-1227.

STEPHEN, K.D., CLARK, J.D. & GARDINER, A.R. 2001. Outcrop-based stochastic modelling of turbidite amalgamation and its effects on hydrocarbon recovery. *Petroleum Geoscience*, **7**, 163-172.

STEPHENSON, D.B., DIAZ, H.F. & MURNANE, R.J. 2008. Definition, diagnosis, and origin of extreme weather and climate events. Cambridge University Press: New York.

STRICKLAND, R.F., PURVIS, D.C. & BLASINGAME, T.A. 2011. Practical aspects of reserves determinations for shale gas. *North American unconventional gas conference and exhibition*. Society of Petroleum Engineers.

TEN HAVEN, H., DE LEEUW, J., RULLKÖTTER, J. & DAMSTÉ, J.S. 1987. Restricted utility of the pristane/phytane ratio as a palaeoenvironmental indicator. *Nature*, **330**, 641.

TAYLOR, K.G., MACQUAKER, J.H.S. and SHAW, H., 2014. Diagenetic alterations in a silt-and clay-rich mudstone succession: an example from the Upper Cretaceous Mancos Shale of Utah, USA. *Clay Minerals*, 49(2), pp.213-227.

THOMAS, M. 1986. Diagenetic sequences and K/Ar dating in Jurassic sandstones, central Viking Graben; effects on reservoir properties. *Clay Minerals*, **21**, 695-710.

THOMAS, R.L. & BLOXAM, T.W. 1969. Some observations on the distribution of quartz, organic carbon, sulphur and iron in the *Gastrioceras Subcrenatum* marine band of the South Wales Coalfield. Sheffield (1968).

TIMMERMAN, M.J., HEEREMANS, M., KIRSTEIN, L.A., LARSEN, B.T., SPENCER-DUNWORTH, E.-A. & SUNDVOLL, B. 2009. Linking changes in tectonic style with magmatism in northern Europe during the late Carboniferous to latest Permian. *Tectonophysics*, **473**, 375-390.

TINNIN, B., BELLO, H. and MCCHESENEY, M., 2014. Multi-source data integration to predict well performance: Eagle Ford sweet spot mapping. In *San Antonio: AAPG/STGS Eagle Ford Plus Adjacent Plays & Extensions Workshop*.

- TRIBOVILLARD, N., ALGEO, T., BAUDIN, F. & RIBOULLEAU, A. 2012. Analysis of marine environmental conditions based on molybdenum–uranium covariation—Applications to Mesozoic paleoceanography. *Chemical Geology*, **324**, 46-58.
- TRIBOVILLARD, N., ALGEO, T.J., LYONS, T. & RIBOULLEAU, A. 2006. Trace metals as paleoredox and paleoproductivity proxies: An update. *Chemical Geology*, **232**, 12-32, doi: <https://doi.org/10.1016/j.chemgeo.2006.02.012>.
- TUREKIAN, K.K. & WEDEPOHL, K.H. 1961. Distribution of the elements in some major units of the earth's crust. *Geological Society of America Bulletin*, **72**, 175-192.
- TYSON, R. 1987. The genesis and palynofacies characteristics of marine petroleum source rocks. *Geological Society, London, Special Publications*, **26**, 47-67.
- USEIA. 2011. World shale gas resources: an initial assessment of 14 regions outside the United States. US Department of Energy.
- VAN DER WEIJDEN, C.H. 2002. Pitfalls of normalization of marine geochemical data using a common divisor. *Marine geology*, **184**, 167-187.
- VEEVERS, J.J. & POWELL, C.M. 1987. Late Paleozoic glacial episodes in Gondwanaland reflected in transgressive-regressive depositional sequences in Euramerica. *Geological Society of America Bulletin*, **98**, 475-487.
- VER STRAETEN, C.A., GRIFFING, D.H. & BRETT, C.E. 1994. The lower part of the Middle Devonian Marcellus 'shale,' central to western New York State: Stratigraphy and depositional history. *New York State Geological Association, 66th Annual Meeting Field Trip Guidebook*, 271-321.
- VICKERSTAFF, A. 2019. Fracking is finished in the UK – thanks to the power of public protest. *The Guardian*.
- VINOGRADOV, A.P. 1959. Geochemistry of rare and dispersed chemical elements in soils.
- WALKER, R.G. 1966. Shale Grit and Grindslow shales; transition from turbidite to shallow water sediments in the upper Carboniferous of northern England. *Journal of sedimentary research*, **36**, 90-114.

- WALPER, J.L. 1977. Paleozoic tectonics of the southern margin of North America.
- WANG, G. & CARR, T.R. 2013. Organic-rich Marcellus Shale lithofacies modeling and distribution pattern analysis in the Appalachian Basin. *AAPG Bulletin*, **97**, 2173-2205.
- WATERS, C.N. & CONDON, D.J. 2012. Nature and timing of Late Mississippian to Mid-Pennsylvanian glacio-eustatic sea-level changes of the Pennine Basin, UK. *Journal of the Geological Society*, **169**, 37-51.
- WATERS, C.N., JONES, N.S., COLLINSON, J.D. & CLEAL, C.J. 2011. Craven Basin and southern Pennines. Geological Society of London.
- WATERS, C.N., WATERS, R.A., BARCLAY, W.J. & DAVIES, J.R. 2009. A lithostratigraphical framework for the Carboniferous successions of southern Great Britain (Onshore). British Geological Survey.
- WEBSTER, R.L. 1982. Analysis of petroleum source rocks of the Bakken Formation (Devonian and Mississippian) in North Dakota.
- WEBSTER, R.L. 1987. Petroleum source rocks and stratigraphy of the Bakken Formation in North Dakota.
- WEDEPOHL, K., HEINRICHS, H. & BRIDGWATER, D. 1991. Chemical characteristics and genesis of the quartz-feldspathic rocks in the Archean crust of Greenland. *Contributions to Mineralogy and Petrology*, **107**, 163-179.
- WEDEPOHL, K.H. 1969-1978. Handbook of Geochemistry. SpringerVerlag.
- WEHRLI, B. & STUMM, W. 1988. Oxygenation of vanadyl (IV). Effect of coordinated surface hydroxyl groups and hydroxide ion. *Langmuir*, **4**, 753-758.
- WENDT, A.K., ARTHUR, M.A., SLINGERLAND, R., KOHL, D., BRACHT, R. & ENGELDER, T. 2015. Geochemistry and depositional history of the Union Springs Member, Marcellus Formation in central Pennsylvania. *Interpretation*, **3**, SV17-SV33.
- WENGER, L.M., DAVIS, C.L., EVENSEN, J.M., GORMLY, J.R. & MANKIEWICZ, P.J. 2004. Impact of modern deepwater drilling and testing fluids on geochemical evaluations. *Organic Geochemistry*, **35**, 1527-1536.

- WHITELAW, P., UGUNA, C.N., STEVENS, L.A., MEREDITH, W., SNAPE, C.E., VANE, C.H., MOSS-HAYES, V. & CARR, A.D. 2019. Shale gas reserve evaluation by laboratory pyrolysis and gas holding capacity consistent with field data. *Nature communications*, **10**, 1-10.
- WILLIAMS, L.B. & FERRELL, R.E. 1991. Ammonium substitution in illite during maturation of organic matter. *Clays and Clay Minerals*, **39**, 400-408.
- WILSON, R.D. and SCHEIBER, J., 2015. Sedimentary facies and depositional environment of the Middle Devonian Genesee Formation of New York, USA. *Journal of Sedimentary Research*, *85*(11), pp.1393-1415.
- WINTSCH, R.P. & KVALE, C.M. 1994. Differential mobility of elements in burial diagenesis of siliciclastic rocks. *Journal of sedimentary research*, **64**, 349-361.
- WISEALL, A., CUSS, R., HOUGH, E. & KEMP, S. 2018. The role of fault gouge properties on fault reactivation during hydraulic stimulation; an experimental study using analogue faults. *Journal of Natural Gas Science and Engineering*, **59**, 21-34.
- WITHNALL, A. 2014. David Cameron goes 'all out for shale' with tax boost for councils willing to approve projects. *Independent*.
- WOODCOCK, N. & STRACHAN, R. 2012. Geological History of Britain and Ireland. Wiley-Blackwell.
- WORDEN, R., SMALLEY, P. & BARCLAY, S. 2003. H₂S and diagenetic pyrite in North Sea sandstones: due to TSR or organic sulphur compound cracking? *Journal of Geochemical Exploration*, **78**, 487-491.
- WORTHINGTON, R.P. & WALSH, J.J. 2011. Structure of Lower Carboniferous basins of NW Ireland, and its implications for structural inheritance and Cenozoic faulting. *Journal of Structural Geology*, **33**, 1285-1299.
- WRIGHT, L. 2016. The Potential of Shale Gas In The Bowland-Hodder, Is It The Next Barnett?
- YANG, S., HORSFIELD, B., MAHLSTEDT, N., STEPHENSON, M. & KÖNITZER, S. 2016. On the primary and secondary petroleum generating characteristics of the Bowland Shale, northern England. *Journal of the Geological Society*, **173**, 292-305.

ZAHID, S., BHATTI, A.A., AHAMAD KHAN, H. and AHAMAD, T., 2007, January. Development of unconventional gas resources: stimulation perspective. In *Production and Operations Symposium*. Society of Petroleum Engineers.

ZHOU, H.T., LI, D.Y., LIU, X.T., DU, Y.S. and GONG, W., 2019. Sweet spot prediction in tight sandstone reservoir based on well-bore rock physical simulation. *Petroleum Science*, 16(6), pp.1285-1300.